



# Politecnico di Torino

Thesis of master's degree

Analysis of Deep Tunnels in bimrock

Supervisors:

Prof. Monica Barbero

Prof. Maria Lia Napoli

Candidate:

Amirmohammad Vakili

March-April 2026

## Contents

1	Introduction.....	7
2	General Background on Complex Geological Formations.....	8
2.1	Complex Formations and Mélanges.....	12
2.1.1	Knowledge Aspects and Possible Genesis of Mélanges .....	15
2.2	From Mélanges to Bimrocks: Engineering Interpretation of Block-in-Matrix Materials .....	16
2.2.1	Engineering Challenges in Tunnelling Through Bimrocks .....	18
3	Bimrocks.....	20
3.1	Definition and Engineering Meaning of Bimrocks .....	20
3.1.2	Morphological features of Bimrocks and site investigation .....	24
3.2	Definition of geometrical configuration .....	26
3.3	Volumetric Block Proportion (VBP).....	30
4	Methodology:.....	32
4.1	Numerical approach and software .....	32
4.2	Geometrical model .....	32
4.3	Material properties .....	34
4.4	Boundary conditions.....	36
4.5	Loading conditions .....	37
4.6	Mesh generation .....	37
4.7	Analysis type and output parameters .....	38
5	Results of the numerical analysis: .....	41
5.1	Internal pressure vs. tunnel convergence.....	42
5.1.1	Analysis without inclusions: (VBP = 0%) .....	42
5.1.2	Analysis with inclusions: (VBP = 25%) .....	44
5.1.3	Analysis with Inclusions: VBP = 40% .....	50
5.2	Analysis of radial displacement from the sidewall to the external boundary 59	
5.2.1	Radial displacement from the sidewall until the external for a VBP=25% 59	
5.2.2	Radial displacement from the sidewall to the external boundary for a VBP = 40% .....	63

5.3	Analysis of Radial displacement along the tunnel boundary.....	67
5.3.1	Radial displacement along the tunnel boundary for VBP = 25%.....	67
5.3.2	Radial displacement along the tunnel boundary for VBP = 40%.....	70
5.4	Comparative Discussion:.....	73
5.5	Analysis of radial displacement at the side walls: .....	76
5.5.1	Radial displacement at the right sidewall.....	76
5.5.2	Radial displacement at the crown .....	79
5.5.3	Radial displacement at the left sidewall.....	81
5.5.4	Summary of the displacement at the sidewalls and the crown for different VBPs .....	83
5.6	Plastic zone extent for VBP = 25% and 40%:.....	86
5.6.1	Plastic zone extent for VBP = 25%: comparison between 0° and 90° configurations .....	87
6	Conclusions .....	89

## Figure index:

Figure 2.1 Summarizes the main criteria adopted by the Associazione Geotecnica Italiana (A.G.I., 1979) for the identification of complex geological formations. ....	9
Figure 2.2 Example of a structurally complex turbiditic succession, characterized by alternating sandstone and shale layers, representative of class B1 according to the A.G.I. (1979) classification.....	10
Figure 2.3 Example of a <i>mélange</i> deposit characterized by a chaotic block-in-matrix structure (after Medley, 2001). ....	12
Figure 2.4 Geographical distribution of the Franciscan Complex in the San Francisco Bay Area (after Medley, 1994). ....	13
Figure 2.5 Examples of block-in-matrix geological formations at different scales according to Edmund Medley (1994) .....	14
Figure 3.1 Illustrated different VBP% simulation.....	31
Figure 4.1 The geometry assumed in the RS2 .....	34
Figure 4.2 The model and boundaries that considered in RS2 .....	36
Figure 4.3 Ground reaction curve (Hoek et al., 1998).....	39
Figure 5.1 The values of radial displacement of matrix for VBP 0% vs. internal pressure .....	43
Figure 5.2 The diagram of radial displacement for 0-degree orientations for VBP 25% vs. internal pressure.....	45
Figure 5.3 The diagram of radial displacement for 45-degree orientations for VBP 25% vs. internal pressure .....	46
Figure 5.4 The diagram of radial displacement for 90-degree orientations for VBP 25% vs. internal pressure .....	47
Figure 5.5 The figure of max radial displacement for 0-45-90-degree orientations for VBP 25% vs. internal pressure .....	48
Figure 5.6 The diagram of radial displacement for 0-degree orientations for VBP 40% vs. internal pressure.....	51
Figure 5.7 The diagram of radial displacement for 45-degree orientations for VBP 40% vs. internal pressure .....	53
Figure 5.8 The diagram of radial displacement for 90-degree orientations for VBP 40% vs. internal pressure .....	55
Figure 5.9 The figure of max radial displacement for 0-45-90-degree orientations for VBP 40% vs. internal pressure .....	57
Figure 5.10 The comparing of internal pressure vs. Radial displacement in VBP 25%-40%-55%-70%.....	58
Figure 5.11 The figure of radial displacement for 0-degree orientations for VBP 25% vs. distance until external boundary .....	60
Figure 5.12 The figure of radial displacement for 45-degree orientations for VBP 25% vs. distance until external boundary .....	61

Figure 5.13 The figure of radial displacement for 90-degree orientations for VBP 25% vs. distance until external boundary .....	62
Figure 5.14 The figure of radial displacement for 0-degree orientations for VBP 40% vs. distance until external boundary .....	63
Figure 5.15 The figure of radial displacement for 45-degree orientations for VBP 25% vs. distance until external boundary .....	64
Figure 5.16 The figure of radial displacement for 90-degree orientations for VBP 25% vs. distance until external boundary .....	65
Figure 5.17 The figure of radial displacement for 0-degree orientations for VBP 25% vs. along the tunnel boundary.....	67
Figure 5.18 The figure of radial displacement for 45-degree orientations for VBP 25% vs. along the tunnel boundary.....	68
Figure 5.19 The figure of radial displacement for 90-degree orientations for VBP 25% vs. along the tunnel boundary.....	69
Figure 5.20 The figure of radial displacement for 0-degree orientations for VBP 40% vs. along the tunnel boundary.....	70
Figure 5.21 The figure of radial displacement for 45-degree orientations for VBP 40% vs. along the tunnel boundary.....	71
Figure 5.22 The figure of radial displacement for 90-degree orientations for VBP 40% vs. along the tunnel boundary.....	72
Figure 5.23 The max and the minimum radial displacement along the tunnel boundary in condition of VBP 25%.....	74
Figure 5.24 The max and the minimum radial displacement along the tunnel boundary in condition of VBP 40%.....	74
Figure 5.25 The max and the minimum radial displacement along the tunnel boundary in condition of VBP 40% and 25% .....	75
Figure 5.26 The values of displacement at crown orientations for VBP 40% and 25% .....	83
Figure 5.27 The values of displacement at left sidewall orientations for VBP 40%,55%,70% and 25%.....	84
Figure 5.28 The values of displacement at right sidewall orientations for VBP 40% and 25% .....	85
Figure 5.29 The plastic zone at VBP 25% .....	86
Figure 5.30 The plastic zone at VBP 40%.....	86
Figure 5.31 The comparison of plastic zone in 90-degree orientation .....	87
Figure 5.32 The comparison of plastic zone in 0-degree orientation .....	88

**Table index:**

Table 4.1 Input parameters for the matrix and blocks (Napoli et al., 2021) .....	35
Table 4.2 The initial state of stress .....	37
Table 5.1 The values of radial displacement of matrix for VBP 0% vs. internal pressure .....	43
Table 5.2 The values of radial displacement for 0-degree orientations for VBP 25% vs. internal pressure .....	45
Table 5.3 The values of radial displacement for 45-degree orientations for VBP 25% vs. internal pressure .....	46
Table 5.4 The values of radial displacement for 90-degree orientations for VBP 25% vs. internal pressure .....	47
Table 5.5 The values of max radial displacement for 0-45-90-degree orientations for VBP 25% vs. internal pressure .....	48
Table 5.6 The values of radial displacement for 0-degree orientations for VBP 40% vs. internal pressure .....	50
Table 5.7 The values of radial displacement for 45-degree orientations for VBP 40% vs. internal pressure .....	52
Table 5.8 The values of radial displacement for 90-degree orientations for VBP 40% vs. internal pressure .....	54
Table 5.9 The values of max radial displacement for 0-45-90-degree orientations for VBP 40% vs. internal pressure .....	56
Table 5.10 The values of radial displacement at right sidewall for 0-degree orientations for VBP 40% and 25% .....	77
Table 5.11 The values of radial displacement at right sidewall for 45-degree orientations for VBP 40% and 25% .....	77
Table 5.12 The values of radial displacement at right sidewall for 90-degree orientations for VBP 40% and 25% .....	78
Table 5.13 The values of radial displacement at crown for 0-degree orientations for VBP 40% and 25% .....	79
Table 5.14 The values of radial displacement at crown for 45-degree orientations for VBP 40% and 25% .....	80
Table 5.15 The values of radial displacement at crown sidewall for 90-degree orientations for VBP 40% and 25% .....	80
Table 5.16 The values of radial displacement at left sidewall for 0-degree orientations for VBP 40% and 25% .....	81
Table 5.17 The values of radial displacement at left sidewall for 45-degree orientations for VBP 40% and 25% .....	82
Table 5.18 The values of radial displacement at left sidewall for 90-degree orientations for VBP 40% and 25% .....	82

# 1 Introduction

Underground construction frequently involves geological materials whose mechanical behaviour cannot be described in a simple or uniform manner. The ground is often composed of constituents with markedly different properties, whose interaction governs the overall response of the rock mass. Among these materials, block-in-matrix rocks (bimrocks) represent a particularly complex class of geological formations. Bimrocks consist of competent rock blocks embedded within a weaker, fine-grained matrix, and their internal structure is characterized by strong heterogeneity.

The blocks within bimrocks vary widely in size and are irregularly distributed in space, leading to highly variable mechanical behaviour. Due to this heterogeneity, bimrocks do not respond in the same way as conventional soils or rock masses, and their behaviour cannot be reliably predicted using standard soil or rock mechanics approaches. The interaction between blocks and matrix, together with their spatial arrangement, results in significant variability in stiffness, strength, and deformation patterns.

Tunnel excavation in bimrock formations further amplifies this complexity. Variations in block content, size, and orientation may locally increase stiffness or, conversely, promote deformation in matrix-dominated zones. These local differences strongly influence stress redistribution around the excavation, the extent of plastic zones, and the magnitude of tunnel convergence. Therefore, traditional tunnel design methods based on homogeneous ground assumptions may be inadequate when applied to bimrock formations, requiring more advanced modelling strategies.

The objective of this thesis is to investigate the influence of bimrock heterogeneity on ground response during the excavation of a circular tunnel. To achieve this, a numerical approach is adopted in which the geometry and spatial distribution of rock blocks are generated using a stochastic procedure. This allows the analysis of multiple realistic configurations characterized by different volumetric block proportions and block orientations. For each configuration, finite element analyses are performed, and the results are compared with a reference model consisting solely of the matrix material.

The analyses focus on stress redistribution, tunnel convergence, displacement evolution, and the development of plastic zones within the bimrock mass. By explicitly accounting for block–matrix interaction and material variability, this study aims to provide a clearer understanding of tunnel behaviour in heterogeneous geological conditions. The results contribute to a more reliable interpretation of the mechanical behaviour of bimrocks when subjected to excavation processes.

## 2 General Background on Complex Geological Formations

Complex geological formations are characterized by a highly heterogeneous and irregular internal structure. They are generally composed of competent rock fragments embedded within a weaker matrix, arranged in a chaotic and spatially variable manner (Raymond, 1984; Festa et al., 2010). They typically form through long and complex geological processes, such as tectonic deformation, faulting, gravitational movements, and the mechanical mixing of materials with different origins and properties (Cowan, 1985). As a result of these processes, such formations cannot be treated as conventional soils or rock masses.

From an engineering perspective, this heterogeneity represents a significant challenge. The mechanical behaviour of complex geological formations cannot be adequately described using classical assumptions based on material homogeneity (Lindquist & Goodman, 1994). Stress redistribution, deformation patterns, and failure mechanisms depend strongly on the interaction between the rock blocks and the surrounding matrix, as well as on their spatial arrangement (Medley, 1994; Medley, 2001). Consequently, zones located very close to one another may exhibit markedly different mechanical responses under similar loading conditions.

A key aspect contributing to the complexity of these formations is the geometry of the rock blocks. Block size, shape, and orientation play an important role in governing the overall mechanical response (Medley, 1994). Large blocks may locally increase stiffness and alter stress paths, while matrix-dominated zones tend to deform more easily and may experience plasticization. In addition, elongated or preferentially oriented blocks can influence the direction in which deformation develops. For this reason, the stress state and displacement field around underground excavations depend not only on the volumetric proportion of blocks, but also on their individual geometrical characteristics (Lindquist & Goodman, 1994).

Several geological units can be classified as complex formations, including tectonic mélanges, fault breccias, chaotic sedimentary deposits, and mass-wasting materials (Raymond, 1984; Festa et al., 2010). Although these units originate in different geological environments, they share a common structural feature: the coexistence of mechanically competent rock blocks and a weaker surrounding matrix, arranged in an irregular and often unpredictable manner. Block sizes may range from a few centimetres to several metres, and their spatial distribution can vary significantly over short distances (Medley, 2001). In Italy, such formations are widely represented by tectonically disturbed units within the Apennine chain (Festa et al., 2010).

To support engineering interpretation, several descriptive and classification approaches have been proposed in the literature to identify and describe complex geological formations. However, these methods are generally based on qualitative criteria and are mainly intended for geological characterization rather than mechanical analysis. As a result, they provide limited guidance for defining the mechanical

parameters required for numerical modelling. Detailed geological investigations, including field mapping, core logging, and photographic documentation, are therefore essential to identify block size distributions, matrix properties, and the internal structure of the formation (A.G.I., 1979; Medley, 1994).

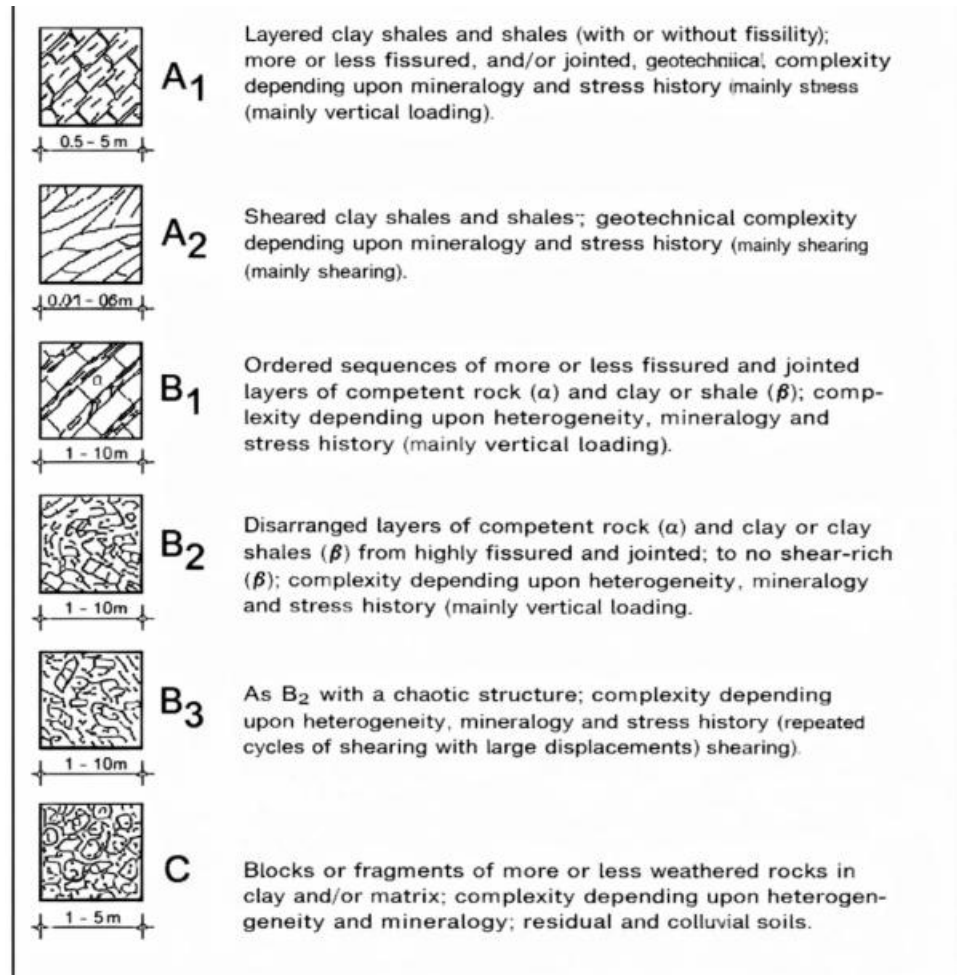


Figure 2.1 Summarizes the main criteria adopted by the Associazione Geotecnica Italiana (A.G.I., 1979) for the identification of complex geological formations.

Figure 2.1 summarizes the main criteria adopted for the identification of complex geological formations, according to the classification proposed by the Associazione Geotecnica Italiana (A.G.I., 1979). The classification distinguishes between:

- (A) stratified clay shales, with or without shear planes.
- (B) internally stratified weak and competent rocks characterized by geometrically chaotic structures or disordered class B sequences.
- (C) chaotic block-in-matrix mixtures consisting of rock fragments embedded within a clayey matrix (Manfredini et al., 1985; D'Elia et al., 1986).

Although the A.G.I. classification provides a useful geological framework, its descriptive nature does not directly address the mechanical implications of block–matrix interaction. For engineering applications, additional interpretation is therefore required to translate geological observations into parameters suitable for numerical modelling. (Figure 2.2)

Within this broader context, the present thesis investigates the mechanical response of tunnels excavated in heterogeneous block-in-matrix formations through numerical modelling, with particular emphasis on the influence of volumetric block proportion and block configuration.



*Figure 2.2 Example of a structurally complex turbiditic succession, characterized by alternating sandstone and shale layers, representative of class B1 according to the A.G.I. (1979) classification*

This classification is based on the internal structure and degree of disorder of the formations and distinguishes between stratified rocks, disarranged layered systems, and chaotic block-in-matrix assemblages. Although mainly descriptive, it provides a useful reference for recognizing geological conditions in which strong heterogeneity and block–matrix interaction is expected (Festa et al., 2010).

In recent decades, the expansion of infrastructure in geologically complex terrains has significantly increased engineering interest in block-in-matrix formations. The limitations of traditional design approaches, which often rely on equivalent homogeneous assumptions, have encouraged the development of numerical and stochastic methods capable of explicitly accounting for geological variability and block–matrix interaction (Medley, 1994; Carranza-Torres & Fairhurst, 2000). In this context, recent research has further emphasized the importance of incorporating heterogeneity into mechanical analyses. For instance, Napoli et al. (2018) demonstrated, through stochastic numerical simulations, that the mechanical response of bimrocks cannot be reliably represented using simplified homogeneous models, particularly when block proportion and spatial variability strongly influence deformation mechanisms.

These findings reinforce the need for modelling strategies that explicitly represent geometric variability and material contrast within complex geological formations. Within this broader framework, the present thesis investigates the mechanical response of tunnels excavated in heterogeneous block-in-matrix formations through numerical modelling, with particular emphasis on the influence of volumetric block proportion and block configuration on deformation patterns and stability conditions.

## 2.1 Complex Formations and Mélanges

Complex geological formations are characterized by pronounced heterogeneity across multiple spatial scales, resulting from the combined effects of tectonic deformation, sedimentary processes, and gravitational reworking (Raymond, 1984; Festa et al., 2010). Unlike well-stratified soil or rock units, these formations generally lack a regular internal structure and are often marked by a chaotic arrangement of their constituents.

A common feature of complex formations is the coexistence of materials with markedly different mechanical properties within the same geological unit (Lindquist & Goodman, 1994). Competent rock elements may be embedded within weak, fine-grained, and highly deformable materials. Therefore, their mechanical behaviour cannot be adequately described using a single set of representative parameters, since the response depends strongly on the spatial distribution of the different components and on the scale of observation (Medley, 1994).

Among complex formations, *mélanges* represent one of the most extreme and representative cases. *Mélanges* are block-in-matrix geological formations composed of rock blocks with variable lithology, size, shape, and mechanical properties embedded within a continuous and mechanically weaker matrix (Medley, 2001). The matrix is often clayey, tectonically sheared, or highly fractured, while the distribution of blocks is irregular and chaotic. Block dimensions may range from a few centimetres to several metres, and the block-to-matrix proportion can vary significantly over short distances.



*Figure 2.3 Example of a *mélange* deposit characterized by a chaotic block-in-matrix structure (after Medley, 2001).*

From a genetic point of view, mélanges may originate from different geological processes. Many mélanges are associated with tectonic activity related to plate convergence and subduction, where intense deformation leads to the fragmentation and mixing of materials from different sources (Cowan, 1985). Other mélanges may form through sedimentary or mixed tectono-sedimentary mechanisms (Festa et al.,

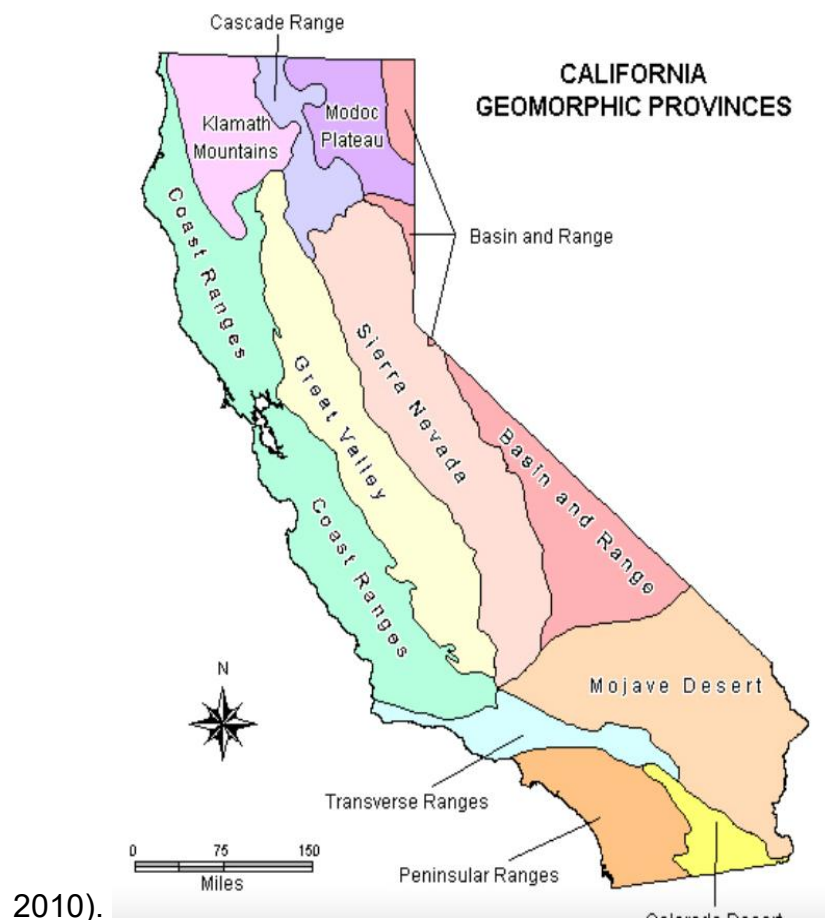


Figure 2.4 Geographical distribution of the Franciscan Complex in the San Francisco Bay Area (after Medley, 1994).

From an engineering standpoint, the mechanical behaviour of *mélanges* is strongly scale dependent (Medley, 1994) (Figure 2.5). Laboratory-scale tests often fail to capture the true response of these materials at the scale relevant to engineering works. For low to moderate block contents, deformation and plasticization tend to localize within the matrix, while blocks mainly contribute to stress redistribution and local stiffening effects (Lindquist & Goodman, 1994).

Due to their heterogeneity and chaotic structure, *mélanges* pose serious challenges to conventional geotechnical investigation and design approaches. Classical rock mass classification systems, such as RMR or Q, are generally based on assumptions of homogeneity and regular discontinuity patterns and may therefore provide unreliable results when applied to *mélanges* (Medley, 2001).

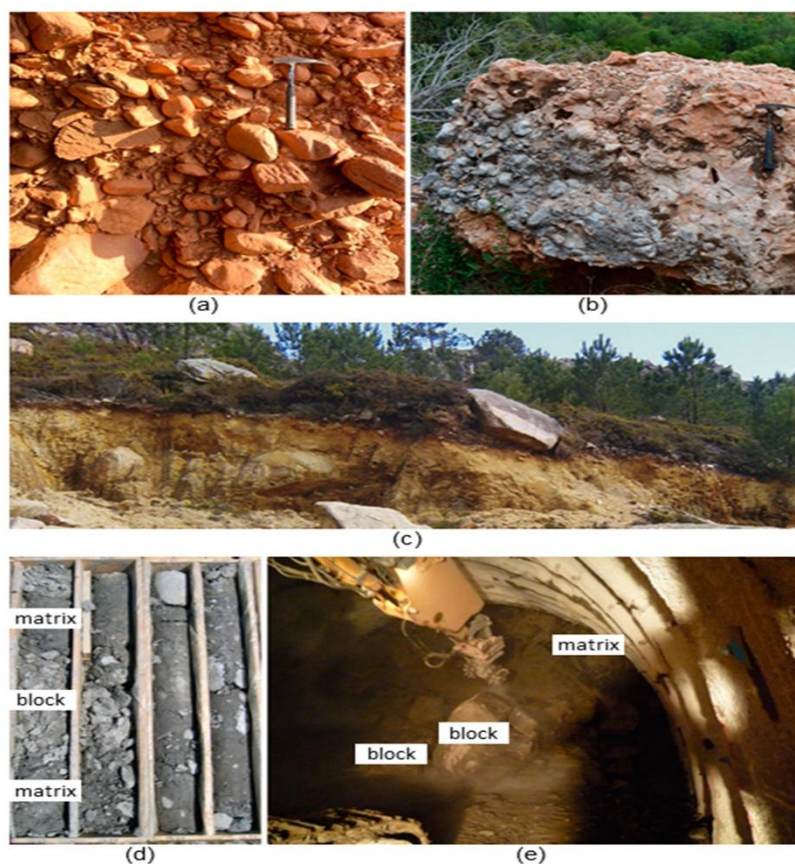


Figure 2.5 Examples of block-in-matrix geological formations at different scales according to Edmund Medley (1994)

### **2.1.1 Knowledge Aspects and Possible Genesis of Mélanges**

The term *mélange* was first introduced by Greenly (1919) based on geological observations carried out in Wales, where chaotic rock assemblages were identified within a schistose matrix. Early studies interpreted the origin of *mélanges* as the result of intense shearing mechanisms acting within tectonically active zones. Subsequent investigations expanded this interpretation, suggesting that *mélanges* could not be explained by a single genetic mechanism and that their formation may involve different geological processes operating at various spatial and temporal scales (Raymond, 1984; Festa et al., 2010).

Several authors have highlighted the limitations of purely descriptive definitions of *mélanges* when applied to engineering problems (Medley, 1994). From a structural point of view, *mélanges* are characterized by the absence of internal continuity and by the inclusion of lithologically diverse rock blocks within a weak and highly deformable matrix (Lindquist & Goodman, 1994).

Different genetic models have been proposed to explain the formation of *mélanges*. In many cases, *mélanges* are associated with convergent tectonic settings and subduction zones, where intense deformation, fragmentation, and material mixing occur (Cowan, 1985). Other *mélanges* may originate from sedimentary processes or from a combination of sedimentary and tectonic mechanisms (Festa et al., 2010).

The engineering significance of these formations lies in their mechanical complexity. The strong contrast between competent blocks and weak matrix materials results in non-uniform stress distribution and highly localized deformation mechanisms (Medley, 2001). Well-known examples include the Franciscan Complex of California, extensively studied as a reference case for understanding *mélange* behaviour (Medley, 1994).

## 2.2 From Mélanges to Bimrocks: Engineering Interpretation of Block-in-Matrix Materials

Although mélanges are primarily defined from a geological perspective, engineering analysis requires a framework that explicitly accounts for mechanical behaviour and scale effects. This need led to the development of the bimrock (block-in-matrix rock) concept.

While geological classifications focus mainly on origin and structural characteristics, the bimrock concept emphasizes mechanical behaviour and the interaction between competent rock blocks and a weaker surrounding matrix (Medley, 1994; Medley, 2001). This shift in perspective enables complex formations to be interpreted in terms that are directly relevant to engineering analysis and numerical modelling.

It is important to recognize that mélanges and bimrocks are related but not identical concepts. Mélanges are defined based on geological processes and structural features, whereas bimrocks are characterized according to their mechanical response at the scale of interest. A geological mélange may behave as a bimrock when the mechanical contrast between blocks and matrix becomes significant for excavation stability. Conversely, bimrock conditions may also arise in formations that are not strictly tectonic mélanges, such as mass-transport deposits or chaotic sedimentary units (Raymond, 1984; Festa et al., 2010).

One of the key aspects distinguishing bimrocks from conventional rock masses is the strong influence of scale. Medley (1994) emphasized that the mechanical behaviour of block-in-matrix materials depends largely on the relative size of the blocks with respect to the characteristic dimension of the engineering problem. When blocks are small relative to the excavation size, the material may respond similarly to a heterogeneous soil or weak rock mass. As block size increases, stiffness contrasts become more pronounced, and stress redistribution mechanisms begin to govern the deformation pattern.

Within this framework, the volumetric block proportion (VBP) plays a fundamental role. Low VBP values typically correspond to matrix-dominated behaviour, where deformation concentrates within the weaker material. As the proportion of blocks increases, block–matrix interaction becomes more significant and may lead to increased overall stiffness and more complex failure mechanisms (Lindquist & Goodman, 1994; Medley, 2001). At intermediate VBP ranges, the mechanical response becomes particularly sensitive to block geometry and spatial distribution, rendering simplified homogeneous assumptions unreliable.

Another important implication of bimrock behaviour concerns the concept of representative elementary volume (REV). In relatively homogeneous rock masses, it is often possible to define an equivalent material characterized by averaged mechanical parameters. In bimrocks, however, the irregular distribution and wide size variability of blocks may prevent the identification of a representative volume, especially when block dimensions approach the tunnel diameter (Medley, 1994). The absence of clear scale separation therefore justifies the adoption of explicit numerical modelling strategies.

From a tunnelling perspective, bimrock conditions may significantly influence excavation response. Competent blocks can locally restrain deformation and alter stress trajectories, whereas the surrounding matrix may undergo progressive yielding and plasticization. The coexistence of these behaviours frequently produces non-uniform displacement patterns and complex plastic zone development around the tunnel boundary. Consequently, engineering analyses must account not only for material properties but also for geometric factors such as block size, orientation, and spatial arrangement.

The increasing recognition of bimrocks in underground construction has encouraged the development of modelling strategies that explicitly incorporate block geometry. Rather than representing the ground as an equivalent homogeneous medium, these approaches aim to reproduce the heterogeneous structure observed in the field, enabling a more realistic assessment of deformation and stability during excavation (Carranza-Torres & Fairhurst, 2000). Within this framework, the present thesis investigates the influence of volumetric block proportion and block configuration on tunnel behaviour through numerical simulations.

By introducing the bimrock concept as an engineering interpretation of complex geological formations, this section establishes the conceptual bridge between the geological background discussed earlier and the numerical modelling approach adopted in the following chapters. The focus shifts from genetic description toward mechanical representation, highlighting the fundamental role of geometry, scale effects, and block–matrix interaction in underground excavation analysis.

### **2.2.1 Engineering Challenges in Tunnelling Through Bimrocks**

The excavation of tunnels in block-in-matrix formations presents significant challenges that differ from those encountered in more homogeneous rock masses. The coexistence of mechanically competent blocks and a weaker matrix led to a highly variable mechanical response, where deformation and stress redistribution are strongly influenced by local geometry and material contrast (Medley, 1994; Lindquist & Goodman, 1994). As a result, conventional design assumptions based on equivalent homogeneous media may not adequately capture the behaviour of these formations.

One of the main difficulties in tunnelling through bimrocks is the presence of pronounced spatial variability. Even within short excavation lengths, the distribution and orientation of blocks may change considerably, producing localized variations in stiffness and strength. These variations can lead to asymmetric displacement patterns, irregular development of plastic zones, and unpredictable excavation performance. In matrix-dominated areas, deformation may evolve gradually, while in block-rich zones the ground may behave in a stiffer and more brittle manner.

Another critical aspect concerns the scale dependency of mechanical behaviour. When the size of blocks becomes comparable to the tunnel diameter, the excavation process may no longer be represented using simplified continuum assumptions. Individual blocks can alter stress trajectories and locally modify the interaction between the ground and the support system. This effect is particularly relevant during the early stages of excavation, when stress redistribution occurs around the advancing face and deformation begins to develop (Hoek & Brown, 1980; Carranza-Torres & Fairhurst, 2000).

From a practical engineering perspective, the characterization of bimrocks also poses challenges during site investigation. Standard laboratory tests may provide information primarily about the matrix or isolated blocks but rarely capture the combined mechanical behaviour of the heterogeneous system. Borehole observations and geological mapping may reveal strong variability in block size and distribution, making it difficult to define representative mechanical parameters. Consequently, design approaches based solely on averaged properties may lead to significant uncertainties.

The interaction between excavation and support installation represents another important factor. In bimrock conditions, support response may vary depending on local block configuration and matrix behaviour. Blocks may provide temporary stability by bridging the excavation boundary, while matrix-dominated regions may experience progressive yielding and require more effective confinement. This complex interaction highlights the need for analysis methods capable of representing the progressive evolution of deformation during excavation.

Given these challenges, numerical modelling has become an essential tool for investigating tunnel behaviour in bimrock formations. Advanced modelling approaches allow the explicit representation of block geometry and enable the evaluation of stress

redistribution, displacement development, and plastic zone formation under different conditions. By incorporating geometrical variability into the analysis, numerical simulations can provide insights that are difficult to obtain through analytical methods alone (Carranza-Torres & Fairhurst, 2000).

Within this framework, the present thesis investigates how variations in volumetric block proportion and block configuration influence the mechanical response of tunnels excavated in bimrock materials. The modelling strategy adopted in the following chapters aims to capture the interaction between blocks and matrix, providing a deeper understanding of deformation mechanisms and stability conditions associated with heterogeneous ground.

These limitations highlight the need for numerical approaches capable of explicitly representing geometric variability and block–matrix interaction, which forms the basis of the modelling strategy adopted in this thesis.

## 3 Bimrocks

### 3.1 Definition and Engineering Meaning of Bimrocks

The terminology used to describe block-in-matrix materials has evolved primarily to address the limitations of classical geological and geotechnical classifications when applied to highly heterogeneous rock masses. An early engineering-oriented description was introduced by Raymond (1984), who referred to these materials as *structurally complex rock masses*. Subsequently, Medley (1994) formally introduced the term *bimrock* (block-in-matrix rock) to describe geological formations such as *mélanges* and *olistostromes* from a geotechnical perspective.

Bimrocks are defined as heterogeneous rock masses composed of competent rock blocks embedded within a weaker and continuous matrix. From an engineering standpoint, the geological origin of the formation is not the primary focus; rather, the material is characterized based on the mechanical contrast between blocks and matrix and on their spatial interaction. In general, bimrocks consist of a mixture of stiff rock clasts surrounded by a matrix with significantly lower mechanical properties, leading to a highly non-uniform mechanical response.

A defining characteristic of bimrocks is their strong scale dependency. At laboratory scale, a bimrock specimen may appear relatively homogeneous if the size of the blocks is small compared to the sample dimensions. However, at the scale of engineering works such as tunnels or underground excavations, the same material may exhibit highly irregular behaviour. In these conditions, individual blocks can locally control stress redistribution, deformation patterns, and failure mechanisms, resulting in asymmetric convergence and localized plasticization.

For engineering purposes, it is therefore essential to distinguish between blocks that are mechanically significant and those that can be considered part of the matrix. Medley (1994, 2001) proposed the concept of a block–matrix threshold, defined through a characteristic engineering dimension of the problem under consideration. Blocks with dimensions smaller than a fraction of this characteristic length can be treated as matrix material, whereas larger blocks must be explicitly considered as discrete inclusions. This threshold depends on the scale of the engineering problem and highlights the importance of block size relative to excavation dimensions.

In addition to block size, other geometrical parameters such as block shape, orientation, and spatial distribution influence the mechanical behaviour of bimrocks. As the volumetric proportion of blocks increases, the overall stiffness of the rock mass generally increases, while deformation tends to decrease.

Due to these characteristics, bimrocks pose significant challenges to conventional geotechnical characterization and design approaches. Classical rock mass classification systems and simplified equivalent-continuum models are typically based on assumptions of homogeneity and continuity that are not valid for block-in-matrix

materials. When applied to bimrocks, such approaches may lead to overly conservative or misleading predictions, especially in tunnelling applications. For this reason, engineering analyses of bimrocks often require dedicated modelling strategies that explicitly account for block–matrix interaction and scale effects.

### 3.1.1.1 Identification and recognition of Bimrocks

As previously discussed, neglecting the presence of block-in-matrix rocks (bimrocks) within a rock mass represents a common yet potentially critical source of error in engineering design. Because heterogeneous formations of this type are widely distributed worldwide, their correct identification and classification during the preliminary investigation phase are essential (Medley, 1994; Napoli et al., 2021). An incomplete understanding of the geological structure during site characterization may lead to inaccurate predictions of global behaviour and, consequently, to inaccurate predictions of deformation and stability during excavation (Napoli et al., 2021).

For this reason, the classification of bimrocks should rely on systematic observational approaches derived from geological studies of complex formations (Medley, 1994). These approaches rely on the recognition of geomorphological and geological indicators reflecting the origin, internal structure, and spatial variability of the rock mass. In heterogeneous rock masses, the distribution of competent blocks within a weaker matrix and the mechanical contrast between these components strongly influence the overall response of the formation, particularly in tunnelling applications (Napoli et al., 2021).

The correct identification of a bimrock typically requires a detailed geological assessment carried out by experienced geologists through field surveys and geological mapping. Mélange-type formations often exhibit irregular or undulating topography, where resistant rock blocks emerge from a more erodible matrix. This geomorphological expression reflects the intrinsic heterogeneity of the deposit and the different weathering resistance between blocks and matrix materials (Medley, 1994). However, irregular morphology alone cannot be considered sufficient to uniquely identify a bimrock, since similar features may also occur in stratified clayey deposits or alternating lithological sequences.

In many cases, the matrix of bimrocks is predominantly clay-rich and may display a scaly or foliated fabric associated with shear deformation processes. These structural features can develop preferential orientations that significantly influence the mechanical behaviour of the rock mass. The presence of such anisotropy becomes particularly relevant in underground excavations, where stress redistribution interacts with the heterogeneous fabric of the formation (Napoli et al., 2021).

Bimrocks are frequently highly erodible and may be easily reshaped by surface processes. On slopes, they often appear as poorly vegetated areas and are commonly associated with shallow landslides or surface instabilities. These geomorphological characteristics provide indirect but meaningful indicators of mechanically weak and heterogeneous materials (Medley, 1994).

Field investigations may reveal the coexistence of blocks with different lithologies within the same formation, such as limestone blocks embedded in arenaceous or clayey matrices or isolated serpentinite inclusions within weaker surrounding materials. However, the presence of specific lithologies alone is not sufficient to define a bimrock. What characterizes these formations is the mechanical contrast between blocks and matrix, as well as their spatial distribution within the rock mass (Napoli et al., 2021).

A particularly important distinction must be made between bimrocks and colluvial deposits. Surface processes may erode and rework complex formations, producing materials that resemble colluvium in appearance. Nevertheless, colluvial deposits are typically characterized by discontinuous or randomly oriented fabrics, whereas bimrocks often preserve a more persistent internal structure, such as a continuous foliation within the matrix. This structural continuity represents a key criterion for distinguishing block-in-matrix rocks from superficial deposits (Medley, 1994).

These considerations highlight that the recognition of bimrocks cannot rely solely on laboratory testing or limited sampling, since such approaches may fail to capture the internal variability of the formation. Instead, a comprehensive observational strategy is required, integrating field mapping, outcrop analysis, and careful interpretation of lithological and structural features. Only through such an integrated investigation can a reliable identification of bimrocks be achieved, enabling a more appropriate interaction between the geological material and the engineered structure (Napoli et al., 2021).

### **3.1.2 Morphological features of Bimrocks and site investigation**

The morphology of the study area represents one of the first and most valuable sources of information for recognizing the presence of bimrocks during the early stages of site investigation. Surface observations often reveal rock blocks emerging from a softer surrounding material, creating irregular slopes, localized relief contrasts, or blocky ridges that reflect the heterogeneous nature of the formation. These geomorphological expressions are commonly linked to differential weathering processes, where more competent blocks resist erosion while the weaker matrix progressively degrades (Medley, 1994).

Vegetation patterns may also provide useful, although indirect, clues. Areas where large blocks are exposed can locally support trees or sparse vegetation due to their higher mechanical stability, whereas the surrounding matrix is frequently covered by grass or low shrubs. While vegetation alone cannot be considered a diagnostic indicator, it becomes meaningful when interpreted together with geological mapping and field observations (Medley, 1994).

After identifying a potential bimrock within the investigation area, a preliminary evaluation of the intrinsic characteristics of both blocks and matrix is required. This stage typically involves assessing lithology, degree of fracturing, and structural continuity. Highly fractured blocks may lose part of their mechanical competence and begin to behave similarly to the surrounding matrix. In such cases, the mechanical contrast that defines bimrocks becomes less pronounced, highlighting the importance of considering both geological and mechanical aspects simultaneously (Napoli et al., 2021).

The investigation of bimrocks rarely relies on a single method and instead requires the integration of surface observations with subsurface exploration. Geotechnical drilling remains one of the most common tools for identifying block-in-matrix structures at depth, as core samples allow direct observation of lithological variability, block occurrence, and matrix characteristics along the borehole (Medley, 1994). However, drilling in heterogeneous formations presents specific challenges. Because of the strong mechanical contrast between blocks and matrix, the drilling process may disturb or wash out weaker materials while leaving competent blocks relatively intact. As a result, recovered cores may not always represent the in-situ structure accurately, particularly when block dimensions approach or exceed the borehole diameter (Medley, 1994; Sonmez and Tuncay, 2008).

Directional drilling techniques may provide additional insight by revealing the orientation of blocks and foliations within the matrix, which becomes especially relevant when anisotropy is expected to influence mechanical behaviour. This information is particularly valuable in underground excavations, where stress redistribution interacts with the heterogeneous fabric of the rock mass (Napoli et al., 2021). Nevertheless, drilling data should always be interpreted together with surface

mapping and geological reasoning, since isolated boreholes cannot fully capture the spatial variability typical of bimrocks.

Sampling for laboratory testing also requires careful consideration. Standard procedures may produce misleading results if samples are obtained predominantly from either the matrix or isolated blocks. In many cases, double or triple coring is necessary to obtain representative material for laboratory characterization. Even so, laboratory tests generally describe local properties and must be interpreted cautiously when extrapolated to engineering-scale behaviour (Napoli et al., 2021).

Overall, these aspects highlight the importance of adopting an integrated investigation strategy when dealing with bimrocks. A combination of detailed field mapping, geomorphological interpretation, drilling data, and engineering judgement is essential for understanding the internal structure of the material and for defining realistic mechanical parameters that can support reliable design decisions (Medley, 1994; Napoli et al., 2021).

### 3.2 Definition of geometrical configuration

The study of the mechanical behaviour of complex block-in-matrix formations requires a geometric representation that is consistent with both geological observations and engineering modelling needs. In bimrocks, the global response of the rock mass is strongly influenced by the presence of competent blocks embedded within a weaker matrix, as well as by their size, shape, spatial distribution, and volumetric proportion (Medley, 1994; Napoli et al., 2021). For this reason, the definition of geometry represents a fundamental step linking geological interpretation to numerical analysis.

From a modelling perspective, it is often insufficient to describe the material using only equivalent mechanical properties of the matrix. When block dimensions become comparable to the characteristic size of the engineering problem, such as tunnel diameter or excavation height, the explicit representation of blocks becomes necessary. Under these conditions, blocks may significantly influence stress redistribution, deformation localization, and failure mechanisms around underground excavations (Napoli et al., 2021).

A key aspect of geometric characterization concerns the definition of block size. Since blocks are inherently three-dimensional objects, their real dimensions can only be fully described in a three-dimensional domain. However, direct measurement of 3D geometry in situ is rarely feasible, and block dimensions are commonly inferred from two-dimensional observations such as outcrops, excavation faces, or core samples obtained during geotechnical drilling (Medley, 1994). As discussed in previous research carried out within the PoliTo framework, block geometry must often be interpreted through engineering-scale considerations rather than through purely geological measurements (Dadone, 2018).

One widely adopted parameter for describing block size is the chord length, defined as the apparent intersection length between a block and an observation line or surface. Chord-based measurements provide useful information but do not correspond directly to the true size of blocks. As a result, they tend to underestimate maximum block dimensions and may introduce bias in the interpretation of size distributions if not properly corrected (Medley, 1994).

The distinction between one-dimensional, two-dimensional, and three-dimensional block size distributions is particularly relevant in bimrocks. While 1D and 2D observations are more accessible in engineering practice, they may not fully represent the actual volumetric contribution of blocks within the rock mass. This discrepancy becomes critical when estimating the Volumetric Block Proportion (VBP), since inaccurate size characterization may lead to significant errors in the evaluation of block content and mechanical behaviour (Napoli et al., 2021).

Conceptual models illustrate how a block population characterized in three dimensions may appear substantially different when sampled through lower-dimensional observations. Large blocks, for example, may be only partially intersected or completely missed by boreholes or exposed surfaces, leading to an apparent reduction in both size and frequency. This effect becomes more pronounced when investigation orientations do not adequately intersect the dominant block geometry or when drilling length is limited (Dadone, 2018).

Despite these limitations, one-dimensional and two-dimensional data remain essential for engineering practice. When combined with geological interpretation, statistical correction procedures, and numerical simulations, they allow a reasonable reconstruction of the three-dimensional block distribution. Such an approach enables the development of representative geometrical models for numerical analysis while acknowledging the uncertainty inherent in block geometry (Napoli et al., 2021).

In this context, stereological methods provide a useful framework for relating measurements obtained in one or two dimensions to the actual three-dimensional geometry of the inclusions. These techniques support the estimation of block size distributions and volumetric proportions, facilitating the generation of numerical models that better reproduce the internal structure of bimrocks (Medley, 1994).

The statistical nature of block size distribution represents another important aspect of geometric characterization. Field observations and drilling data show that block dimensions may vary across several orders of magnitude, from small fragments to blocks comparable in size to the excavation itself. Consequently, the use of a single representative block size is generally inadequate, and cumulative distribution curves are often employed to describe the variability of block populations (Dadone, 2018).

Experimental and numerical studies have demonstrated that block size distribution strongly influences the mechanical response of bimrocks. When block dimensions are large relative to the engineering scale, they contribute significantly to stress redistribution and may limit deformation. Conversely, when blocks are small compared to the excavation size, their influence tends to be averaged within the matrix behaviour, allowing the use of equivalent continuum approaches (Napoli et al., 2021).

For engineering applications, it is therefore essential to define block dimensions relative to a characteristic engineering length. Rather than reproducing exact field geometries, simplified yet representative synthetic block distributions are often generated to reproduce key statistical features such as volumetric proportion, size range, and spatial variability. This strategy allows the main mechanical effects of block–matrix interaction to be captured while maintaining computational efficiency.

Overall, the correct interpretation of block size distributions and their geometric representation play a central role in bimrock analysis. Errors introduced during this stage may propagate throughout the modelling process, leading to unrealistic deformation patterns, inaccurate stress predictions, and unsafe design assumptions. For this reason, geometric characterization represents a critical step that connects geological observation with reliable engineering analysis (Medley, 1994; Napoli et al., 2021; Dadone, 2018).

An additional aspect that must be considered in the geometric characterization of bimrocks is the relationship between block size and the scale of the engineering problem. A block can only be considered mechanically significant if its dimensions are comparable to the characteristic size of the excavation or structure under analysis. Blocks that are small relative to this characteristic dimension may be present in large numbers, but their influence on the global mechanical behaviour of the rock mass tends to be limited (Medley, 1994; Lindquist & Goodman, 1994)

Conceptual models illustrate that blocks with dimensions below a certain threshold cannot be reliably identified as individual rock elements from an engineering standpoint. In such cases, these blocks effectively behave as part of the matrix, and their mechanical contribution is implicitly included in the equivalent properties assigned to the matrix material. This consideration is particularly relevant for tunnel excavation at small to moderate diameters, where only blocks exceeding a minimum characteristic size may influence stress redistribution and deformation patterns.

Studies on bimrocks indicate that the identification of a block–matrix threshold size is essential for distinguishing between mechanically active blocks and matrix material (Medley, 1994). This threshold depends on the characteristic engineering length, such as tunnel diameter or excavation height, and is therefore not an intrinsic property of the rock mass but a scale-dependent parameter. As excavation dimensions increase, blocks previously considered insignificant may become mechanically relevant.

Block size distributions derived from cumulative frequency curves further highlight this scale effect. Even in bimrocks characterized by a relatively high volumetric block proportion, a large fraction of the total block population may consist of small fragments that contribute minimally to global behaviour. Conversely, a small number of large blocks may account for a significant portion of the total block volume and dominate the mechanical response of the system.

This observation explains why bimrocks with similar volumetric block proportions may exhibit markedly different behaviours depending on the size distribution of the blocks. Two formations with identical VBP values may respond differently to excavation if one contains a few large blocks and the other contains many small ones. For this reason, VBP alone is not sufficient to fully describe bimrock behaviour, and it must always be interpreted together with block size distribution and scale considerations. (Napoli et al., 2021; Lindquist & Goodman, 1994)

From an engineering modelling perspective, these concepts justify the use of simplified geometric representations in numerical analyses. Rather than reproducing the full spectrum of block sizes observed in the field, it is often more effective to explicitly model only those blocks that exceed the block–matrix threshold size, while incorporating smaller blocks into the matrix properties (Napoli et al., 2021). This approach allows the key mechanical effects of block–matrix interaction to be captured without excessive computational complexity.

In conclusion, the geometric characterization of bimrocks requires a careful balance between geological realism and engineering applicability. Proper identification of block size thresholds, combined with an understanding of scale effects and block size distributions, is fundamental for the development of reliable numerical models and for the correct interpretation of bimrock behaviour in underground excavations.

### 3.3 Volumetric Block Proportion (VBP)

The Volumetric Block Proportion (VBP) is defined as the ratio between the volume of competent rock blocks and the total volume of the rock mass (Medley, 1994; Lindquist & Goodman, 1994). It represents a key parameter for bimrock characterization, since it directly governs the heterogeneity of the material and strongly influences its mechanical behaviour (Medley, 1994; Napoli et al., 2021).

Previous studies have shown that for low to intermediate VBP values, the mechanical response of bimrocks is governed by a complex interaction between blocks and matrix (Medley, 1994; Lindquist & Goodman, 1994). For  $VBP \approx 25\%$ , behavior is largely matrix-dominated, with blocks acting mainly as stiff inclusions that locally modify the stress field. Plastic deformation tends to localize within the matrix, and tunnel convergence is primarily controlled by matrix strength and stiffness.

For  $VBP \approx 40\%$ , the influence of blocks becomes more pronounced. The increase in block content generally leads to higher overall stiffness and reduced average deformation (Lindquist & Goodman, 1994; Napoli et al., 2021). However, this stiffening effect is accompanied by increased spatial variability in displacement and convergence. Numerical studies indicate that intermediate VBP values often exhibit the largest scatter in mechanical response due to heterogeneous block–matrix interactions at tunnel scale (Napoli et al., 2021).

Focusing on VBP values of 25% and 40% allows investigation of a critical transition regime in which neither the matrix nor the blocks are fully dominant. This range is particularly relevant from an engineering perspective, as it represents conditions where simplified homogeneous assumptions are least reliable (Medley, 1994; Napoli et al., 2021). The selection of these VBP values therefore provides a meaningful basis for evaluating deformation mechanisms and for assessing the limitations of equivalent continuum modeling approaches. (Figure 3.1)

Complex geological formations include a wide range of materials whose internal structure is anything but uniform. These formations often develop through long and dynamic geological histories involving tectonic movements, fault activity, landslides, and the mixing of materials with very different origins. Because of this, they do not behave like typical soils or intact rock masses. Instead, they consist of strong rock fragments surrounded by a weaker matrix, arranged in a way that is irregular and highly variable from point to point.

For engineers, this heterogeneity creates major challenges. The mechanical behaviour of these formations cannot be captured using the common assumption of a single, homogeneous material. The way stresses distribute through the ground and the way deformation develops depend strongly on how the blocks and the surrounding matrix interact. Two locations that are very close to each other may respond completely differently simply because the local block distribution changes.

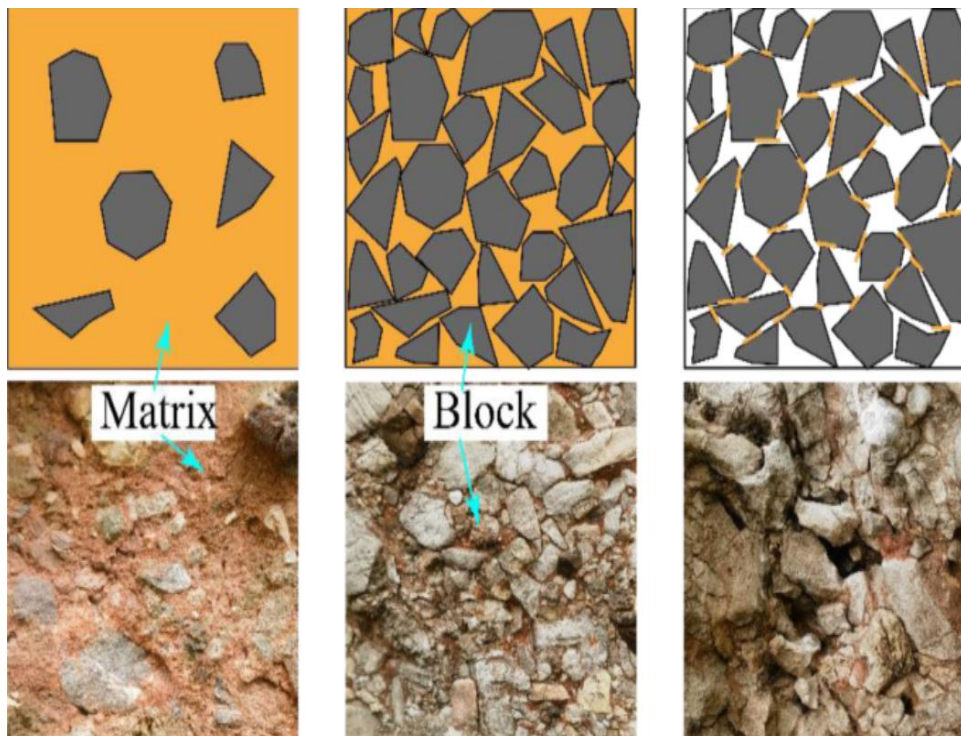


Figure 3.1 Illustrated different VBP% simulation

## 4 Methodology:

### 4.1 Numerical approach and software

By means of numerical modelling, this study investigates the mechanical behaviour of bimrock materials affected by the excavation of a tunnel, and to evaluate the influence of different volumetric block proportions (VBP) on their overall response. Due to variations in block configuration and orientation within the bimrock mass, the extent and distribution of plastic zones as well as the resulting displacement patterns differ significantly from one model to another. These differences highlight the strong dependency of bimrock mechanical behaviour on internal geometry rather than solely on material properties.

Numerical analysis is particularly suitable for the investigation of bimrock systems because of their inherent heterogeneity, characterized by the coexistence of stiff rock blocks embedded in a weaker soil matrix, and their complex stress–strain behaviour, which cannot be adequately captured using simplified analytical solutions.

All simulations were carried out using the finite element method (FEM) implemented in the software RS2, which enables accurate two-dimensional continuum modelling under plane strain conditions. The software provides reliable tools for the evaluation of stress and strain distributions, displacement fields, and the development of plastic deformation, allowing a detailed assessment of the mechanical response of bimrock to tunnel excavation.

### 4.2 Geometrical model

The numerical model represents a two-dimensional plane strain domain corresponding to a bimrock mass. To reduce the time requirement for each simulation, the overall geometry consists of a 100 m × 100 m square domain of homogeneous rock. Within this domain, a central 50 m × 50 m region is defined as the bimrock box, where the heterogeneous block–matrix system is generated. The external domain was introduced to reduce boundary effects and ensure that the excavation response is not influenced by artificial constraints at the model limits.

A circular tunnel with a diameter of 10 m is located within the bimrock region and represents the excavation of interest. This configuration allows the investigation of stress redistribution, displacement, and plastic zone development in the surrounding bimrock material due to tunnelling.

The geometry of the bimrock domain was generated through a stochastic procedure implemented in MATLAB. The resulting block configuration was subsequently exported to AutoCAD for geometric preparation and then imported into RS2 for numerical analysis.

Two different volumetric block proportions (VBP) were considered in this study:

- VBP = 25%
- VBP = 40%

For each VBP value, the size, shape, and spatial distribution of the rock blocks were kept constant to eliminate geometric bias. Only the volumetric proportion of the blocks was varied. To account for the influence of block arrangement and orientation, ten distinct block configurations were generated for each VBP. In addition, each configuration was analysed under three different orientation angles of the blocks, with respect to the horizontal direction ( $0^\circ$ ,  $45^\circ$ , and  $90^\circ$ ).

Blocks were randomly positioned inside the  $50\text{ m} \times 50\text{ m}$  domain while satisfying the prescribed volumetric block proportion within a tolerance of  $1/40$ . The inclusions were modelled as ellipses with an eccentricity equal to 0.5 and random orientation, providing a more realistic representation of natural block geometries compared to circular shapes.

The characteristic engineering dimension  $L_c$ , defined as the tunnel diameter, was set equal to 10 m. Block sizes varied between 5% and 75% of  $L_c$ , in accordance with the criteria proposed by Medley (2004). The size distribution followed a cumulative fractal-based law representative of Franciscan Mélange formations, adopting an approach analogous to that proposed by Barbero et al. (2006) and further applied in Napoli et al. (2018). Overlapping between inclusions was prevented to ensure geometric consistency of the generated configurations.

The resulting bimrock box therefore represents a statistically controlled heterogeneous system in which the spatial arrangement, orientation, and size distribution of blocks directly influence the mechanical response of the excavation. The overall model geometry and boundary conditions are illustrated in (Figure 4.1).

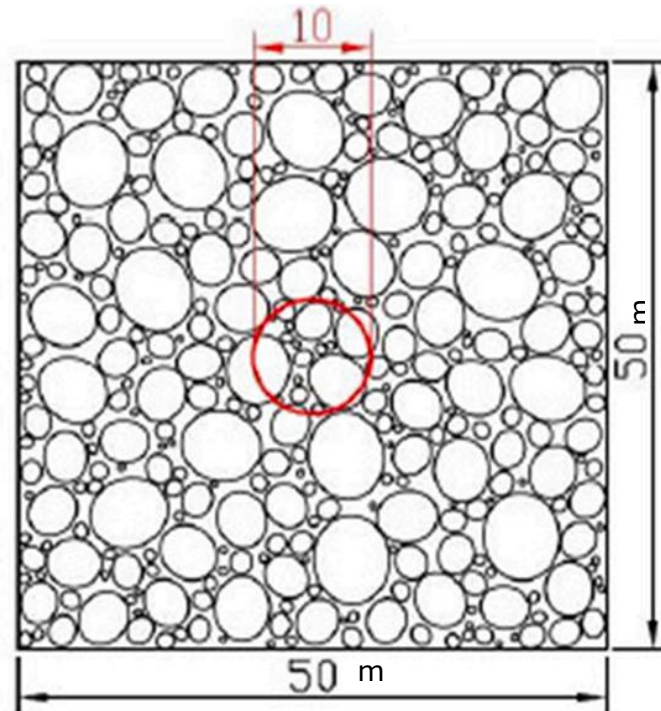


Figure 4.1 The geometry assumed in the RS2

### 4.3 Material properties

The bimrock material was modelled as a two-element system consisting of soil matrix and rock blocks, representing the heterogeneous nature of bimrock formations. Both components were assumed to follow an elastic–plastic constitutive behaviour governed by the Mohr–Coulomb failure criterion, which is commonly used to describe the shear strength of geomaterials.

To analyse the mechanical response of the bimrock mass as the excavation advances, the analyses were performed ten incremental loading stages, in which the internal pressure around the tunnel was gradually reduced up to 0% of the applied load.

In the first loading stage, both the soil matrix and the rock blocks were assumed to behave purely elastically to establish the initial stress–strain state. In the subsequent stages, plastic behaviour was observed exclusively within the bimrock region, where elastoplastic constitutive laws were assigned to the blocks and the surrounding matrix.

The in-situ stress condition was defined by assuming a coefficient of earth pressure at rest equal to  $K_0 = 1$ , implying that the major and minor principal stresses are equal ( $\sigma_1 = \sigma_3$ ).

Distinct mechanical properties were assigned to the soil matrix and the rock blocks, including Young's modulus, Poisson's ratio, cohesion, friction angle, and unit weight. The adopted parameters, reported in table 4.1, were selected based on values reported in the relevant literature to ensure realistic representation of the material behaviour. ( Napoli et al., 2021)

A perfect bonding condition was assumed at the interface between the soil matrix and the rock blocks. This implies that no relative sliding or separation occurs at the interface, ensuring full stress transfer between the two elements throughout the analysis.

Parameter	Matrix	Blocks
E[GPa]	0.04	40.7
$\nu$ [-]	0.3	0.3
$\gamma$ [Kn/m <sup>3</sup> ]	22	27
c[kPa]	65	11000
$\phi$ [°]	28	50

Table 4.1 Input parameters for the matrix and blocks (Napoli et al., 2021)

#### 4.4 Boundary conditions

Boundary conditions were applied to the numerical model to represent realistic in-situ constraints while simultaneously preventing rigid body motion of the domain. These conditions ensure numerical stability and allow a meaningful interpretation of stress redistribution and deformation.

The lateral boundaries of the model were constrained in the horizontal (x) direction, while remaining free in the vertical direction. This condition prevents horizontal displacement of the domain and simulates the confinement provided by the surrounding ground mass.

The upper and lower boundaries were constrained in the vertical (y) direction, while horizontal movement was allowed. This configuration permits lateral deformation while restricting vertical translation of the model.

At the corner nodes, displacements were restrained in both the horizontal and vertical directions to fully eliminate rigid body movement and ensure a stable numerical solution.

This combination of boundary conditions provides an appropriate balance between mechanical realism and computational stability, allowing the development of stress and deformation patterns within the bimrock mass without introducing artificial constraints. (Figure 4.2))

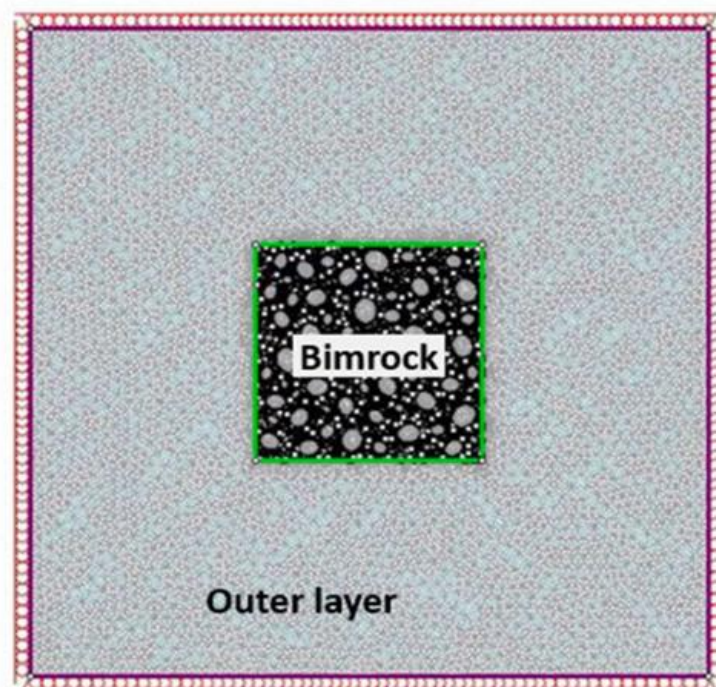


Figure 4.2 The model and boundaries that considered in RS2

## 4.5 Loading conditions

The analyses were conducted under an initial at-rest earth pressure condition with a coefficient  $K_0 = 1$ , implying equal major and minor principal stresses ( $\sigma_1 = \sigma_3$ ) by considering the state of stress at the center of the tunnel. The out-of-plane stress ( $\sigma_z$ ) was calculated according to plane strain conditions using the material Poisson's ratio. Table 4.2.

No external loads or pore water pressures were applied, and the material behaviour was analysed under dry conditions.

Parameter	Value
$\sigma_1$ [MPa]	1.68
$\sigma_3$ [MPa]	1.68
$\sigma_z$ [MPa]	1.008

Table 4.2 The initial state of stress

## 4.6 Mesh generation

The numerical domain was discretized using the finite element method with a graded mesh configuration. A graded mesh was selected to achieve a higher level of accuracy in critical zones while maintaining computational efficiency in less sensitive regions.

The mesh was generated using 6-noded triangular elements, which provide improved representation of stress and strain gradients compared to linear elements and are particularly suitable for problems involving plastic deformation and stress concentration around excavations.

A gradation factor of 0.1 was adopted, allowing a smooth transition from a finer mesh near the tunnel boundary and block interfaces to a coarser mesh farther away from the excavation. This refinement strategy ensures accurate capture of stress concentrations, displacement gradients, and plastic strain localization, especially in the vicinity of the tunnel and within the bimrock domain.

For the excavation boundary, a default number of 100 nodes was assigned to ensure sufficient resolution of the tunnel geometry and a reliable simulation of the stress redistribution induced by excavation.

Mesh sensitivity analyses were performed to verify that the numerical results, including displacement magnitude and extent of plastic zones, were not significantly influenced by the chosen element size. The adopted mesh configuration was found to provide a satisfactory balance between accuracy and computational efficiency and was therefore used consistently in all analyses.

## 4.7 Analysis type and output parameters

The mechanical response of a tunnel excavation is strongly influenced by the progressive advance of the excavation front and by the associated redistribution of stresses within the surrounding ground. In the 1970s, Lombardi first highlighted the importance of considering tunnel excavation as a gradual process, introducing the characteristic curves method (Lombardi, 1979; Hoek & Brown, 1980). With this approach, the excavation problem is no longer treated as purely two-dimensional, but rather as a pseudo-three-dimensional phenomenon, capable of accounting for the evolution of stresses and deformations along the tunnel axis (Panet & Guenot, 1982).

Tunnel excavation induces a progressive reduction of the radial stress acting on the excavation boundary. In the proximity of the excavation face, the minor principal stress tends to vanish, triggering deformation and, in weak ground conditions, the development of plastic zones. Deformation initiates at the excavation face and evolves as the tunnel advances, becoming fully developed at a certain distance behind the face. Consequently, the deformability of the rock mass depends not only on its intrinsic mechanical properties and the initial in-situ stress state, but also on the excavation sequence and the distance from the tunnel face (Vlachopoulos & Diederichs, 2009).

The overall deformation response of the ground may be interpreted as the combined effect of three main phenomena: extrusion of the core ahead of the excavation face, pre-convergence occurring before the tunnel section is fully excavated, and convergence developing behind the face. These mechanisms emphasize the intrinsically three-dimensional nature of the problem, even though simplified two-dimensional approaches are commonly adopted for engineering analyses (Hoek, 1999; Carranza-Torres & Fairhurst, 2000).

Within this conceptual framework, the convergence–confinement method provides an effective tool for post-excavation analysis. In this approach, tunnel excavation is simulated by imposing a progressively decreasing fictitious, internal pressure on the tunnel boundary, representing the gradual loss of confinement provided by the excavation face (Hoek & Brown, 1980; Panet & Guenot, 1982). The surrounding ground is typically assumed to behave as an elasto-plastic medium under an initially isotropic in-situ stress state.

In the present study, a static elastic–plastic analysis was performed for all numerical models to evaluate the mechanical response of the bimrock mass during tunnel excavation. The analyses were carried out using an incremental calculation scheme, which allows the gradual application of loading and ensures numerical stability and convergence, particularly when plastic deformation develops (Carranza-Torres & Fairhurst, 2000). This incremental approach makes it possible to capture the progressive evolution of stress redistribution, deformation, and yielding within the bimrock material as the excavation process advances.

Based on the results obtained by the numerical analysis, the ground reaction curve is calculated, which relates the radial displacement to the radial stress acting at the tunnel boundary. At high values of radial stress, corresponding to pre-excitation conditions, no displacement occurs. As the radial stress decreases, radial displacement progressively develops, initially in an elastic regime (according to figure 4.3). When a critical radial stress is reached due to the advancement of the excavation, plastic deformation initiates and a plastic zone form around the tunnel, (figure 4.3) whose extent is defined by the plastic radius (Hoek & Brown, 1980; Carranza-Torres & Fairhurst, 2000). Further stress reduction results in increased deformation and expansion of the yielded zone.

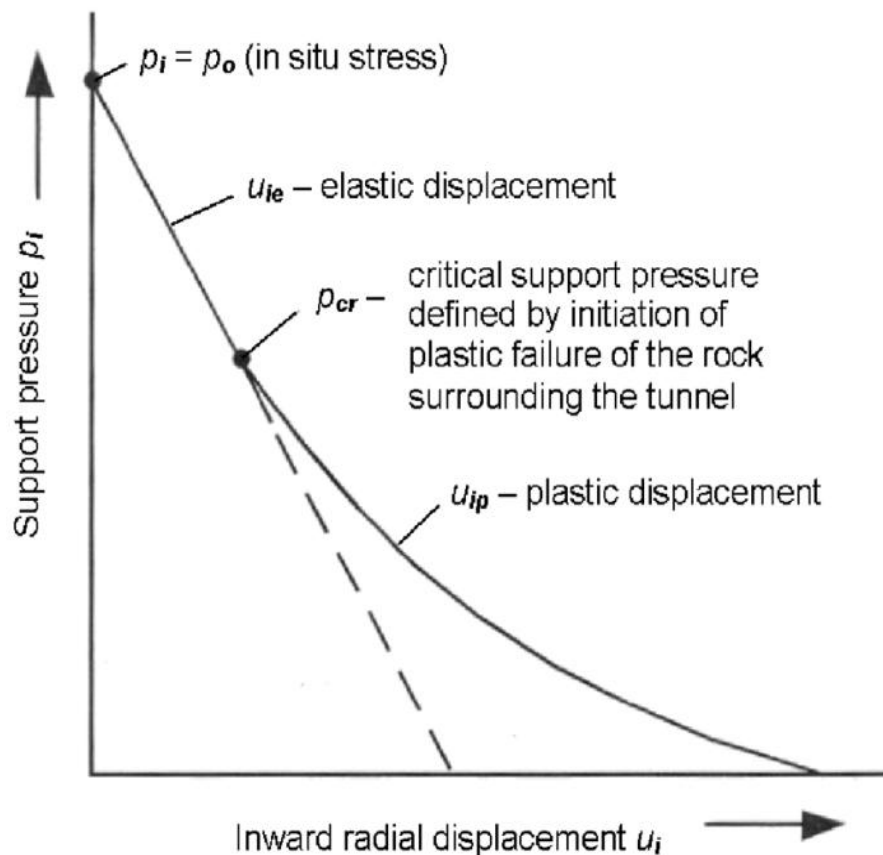


Figure 4.3 Ground reaction curve (Hoek et al., 1998)

In addition to the conceptual interpretation provided by the convergence–confinement approach, several output parameters were analysed in this study to obtain a comprehensive understanding of tunnel behaviour in bimrock formations. These include the distribution of displacement from the tunnel sidewalls to the external boundary of the numerical model, which provides insight into the spatial extent of excavation-induced ground deformation. The displacement along the tunnel boundary was also evaluated to assess tunnel convergence and the degree of deformation symmetry.

Finally, the development and distribution of yielded zones within the bimrock material were analysed to identify plastic deformation patterns and potential failure mechanisms. Together, these output parameters allow a comprehensive assessment of the influence of volumetric block proportion and block configuration on tunnel stability and deformation behavior in bimrock materials.

## 5 Results of the numerical analysis

In this chapter, the results of the numerical simulations performed, presented and discussed. The analyses were carried out using the finite element software Rocscience RS<sup>2</sup>, (chapter 4) considering numerical models explicitly representing the block-in-matrix structure. The blocks were generated with random position and orientation within the surrounding matrix, to reproduce the stochastic nature of bimrock formations. The influence of material heterogeneity on tunnel response was investigated by analyzing different volumetric block proportions.

The analyses focused on volumetric block proportions of 25% and 40%, which are representative of bimrock conditions where both matrix-controlled and block-influenced behaviours coexist.

For each volumetric block proportion, 30 numerical models were generated by varying the position and orientation of the blocks. This allowed the assessment of the influence of stochastic block distribution on tunnel behaviour. Due to the random nature of the block arrangement, the location of maximum tunnel convergence cannot be determined a priori, and significant differences in displacement patterns may arise between different realizations.

Tunnel convergence was evaluated at selected points along the excavation boundary, including the sidewalls and the crown, while the maximum displacement within the entire model domain was also monitored. In addition, the spatial distribution of displacements from the tunnel sidewalls toward the external boundary was analyzed to investigate the extent of excavation-induced ground deformation.

The final part of the analysis focuses on comparing the results obtained for different volumetric block proportions, highlighting the influence of block content and configuration on tunnel convergence, deformation patterns, and the development of plastic zones within the bimrock mass. This approach allows a comprehensive evaluation of tunnel stability and deformation behaviour in heterogeneous block-in-matrix materials, emphasizing the limitations of simplified assumptions and the importance of explicitly accounting for material heterogeneity in numerical analyses.

## 5.1 Internal pressure vs. tunnel convergence

### 5.1.1 Analysis without inclusions: (VBP = 0%)

This section presents the results of the numerical analyses performed for a volumetric block proportion equal to 0% (VBP = 0%), corresponding to a homogeneous matrix without rock inclusions. This condition represents the reference configuration and serves as a baseline for comparison with the heterogeneous bimrock cases investigated in the subsequent sections.

In this configuration, the mechanical response is governed entirely by the matrix material. Due to the absence of blocks, the stress field around the excavation develops in a symmetric and uniform manner, without local perturbations or spatial variability. Consequently, displacement patterns remain concentric around the tunnel boundary, and plastic zones evolve in a regular annular shape.

The numerical simulations were carried out by progressively reducing the internal pressure applied to the tunnel boundary, reproducing the gradual stress release associated with tunnel excavation. The convergence–confinement framework was adopted to evaluate the relationship between internal pressure and radial displacement.

Table 5.1 summarizes the characteristic convergence curve of the homogeneous matrix. At full stress release ( $P_i = 0$  MPa), the maximum radial displacement reaches 1.58 m. As the internal pressure increases, the radial displacement decreases progressively, reaching zero when the applied pressure equals the initial in-situ stress ( $P_i = 1.68$  MPa).

The symmetric and monotonic response observed in this reference case provides a clear benchmark for assessing the influence of block inclusions on stress redistribution, deformation localization, and convergence variability in the bimrock configurations. (Figure 5.1)

Pi [%]	Pi [Mpa]	Radial displacement[m]
0.00%	0.00	1.58
10.00%	0.17	0.59
20.00%	0.34	0.34
30.00%	0.50	0.22
40.00%	0.67	0.17
50.00%	0.84	0.13
60.00%	1.01	0.11
70.00%	1.18	0.08
80.00%	1.34	0.05
90.00%	1.51	0.03
100.00%	1.68	0

Table 5.1 The values of radial displacement of matrix for VBP 0% vs. internal pressure

Internal pressure vs. radial displacement of the matrix

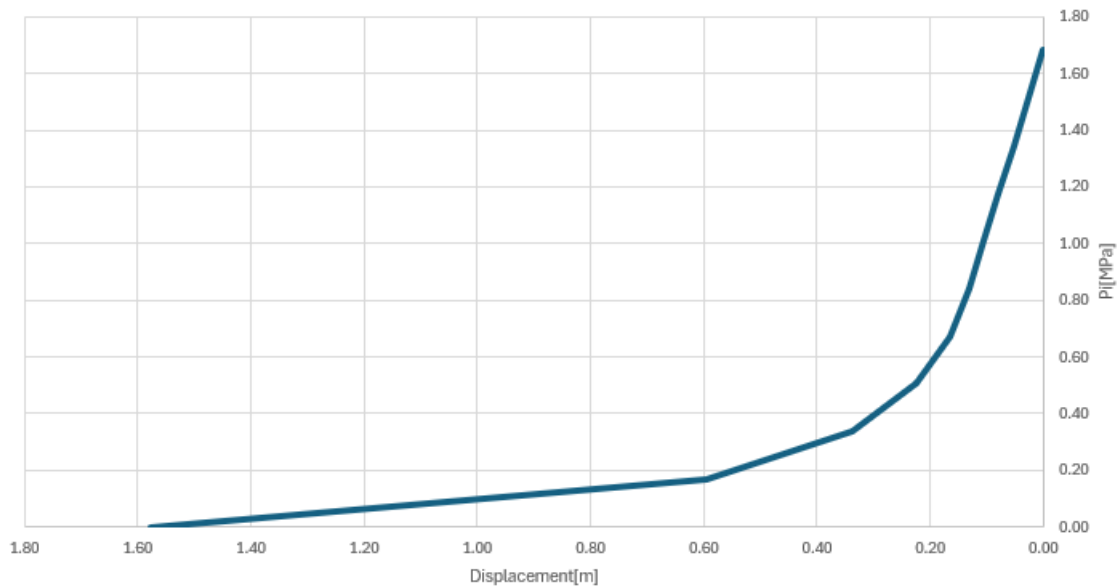


Figure 5.1 The values of radial displacement of matrix for VBP 0% vs. internal pressure

### **5.1.2 Analysis with inclusions: (VBP = 25%)**

This section presents the results of the numerical analyses performed for a volumetric block proportion equal to 25% (VBP = 25%), corresponding to a bimrock mass in which competent rock blocks are embedded within a weaker matrix. This condition represents a typical bimrock configuration in which the mechanical response is mainly governed by the matrix, while the presence of blocks locally modifies stress redistribution and deformation patterns.

Specifically, thirty different block configurations were generated for this VBP value, each characterized by a random spatial distribution of the inclusions within the matrix with three distinct block orientations were considered for each configuration, namely  $0^\circ$ ,  $45^\circ$ , and  $90^\circ$ , to investigate the influence of block orientation relative to the excavation on tunnel response.

The numerical simulations were performed by progressively reducing the internal pressure applied to the tunnel boundary, reproducing the gradual stress release associated with tunnel excavation. Due to the presence of inclusions, the stress field around the excavation becomes locally perturbed, leading to non-uniform displacement patterns and deviations from the symmetric response observed in the homogeneous reference case.

The convergence–confinement framework was adopted to interpret the numerical results. For each configuration and orientation, the relationship between internal pressure and tunnel convergence was evaluated, allowing the mechanical response of the bimrock mass under progressive unloading conditions to be characterized. The results highlight that, at VBP = 25%, deformation remains largely controlled by the matrix, while blocks act as stiff inclusions that locally alter the deformation field and introduce variability in convergence values.

Overall, the analysis at VBP = 25% provides a fundamental reference for understanding the transition from homogeneous behaviour to heterogeneous bimrock response.

0degrees configuration											
Pi [%]	Pi [Mpa]	n_1[m]	n_2[m]	n_3[m]	n_4[m]	n_5[m]	n_6[m]	n_7[m]	n_8[m]	n_9[m]	n_10[m]
0.00%	0.00	1.28	1.45	0.79	1.32	1.36	0.81	0.43	1.15	0.98	1.42
10.00%	0.17	0.45	0.48	0.33	0.44	0.48	0.30	0.20	0.43	0.32	0.49
20.00%	0.34	0.26	0.27	0.21	0.24	0.26	0.18	0.12	0.23	0.16	0.27
30.00%	0.50	0.18	0.18	0.15	0.15	0.17	0.12	0.08	0.16	0.11	0.18
40.00%	0.67	0.14	0.14	0.11	0.11	0.12	0.10	0.06	0.12	0.08	0.13
50.00%	0.84	0.11	0.11	0.09	0.09	0.10	0.08	0.05	0.10	0.07	0.11
60.00%	1.01	0.09	0.09	0.07	0.07	0.08	0.06	0.04	0.08	0.05	0.09
70.00%	1.18	0.07	0.07	0.05	0.05	0.06	0.05	0.03	0.06	0.04	0.06
80.00%	1.34	0.04	0.04	0.04	0.04	0.04	0.03	0.02	0.04	0.03	0.04
90.00%	1.51	0.02	0.02	0.02	0.02	0.02	0.02	0.01	0.02	0.01	0.02
100.00%	1.68	0.00	0.00	0.00	0.00	0.00	0.00	0.00	0.00	0.00	0.00

Table 5.2 The values of radial displacement for 0-degree orientations for VBP 25% vs. internal pressure

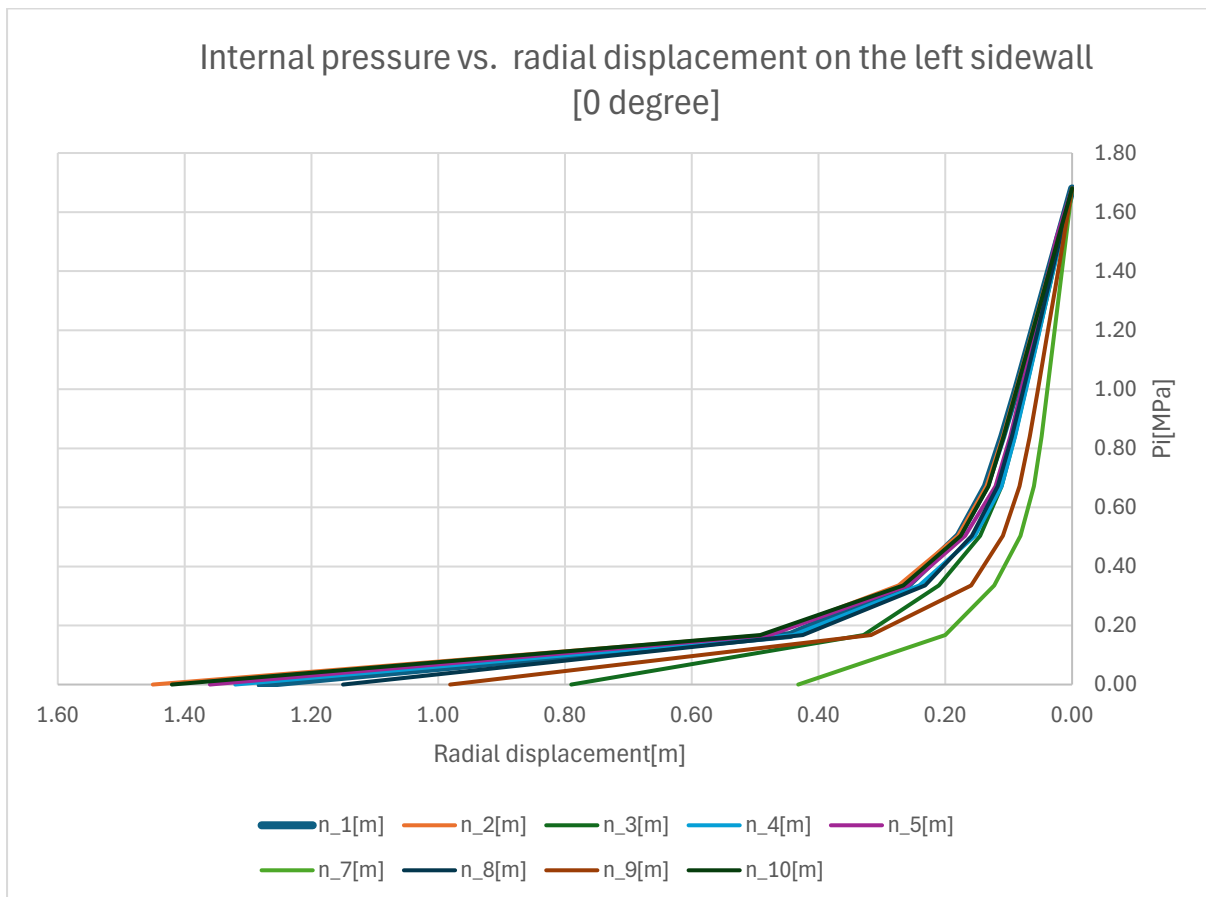


Figure 5.2 The diagram of radial displacement for 0-degree orientations for VBP 25% vs. internal pressure

45degrees configuration											
Pi [%]	Pi [Mpa]	n_1[m]	n_2[m]	n_3[m]	n_4[m]	n_5[m]	n_6[m]	n_7[m]	n_8[m]	n_9[m]	n_10[m]
0.00%	0.00	1.36	0.96	1.30	1.30	1.15	1.24	1.19	0.88	1.41	1.37
10.00%	0.17	0.46	0.34	0.41	0.41	0.42	0.45	0.43	0.36	0.49	0.42
20.00%	0.34	0.24	0.20	0.22	0.23	0.23	0.23	0.25	0.22	0.28	0.23
30.00%	0.50	0.16	0.14	0.16	0.16	0.17	0.15	0.18	0.15	0.18	0.16
40.00%	0.67	0.12	0.10	0.13	0.12	0.13	0.12	0.13	0.11	0.14	0.12
50.00%	0.84	0.09	0.08	0.10	0.10	0.10	0.09	0.11	0.09	0.11	0.10
60.00%	1.01	0.07	0.06	0.08	0.08	0.08	0.07	0.08	0.07	0.09	0.08
70.00%	1.18	0.05	0.04	0.06	0.06	0.06	0.05	0.06	0.05	0.07	0.06
80.00%	1.34	0.04	0.03	0.04	0.04	0.04	0.04	0.04	0.04	0.04	0.04
90.00%	1.51	0.02	0.02	0.02	0.02	0.02	0.02	0.02	0.02	0.02	0.02
100.00%	1.68	0.00	0.00	0.00	0.00	0.00	0.00	0.00	0.00	0.00	0.00

Table 5.3 The values of radial displacement for 45-degree orientations for VBP 25% vs. internal pressure

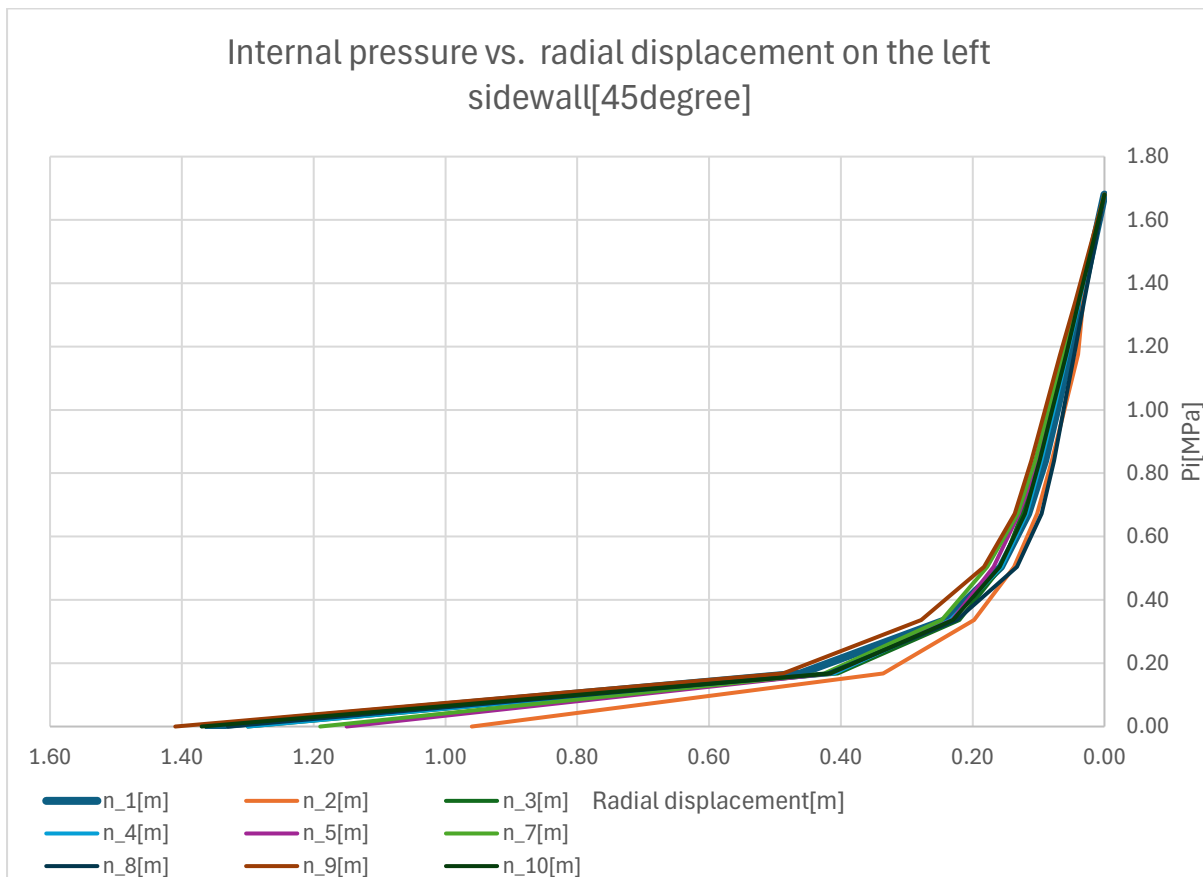


Figure 5.3 The diagram of radial displacement for 45-degree orientations for VBP 25% vs. internal pressure

90degrees configuration											
Pi [%]	Pi [Mpa]	n_1[m]	n_2[m]	n_3[m]	n_4[m]	n_5[m]	n_6[m]	n_7[m]	n_8[m]	n_9[m]	n_10[m]
0.00%	0.00	1.49	1.38	0.67	0.67	1.09	1.10	1.11	1.33	1.45	0.67
10.00%	0.17	0.50	0.44	0.22	0.22	0.39	0.33	0.40	0.42	0.49	0.21
20.00%	0.34	0.26	0.24	0.12	0.12	0.19	0.17	0.21	0.22	0.26	0.11
30.00%	0.50	0.17	0.15	0.08	0.08	0.14	0.11	0.14	0.13	0.18	0.08
40.00%	0.67	0.12	0.11	0.06	0.06	0.11	0.08	0.10	0.10	0.15	0.06
50.00%	0.84	0.09	0.09	0.05	0.05	0.09	0.07	0.08	0.08	0.12	0.05
60.00%	1.01	0.08	0.07	0.04	0.04	0.07	0.05	0.07	0.06	0.10	0.04
70.00%	1.18	0.06	0.05	0.03	0.03	0.05	0.04	0.05	0.05	0.07	0.03
80.00%	1.34	0.05	0.03	0.02	0.02	0.03	0.03	0.03	0.03	0.05	0.02
90.00%	1.51	0.03	0.02	0.01	0.01	0.02	0.01	0.02	0.02	0.02	0.01
100.00%	1.68	0.00	0.00	0.00	0.00	0.00	0.00	0.00	0.00	0.00	0.00

Table 5.4 The values of radial displacement for 90-degree orientations for VBP 25% vs. internal pressure

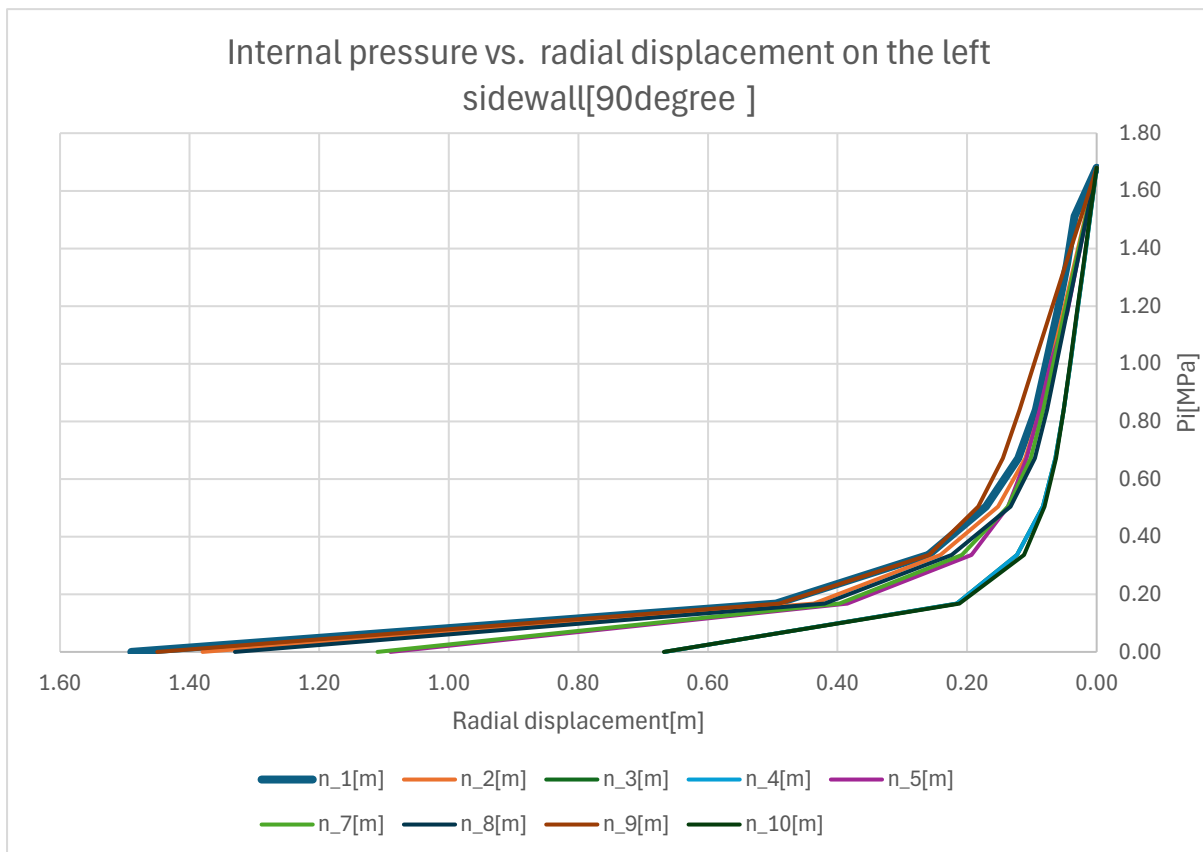


Figure 5.4 The diagram of radial displacement for 90-degree orientations for VBP 25% vs. internal pressure

max Internal pressure vs. radial displacement on the left sidewall		
0degree [m]	45 de- grees[m]	90degree[m]
1.45	1.49	1.41
0.49	0.50	0.49
0.27	0.26	0.28
0.18	0.18	0.18
0.14	0.15	0.14
0.11	0.12	0.11
0.09	0.10	0.09
0.07	0.07	0.07
0.04	0.05	0.04
0.02	0.03	0.02
0.00	0.00	0.00

Table 5.5 The values of max radial displacement for 0-45-90-degree orientations for VBP 25% vs. internal pressure

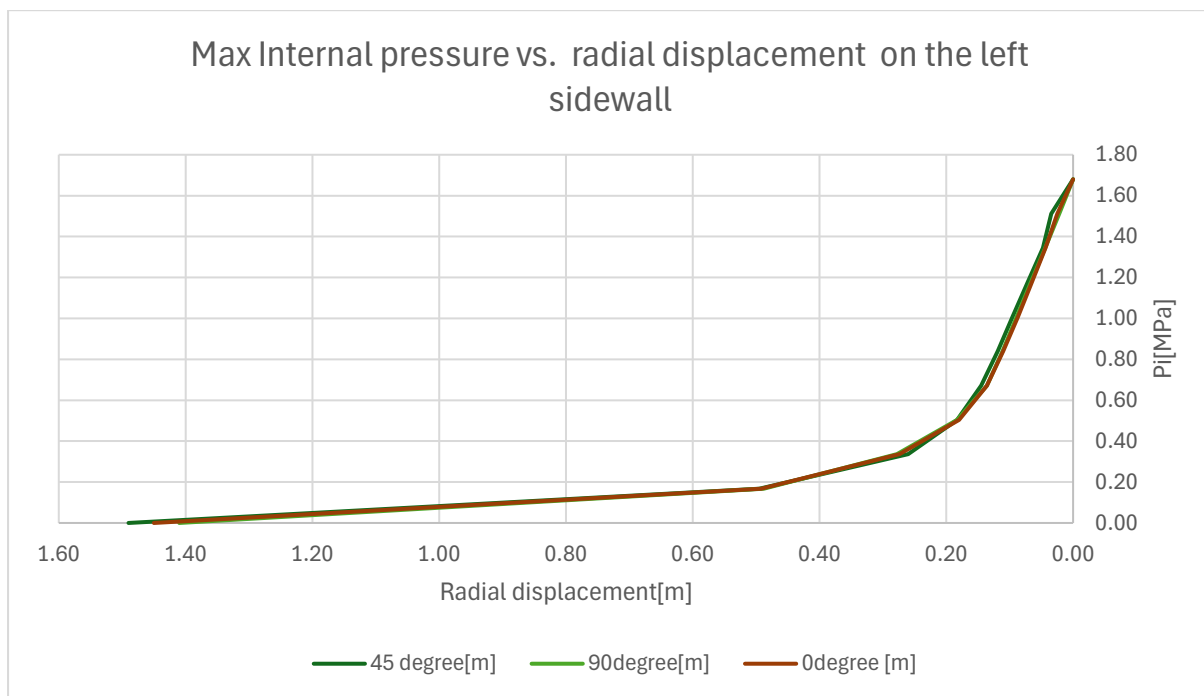


Figure 5.5 The figure of max radial displacement for 0-45-90-degree orientations for VBP 25% vs. internal pressure

Figure 5.5 presents the variation of maximum radial displacement at the left sidewall for  $VBP = 25\%$  under progressive reduction of internal pressure. The max results are shown for three block orientations:  $0^\circ$ ,  $45^\circ$ , and  $90^\circ$ .

Due to the random distribution and orientation of blocks within the bimrock mass, tunnel convergence does not develop uniformly along the excavation boundary. Unlike the homogeneous reference case, the deformation field becomes asymmetric, and the location of maximum displacement may vary depending on the local block arrangement.

The results indicate that block orientation influences the magnitude of convergence. In particular, the highest displacement values are observed for the  $45^\circ$  orientation, reaching a maximum value of 1.49 m under full stress release. The  $0^\circ$  and  $90^\circ$  configurations exhibit slightly lower peak displacements, with maximum values of 1.45 m and 1.41 m, respectively. (Table 5.5)

Although the differences between orientations are moderate, they demonstrate that block alignment relative to the excavation direction affects stress redistribution and deformation localization. These variations confirm that the spatial arrangement and orientation of blocks within the bimrock matrix significantly influence tunnel response.

Overall, the results for  $VBP = 25\%$  highlight the importance of considering geometric variability in numerical modelling, as simplified homogeneous assumptions would not capture the asymmetric deformation patterns observed in heterogeneous configurations.

### 5.1.3 Analysis with Inclusions: VBP = 40%

This section presents the results of the numerical analyses carried out to investigate the relationship between internal pressure reduction and tunnel convergence for the case of VBP equal to 40%. The analyses were performed considering different block orientations ( $0^\circ$ ,  $45^\circ$ , and  $90^\circ$ ), with 10 numerical realizations for each orientation, to capture the influence of material heterogeneity on the excavation response.

The results are expressed in terms of displacement evolution at the tunnel boundary as a function of the applied internal pressure, progressively reduced to simulate the excavation process.

For the  $0^\circ$  configuration, the displacement–pressure curves exhibit a consistent trend across all realizations. At high internal pressure levels, the recorded displacements remain limited, indicating a stable mechanical response of the rock mass. As the internal pressure is gradually reduced, displacement increases smoothly until a critical pressure range is reached, beyond which a rapid growth of convergence is observed.

Although some variability is present among the different realizations, the overall shape of the curves remains similar. This behavior suggests that, for horizontal block orientation, the deformation mechanism is governed by a progressive stress redistribution, with localized effects induced by the presence of blocks becoming more significant at lower confinement levels.

0degrees configuration (VBP40%)											
Pi [%]	Pi [Mpa]	n_1[m]	n_2[m]	n_3[m]	n_4[m]	n_5[m]	n_6[m]	n_7[m]	n_8[m]	n_9[m]	n_10[m]
0.00%	0.00	0.98	0.57	0.54	1.00	0.83	0.88	0.40	0.97	0.95	0.58
10.00%	0.17	0.34	0.17	0.20	0.30	0.29	0.33	0.18	0.29	0.34	0.22
20.00%	0.34	0.18	0.10	0.11	0.17	0.15	0.18	0.12	0.16	0.20	0.13
30.00%	0.50	0.12	0.07	0.08	0.12	0.11	0.12	0.08	0.11	0.12	0.10
40.00%	0.67	0.09	0.06	0.07	0.09	0.08	0.09	0.06	0.08	0.08	0.07
50.00%	0.84	0.07	0.05	0.05	0.08	0.06	0.07	0.05	0.06	0.06	0.06
60.00%	1.01	0.06	0.04	0.04	0.06	0.05	0.06	0.04	0.05	0.05	0.05
70.00%	1.18	0.04	0.03	0.03	0.04	0.04	0.04	0.03	0.04	0.03	0.04
80.00%	1.34	0.03	0.02	0.02	0.03	0.03	0.03	0.02	0.02	0.02	0.02
90.00%	1.51	0.01	0.01	0.01	0.01	0.01	0.01	0.01	0.01	0.01	0.01
100.00%	1.68	0.00	0.00	0.00	0.00	0.00	0.00	0.00	0.00	0.00	0.00

Table 5.6 The values of radial displacement for 0-degree orientations for VBP 40% vs. internal pressure

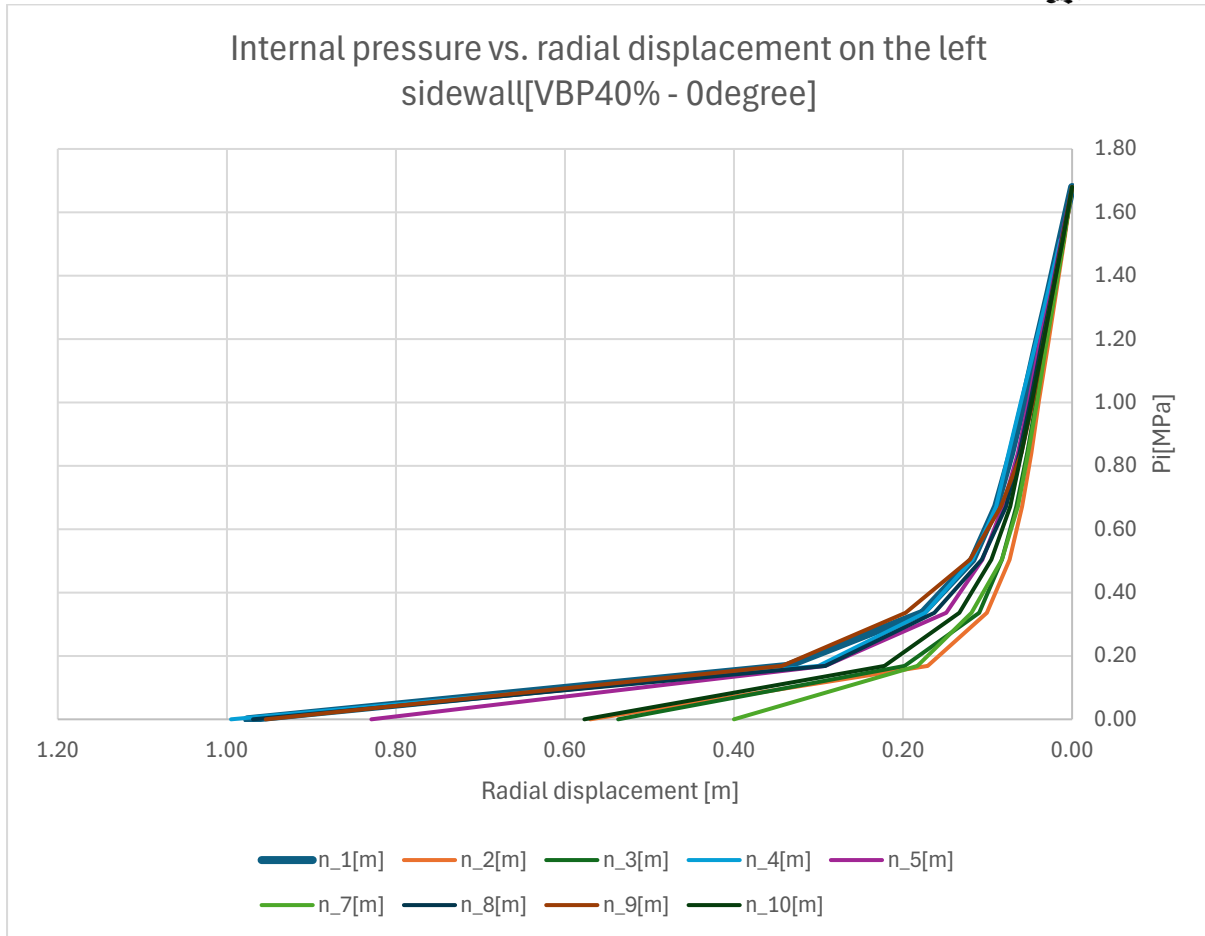


Figure 5.6 The diagram of radial displacement for 0-degree orientations for VBP 40% vs. internal pressure

In the 45° orientation, the displacement–pressure relationship follows the same general trend observed for the 0° case, but with a slightly higher dispersion between realizations. At intermediate pressure levels, some curves show earlier displacement development, indicating a greater sensitivity of the system to internal pressure reduction. (Table 5.7) (Figure 5.7)

As the internal pressure approaches its minimum values, all realizations converge toward a marked increase in displacement, reflecting the onset of extensive plastic deformation around the tunnel. The inclined block arrangement enhances stress interaction effects, leading to a less uniform response compared to the 0° configuration.

45degrees configuration [VBP40%]											
Pi [%]	Pi [Mpa]	n_1[m]	n_2[m]	n_3[m]	n_4[m]	n_5[m]	n_6[m]	n_7[m]	n_8[m]	n_9[m]	n_10[m]
0.00%	0.00	0.83	0.90	0.36	0.71	0.82	0.52	0.82	0.77	0.97	0.77
10.00%	0.17	0.29	0.33	0.14	0.29	0.25	0.18	0.29	0.25	0.30	0.26
20.00%	0.34	0.18	0.19	0.09	0.16	0.13	0.11	0.18	0.15	0.16	0.14
30.00%	0.50	0.12	0.12	0.07	0.11	0.09	0.08	0.13	0.10	0.10	0.10
40.00%	0.67	0.09	0.09	0.05	0.09	0.06	0.06	0.09	0.08	0.08	0.08
50.00%	0.84	0.08	0.07	0.04	0.07	0.05	0.05	0.07	0.06	0.06	0.07
60.00%	1.01	0.06	0.06	0.03	0.06	0.04	0.04	0.06	0.05	0.05	0.05
70.00%	1.18	0.04	0.04	0.03	0.04	0.03	0.03	0.04	0.04	0.04	0.04
80.00%	1.34	0.03	0.03	0.02	0.03	0.02	0.02	0.03	0.03	0.02	0.03
90.00%	1.51	0.01	0.01	0.01	0.01	0.01	0.01	0.01	0.01	0.01	0.01
100.00%	1.68	0.00	0.00	0.00	0.00	0.00	0.00	0.00	0.00	0.00	0.00

Table 5.7 The values of radial displacement for 45-degree orientations for VBP 40% vs. internal pressure

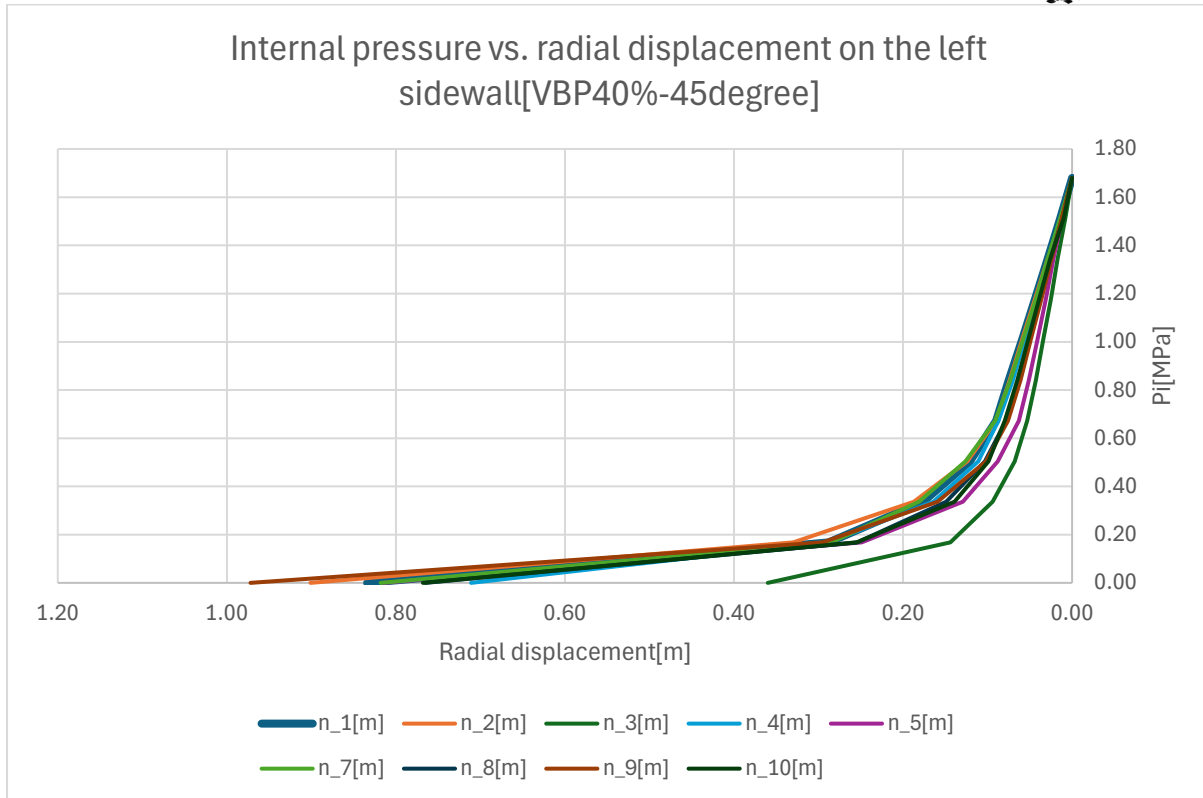


Figure 5.7 The diagram of radial displacement for 45-degree orientations for VBP 40% vs. internal pressure

For the 90° block orientation, the displacement curves show a more gradual evolution at higher pressure levels, followed by a sharp increase in convergence when the internal pressure drops below a threshold value (Table 5.8). Compared to the other configurations, the dispersion among realizations is reduced, particularly at intermediate pressure levels.

This behavior indicates that blocks oriented perpendicular to the excavation direction contribute to a more effective confinement of the tunnel, delaying the onset of significant deformation. However, once the confinement is sufficiently reduced, the displacement increases rapidly, highlighting the non-linear nature of the mechanical response.

90degrees configuration [VBP40%]											
Pi [%]	Pi [Mpa]	n_1[m]	n_2[m]	n_3[m]	n_4[m]	n_5[m]	n_6[m]	n_7[m]	n_8[m]	n_9[m]	n_10[m]
0.00%	0.00	1.04	1.11	0.84	1.02	0.68	1.01	0.88	0.77	0.90	0.56
10.00%	0.17	0.34	0.34	0.26	0.36	0.25	0.36	0.28	0.25	0.33	0.24
20.00%	0.34	0.18	0.19	0.13	0.19	0.15	0.19	0.15	0.14	0.20	0.14
30.00%	0.50	0.12	0.13	0.09	0.13	0.10	0.12	0.11	0.10	0.13	0.10
40.00%	0.67	0.09	0.10	0.07	0.10	0.07	0.09	0.08	0.08	0.10	0.08
50.00%	0.84	0.07	0.08	0.05	0.08	0.06	0.07	0.07	0.06	0.08	0.06
60.00%	1.01	0.06	0.06	0.04	0.06	0.05	0.06	0.05	0.05	0.06	0.05
70.00%	1.18	0.04	0.05	0.03	0.05	0.04	0.04	0.04	0.04	0.05	0.03
80.00%	1.34	0.03	0.03	0.02	0.03	0.02	0.03	0.03	0.03	0.03	0.02
90.00%	1.51	0.01	0.02	0.01	0.02	0.01	0.01	0.01	0.01	0.02	0.01
100.00%	1.68	0.00	0.00	0.00	0.00	0.00	0.00	0.00	0.00	0.00	0.00

Table 5.8 The values of radial displacement for 90-degree orientations for VBP 40% vs. internal pressure

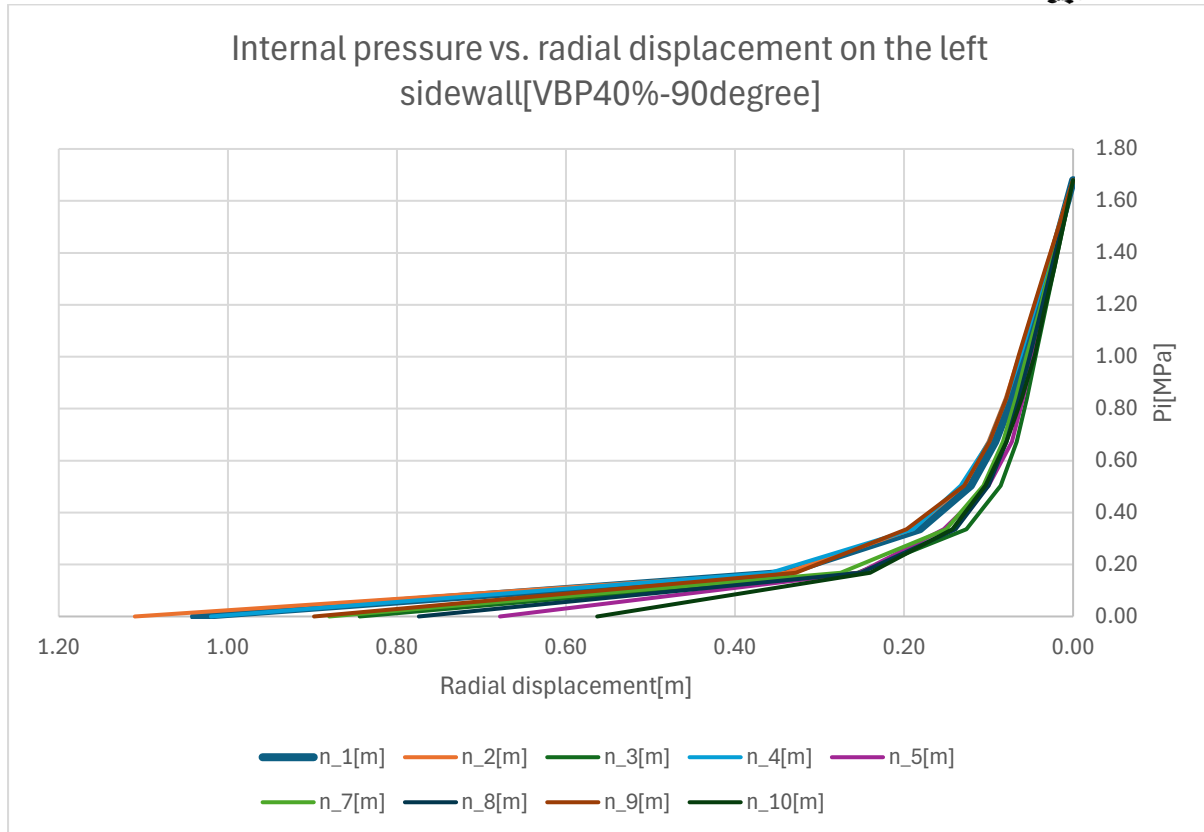


Figure 5.8 The diagram of radial displacement for 90-degree orientations for VBP 40% vs. internal pressure

By comparing the three block orientations, it emerges that:

All configurations exhibit a non-linear relationship between internal pressure and radial displacement. As the internal pressure decreases, convergence increases gradually at first and then accelerates more noticeably as full stress release is approached. This behaviour reflects the progressive mobilization of plastic deformation within the bimrock mass.

Block orientation does not significantly alter the overall shape of the pressure–displacement curves. The general trend remains consistent across the 0°, 45°, and 90° configurations. However, orientation influences the magnitude of the maximum displacement and the level of variability observed at low pressure levels.

In particular, the 90° configuration reaches the highest peak radial displacement (1.11 m) (Table 5.9), while the 0° and 45° orientations show slightly lower maximum values. Although the differences are moderate, they indicate that block alignment relative to the excavation direction affects stress redistribution and deformation localization within the bimrock mass. (Figure 5.9)

The results confirm that, for VBP = 40%, tunnel behaviour is primarily governed by the progressive reduction of internal pressure. Block orientation does not change the global mechanical response but modulates the magnitude and spatial variability of deformation, especially under conditions of significant stress release.

Pi [%]	Pi [Mpa]	Max radial displacement		
		0degree [m]	45degree[m]	90degree [m]
0.00%	0.00	1	0.97	1.11
10.00%	0.17	0.34	0.33	0.36
20.00%	0.34	0.20	0.19	0.20
30.00%	0.50	0.12	0.13	0.13
40.00%	0.67	0.09	0.09	0.10
50.00%	0.84	0.08	0.08	0.08
60.00%	1.01	0.06	0.06	0.06
70.00%	1.18	0.04	0.04	0.05
80.00%	1.34	0.03	0.03	0.03
90.00%	1.51	0.01	0.01	0.02
100.00%	1.68	0	0	0

Table 5.9 The values of max radial displacement for 0-45-90-degree orientations for VBP 40% vs. internal pressure

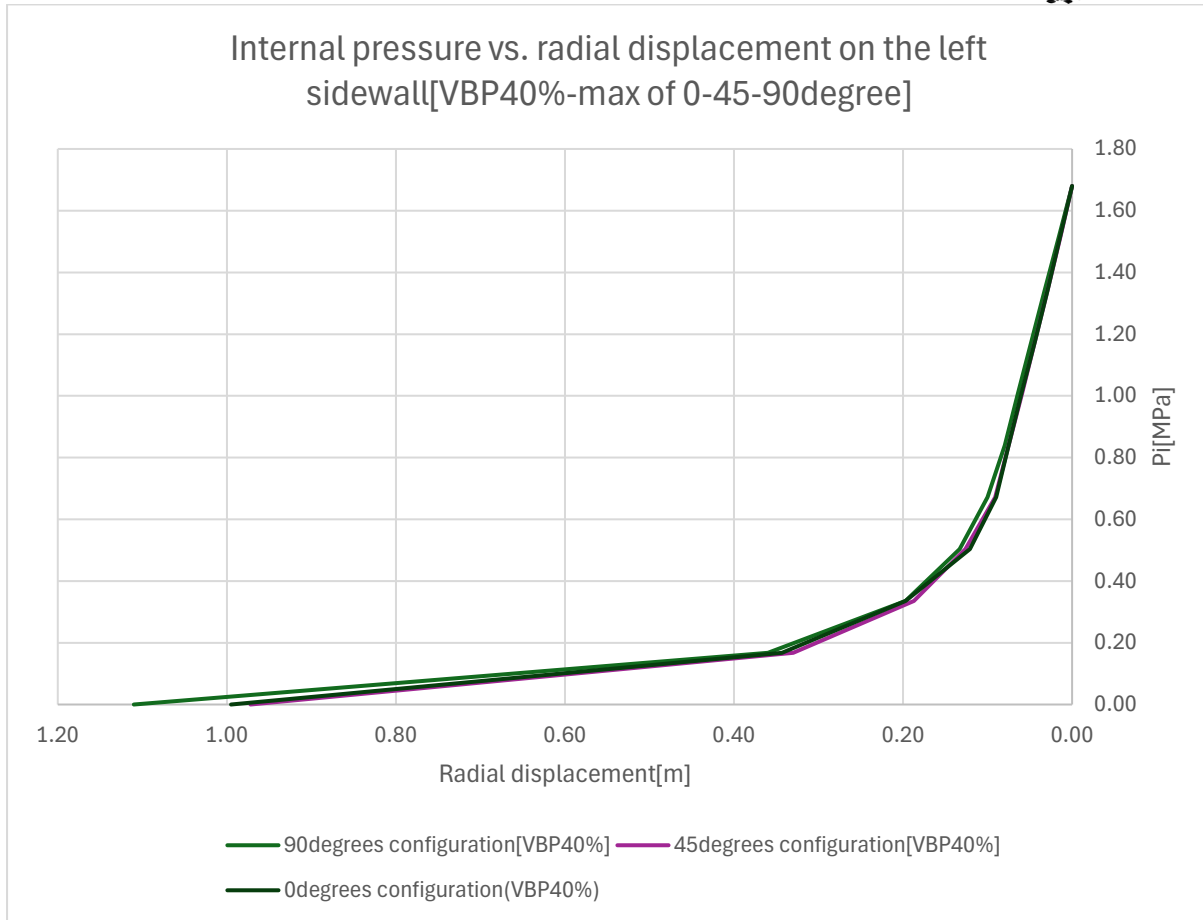


Figure 5.9 The figure of max radial displacement for 0-45-90-degree orientations for VBP 40% vs. internal pressure

By comparing the maximum displacement values corresponding to VBP = 25%, 40%, 55%, and 70%, it can be observed that the magnitude of tunnel convergence decreases with increasing volumetric block proportion. For VBP = 25%, the maximum displacement reaches approximately 1.58 m, whereas for VBP = 70% the maximum displacement is reduced to about 1.15 m. (Figure 5.10)

This trend indicates that increasing the volumetric block proportion leads to a reduction in displacement for a given level of internal pressure reduction. The observed behavior can be attributed to the decrease in the proportion of the weaker matrix material and the corresponding increase in the number of competent rock blocks, which enhances the overall stiffness of the bimrock mass and limits tunnel deformation.

(The values of the 55% and 70% are taken from Dadone,2018).

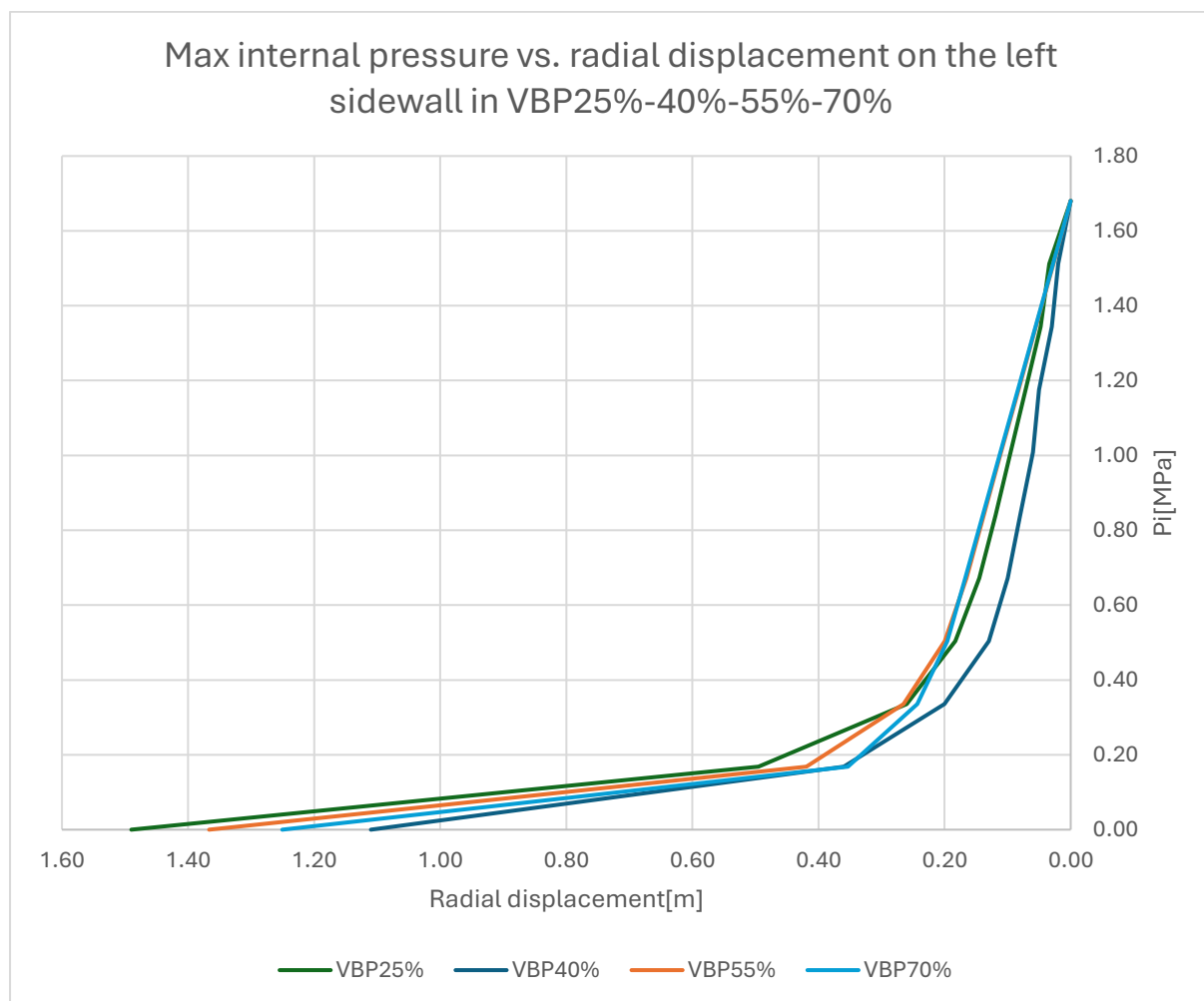


Figure 5.10 The comparing of internal pressure vs. Radial displacement in VBP 25%-40%-55%-70%

## 5.2 Analysis of radial displacement from the sidewall to the external boundary

### 5.2.1 Radial displacement from the sidewall until the external for a VBP=25%

This section examines the variation of total radial displacement with increasing distance from the tunnel sidewall toward the external boundary for the case of VBP equal to 25%. The analyses were performed considering three different block orientations ( $0^\circ$ ,  $45^\circ$ , and  $90^\circ$ ), with ten realizations for each configuration to capture the intrinsic heterogeneity of the bimrock mass.

Figure 5.11 presents the displacement profiles corresponding to the  $0^\circ$  configuration. The results show a rapid decrease in displacement close to the tunnel boundary, followed by a gradual attenuation with increasing distance. The highest displacement values are consistently recorded in the immediate vicinity of the sidewall, reflecting the stress release induced by excavation.

As the distance from the tunnel increases, all realizations exhibit a monotonic reduction of displacement, approaching negligible values at distances on the order of several tens of meters. Although some variability is observed among different realizations—particularly within the near-field region—the overall trend remains consistent. This indicates that, at VBP = 25%, the deformation mechanism is primarily governed by the matrix, while the influence of inclusions remains localized.

The displacement profiles tend to converge in the far-field region, confirming that block–matrix interaction mainly affects the area close to the excavation boundary. This behaviour suggests that, for relatively low block content and horizontal block orientation, the heterogeneity of the bimrock mass does not significantly alter the far-field displacement decay.

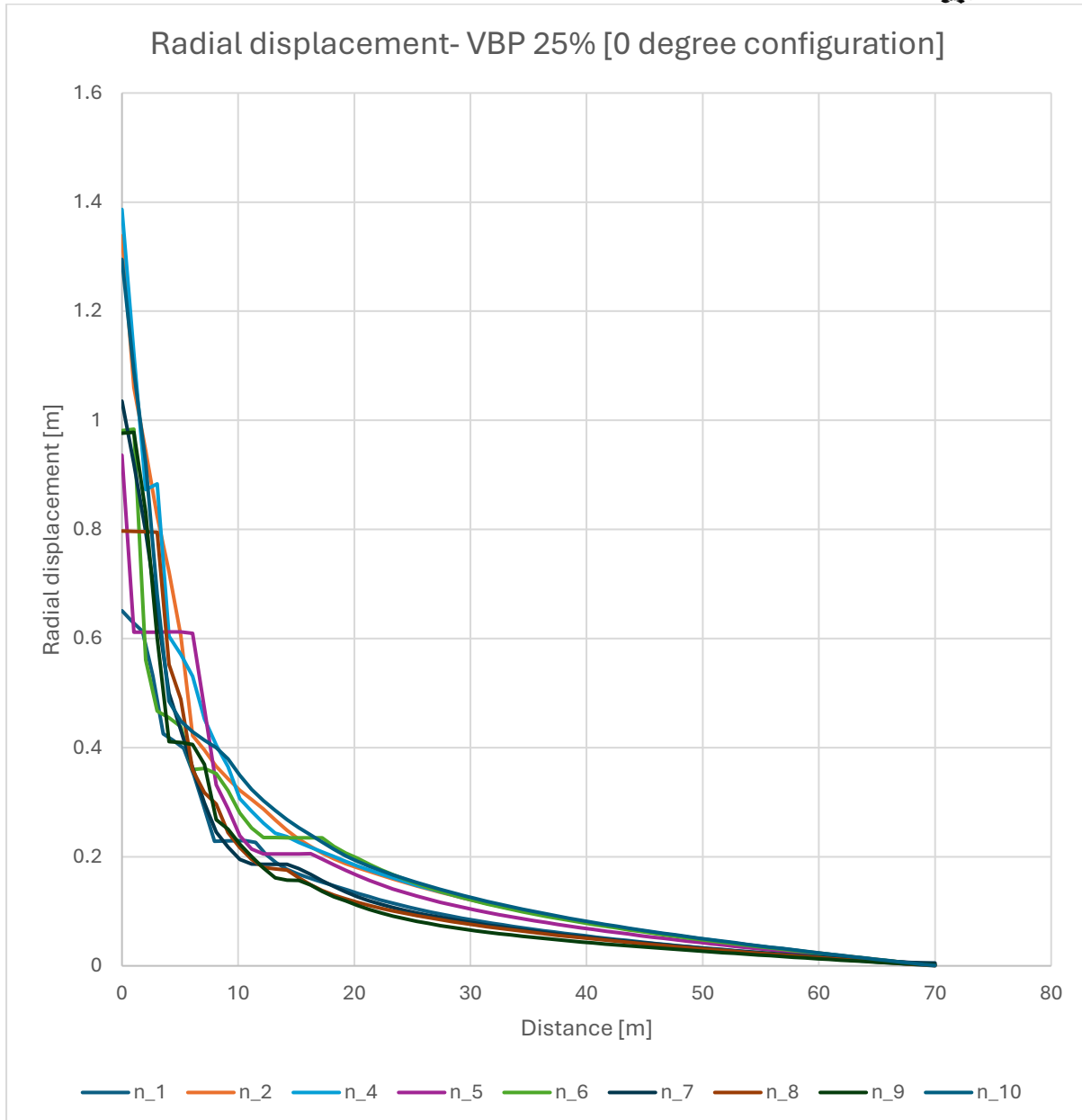


Figure 5.11 The figure of radial displacement for 0-degree orientations for VBP 25% vs. distance until external boundary

In the 45° orientation, the displacement profiles maintain the same general decay trend observed in the 0° case; however, a slightly higher dispersion among realizations is evident, especially near the tunnel sidewall. (Figure 5.12)

The inclined orientation of blocks promotes a more complex interaction between excavation-induced stresses and the heterogeneous material structure. As a result, localized variations in displacement magnitude appear in the near-field zone, while the far-field response remains largely unaffected.

Despite this increased variability, the displacement curves tend to converge toward similarly low values at larger distances, confirming that the global attenuation behavior is preserved even in the presence of inclined inclusions.

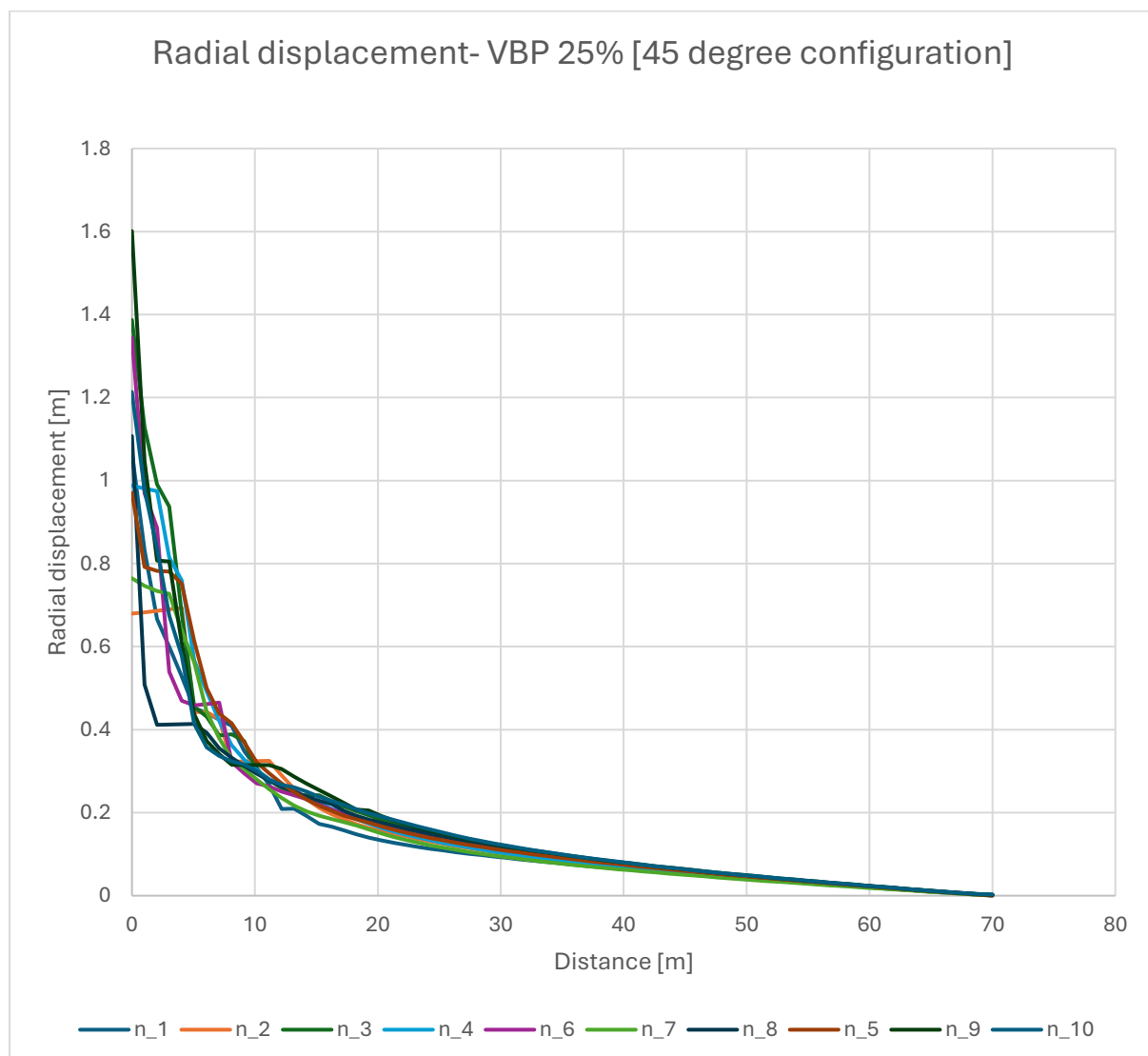


Figure 5.12 The figure of radial displacement for 45-degree orientations for VBP 25% vs. distance until external boundary

For the 90° block orientation, the displacement profiles display the most regular attenuation with distance, with a smoother decay compared to the other configurations. The displacement values near the tunnel boundary remain comparable in magnitude to those observed for 0° and 45°, but the transition toward lower values occurs more gradually and consistently among realizations. (Figure 5.13)

This behavior indicates that blocks oriented perpendicular to the excavation direction tend to redistribute stresses more uniformly away from the tunnel, reducing local irregularities in the displacement field. Consequently, the variability between realizations is slightly reduced, particularly beyond the near-field zone.

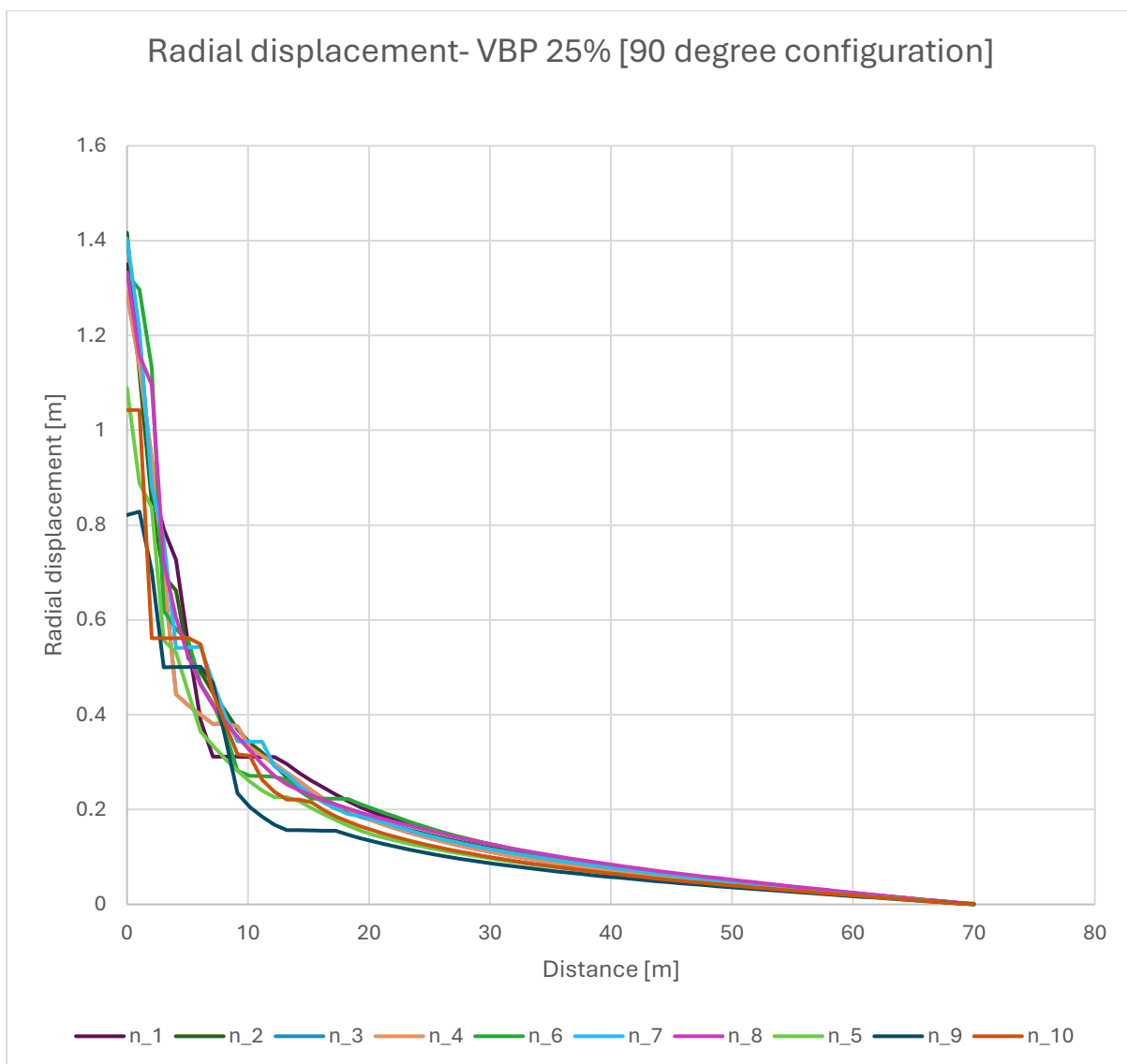


Figure 5.13 The figure of radial displacement for 90-degree orientations for VBP 25% vs. distance until external boundary

## 5.2.2 Radial displacement from the sidewall to the external boundary for a VBP = 40%

This section presents the results of the numerical analyses for VBP equal to 40%, focusing on the evolution of radial displacement with increasing distance from the tunnel sidewall toward the external boundary. Compared to the VBP 25% case, the higher block content leads to a more heterogeneous mechanical response, particularly in the near-field region surrounding the excavation.

For the 0° configuration, the displacement profiles exhibit a sharp reduction immediately beyond the tunnel sidewall, followed by a progressively smoother decay with distance. The highest displacement values are consistently concentrated within the first few meters from the tunnel boundary, confirming the dominant influence of excavation-induced stress release in this region. (Figure 5.14)

Compared to the corresponding VBP 25% case, the curves show a greater dispersion among realizations, especially close to the tunnel. This behavior reflects the increased role of rock blocks in controlling local stiffness and deformation mechanisms. Nevertheless, at larger distances, the displacement curves tend to converge toward low and nearly negligible values, indicating that the far-field response remains relatively insensitive to block arrangement.

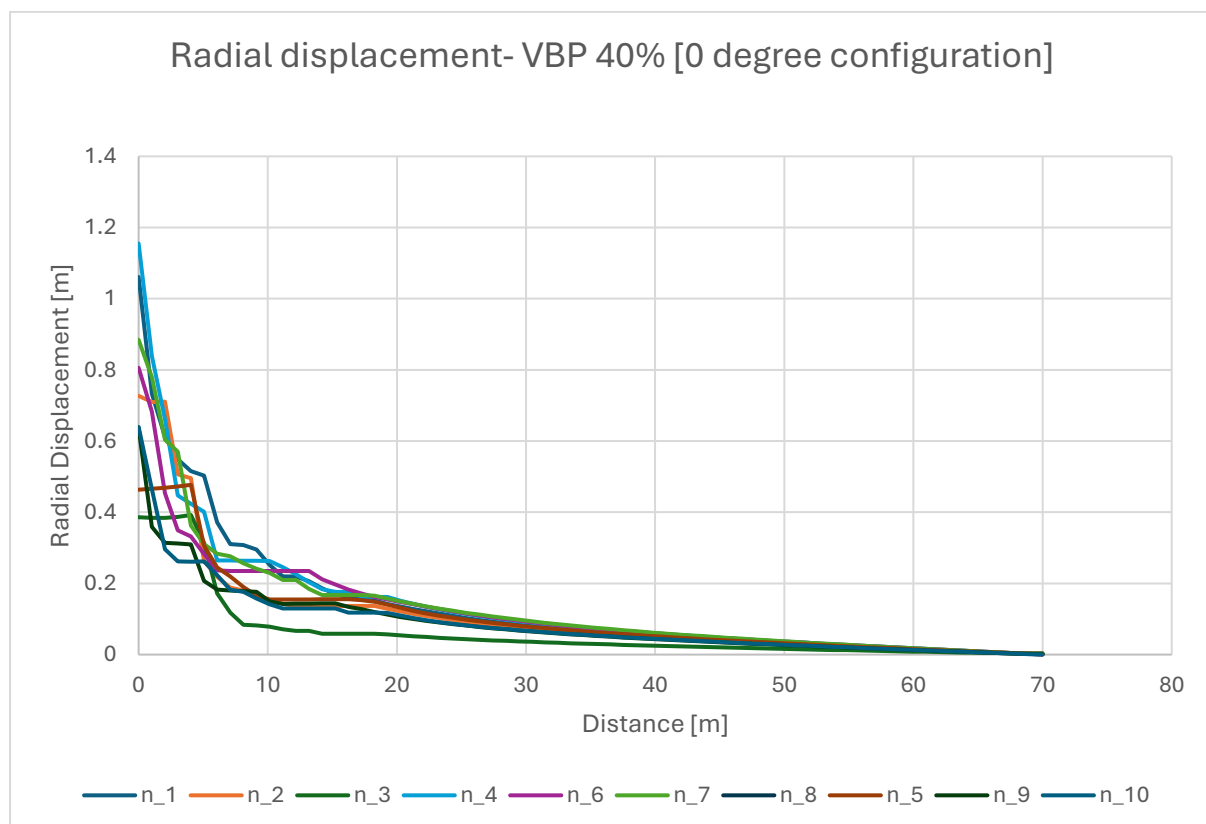


Figure 5.14 The figure of radial displacement for 0-degree orientations for VBP 40% vs. distance until external boundary

In the 45° orientation, the displacement decay remains monotonic but exhibits noticeable variability in the near-field zone. Several realizations display slightly higher displacement levels close to the sidewall compared to the 0° case, suggesting a stronger interaction between inclined blocks and the excavation geometry. (Figure 5.15)

As the distance from the tunnel increases, the displacement curves gradually merge, and differences among realizations become less pronounced. This convergence indicates that, despite the increased heterogeneity associated with higher VBP and inclined blocks, the overall attenuation of deformation with distance is preserved.

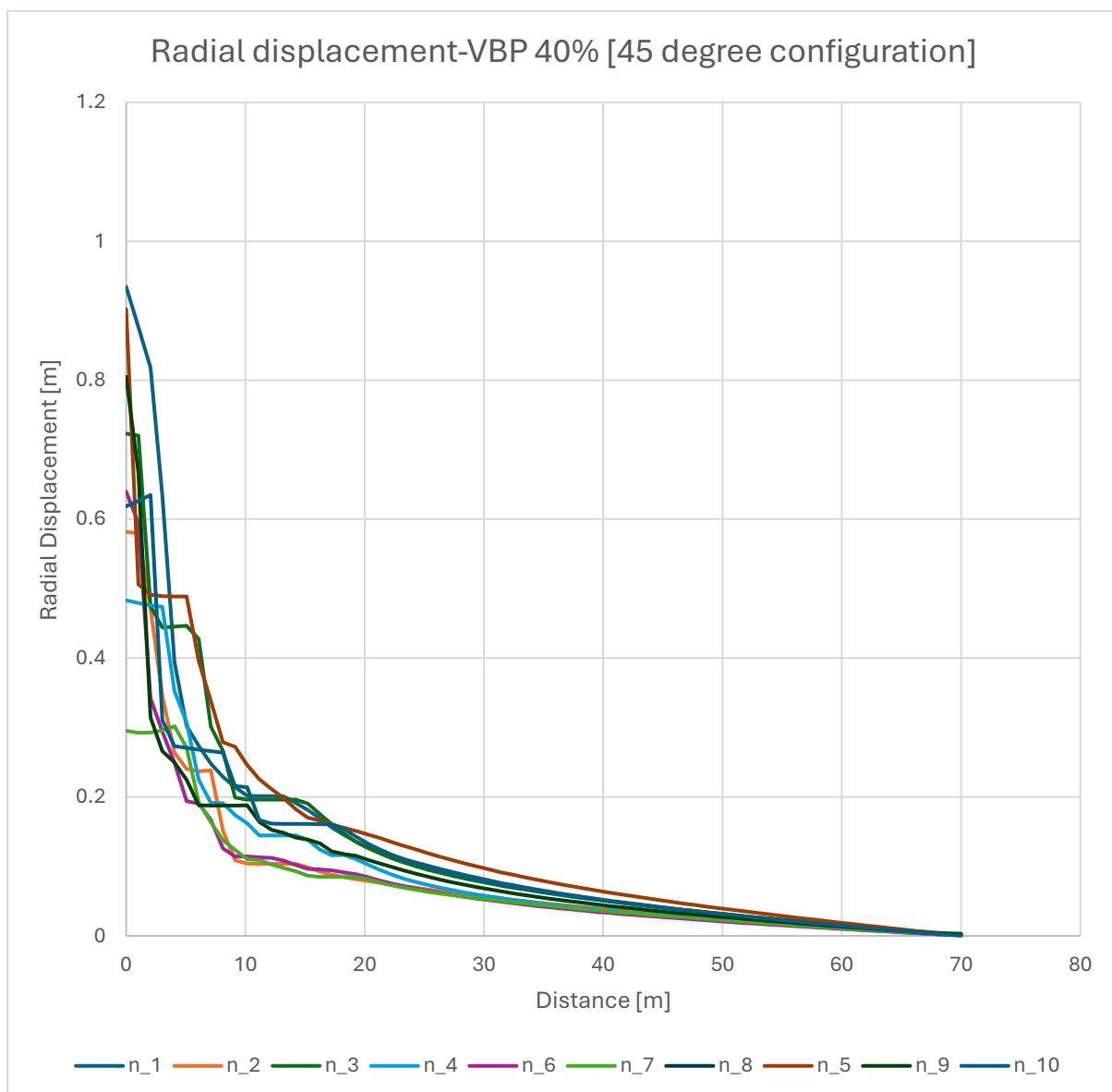


Figure 5.15 The figure of radial displacement for 45-degree orientations for VBP 25% vs. distance until external boundary

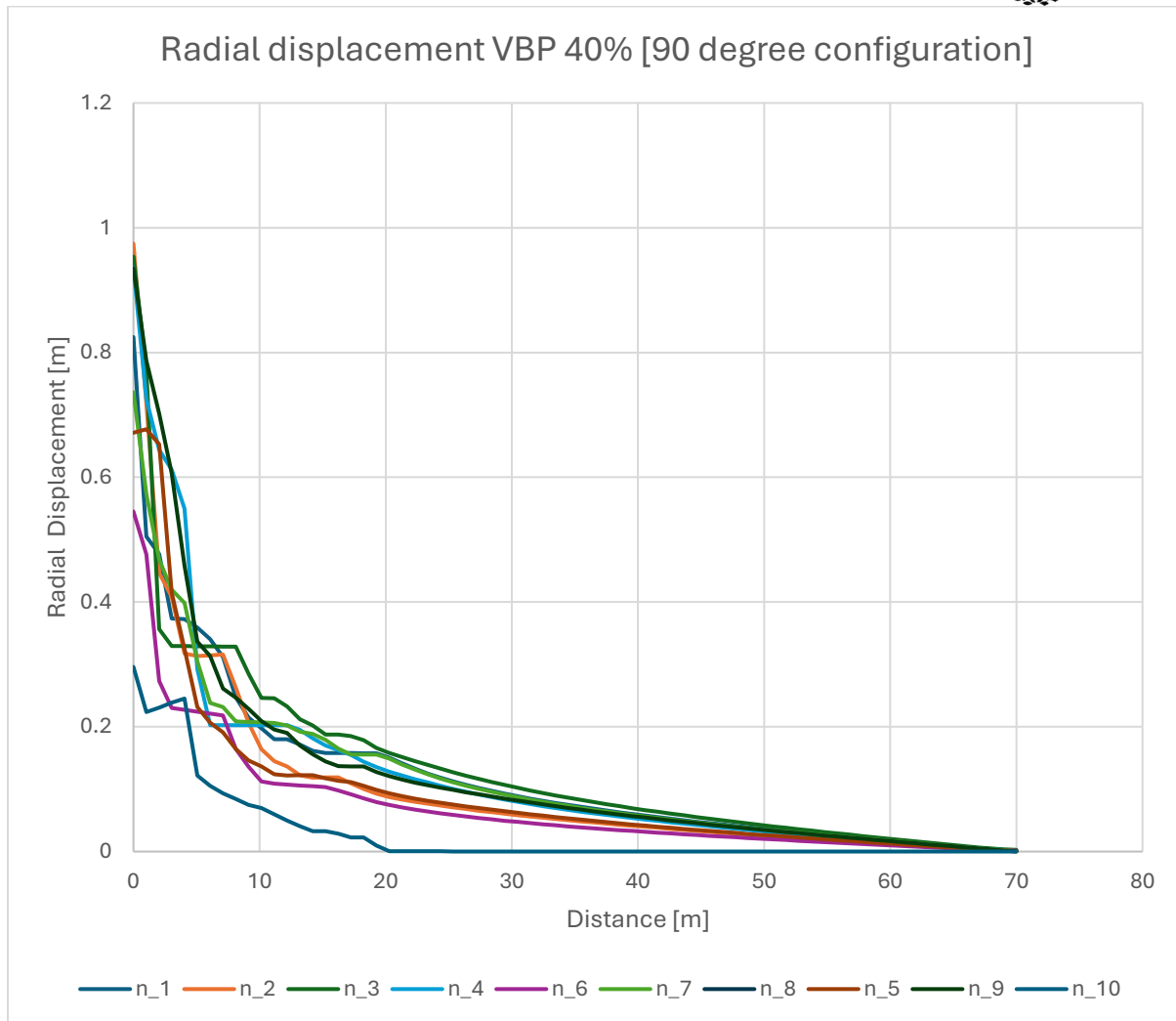


Figure 5.16 The figure of radial displacement for 90-degree orientations for VBP 25% vs. distance until external boundary

The results for  $VBP = 40\%$  clearly highlight the influence of block content on displacement attenuation:

- higher displacement variability is observed near the tunnel boundary compared to lower VBP cases.
- block orientation affects the magnitude and scatter of near-field displacement rather than the global decay trend.
- the far-field displacement consistently approaches negligible values, confirming that deformation remains localized around the excavation.

These findings demonstrate that increasing the volumetric block proportion enhances local heterogeneity and sensitivity to block arrangement, while the overall extent of the disturbed zone remains comparable across different orientations.

## 5.3 Analysis of Radial displacement along the tunnel boundary

### 5.3.1 Radial displacement along the tunnel boundary for VBP = 25%

This section presents and discusses the results of the numerical analyses in terms of total displacement distribution along the tunnel boundary. The objective is to investigate how the volumetric block proportion (VBP) and the orientation of inclusions influence the deformation pattern around the excavation. For each condition, several numerical realizations were considered to account for the inherent variability of bimrock.

For the case with VBP equal to 25%, the displacement profiles along the tunnel boundary show a generally moderate and relatively smooth deformation pattern, although local fluctuations are clearly visible due to the heterogeneous nature of the material. (Figure 5.17)

For 0° block orientation, the displacement curves obtained from different realizations remain relatively close to each other. The deformation along the boundary is uniform, with limited local peaks. This behavior suggests that, at this block content, the response of the tunnel is still largely governed by the matrix, while the blocks mainly induce localized stiffness variations rather than a global change in tunnel convergence.

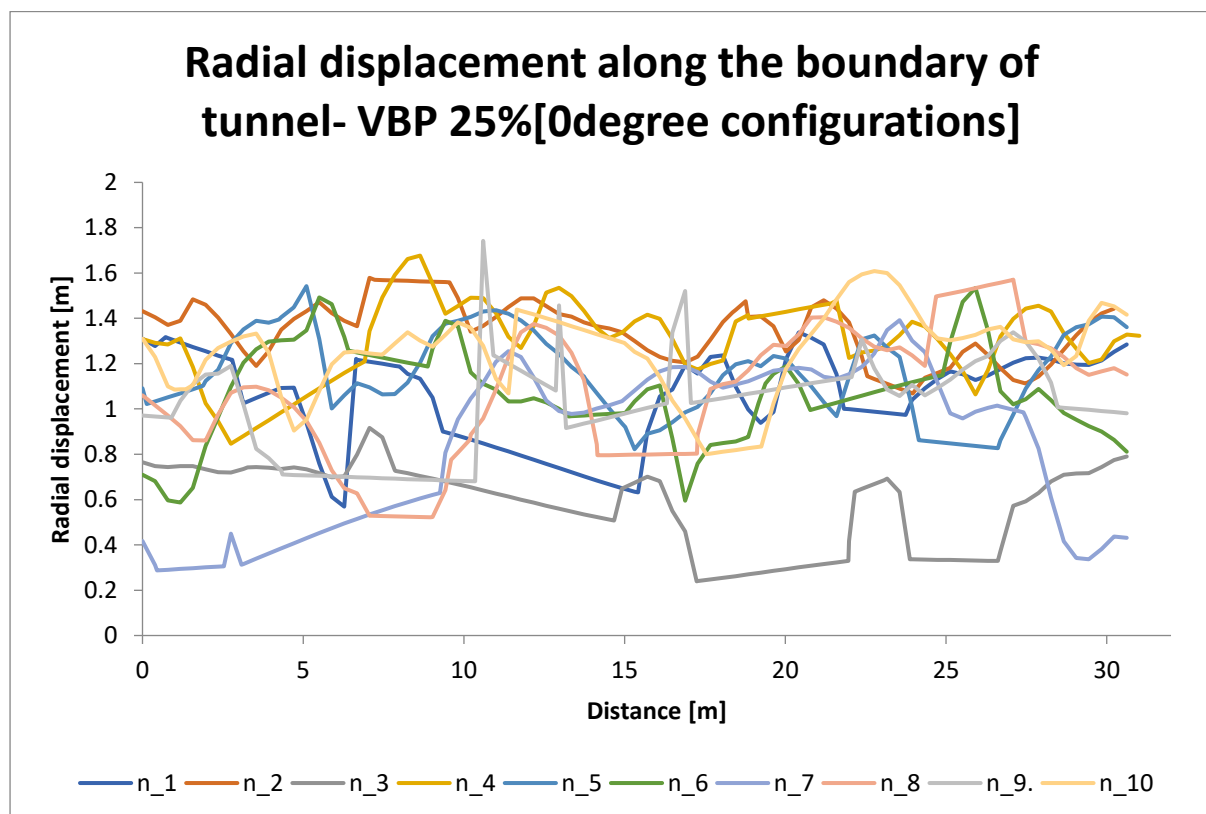


Figure 5.17 The figure of radial displacement for 0-degree orientations for VBP 25% vs. along the tunnel boundary

When the block orientation is increased to  $45^\circ$ , a higher variability among the displacement profiles is observed (Figure 5.18). Local amplification of displacement appears at specific locations along the boundary, indicating a stronger interaction between the excavation-induced stress redistribution and the inclined blocks. Nevertheless, the overall magnitude of displacement remains comparable to the  $0^\circ$  case, confirming that the effect of orientation is more pronounced in terms of spatial variability rather than absolute deformation levels.

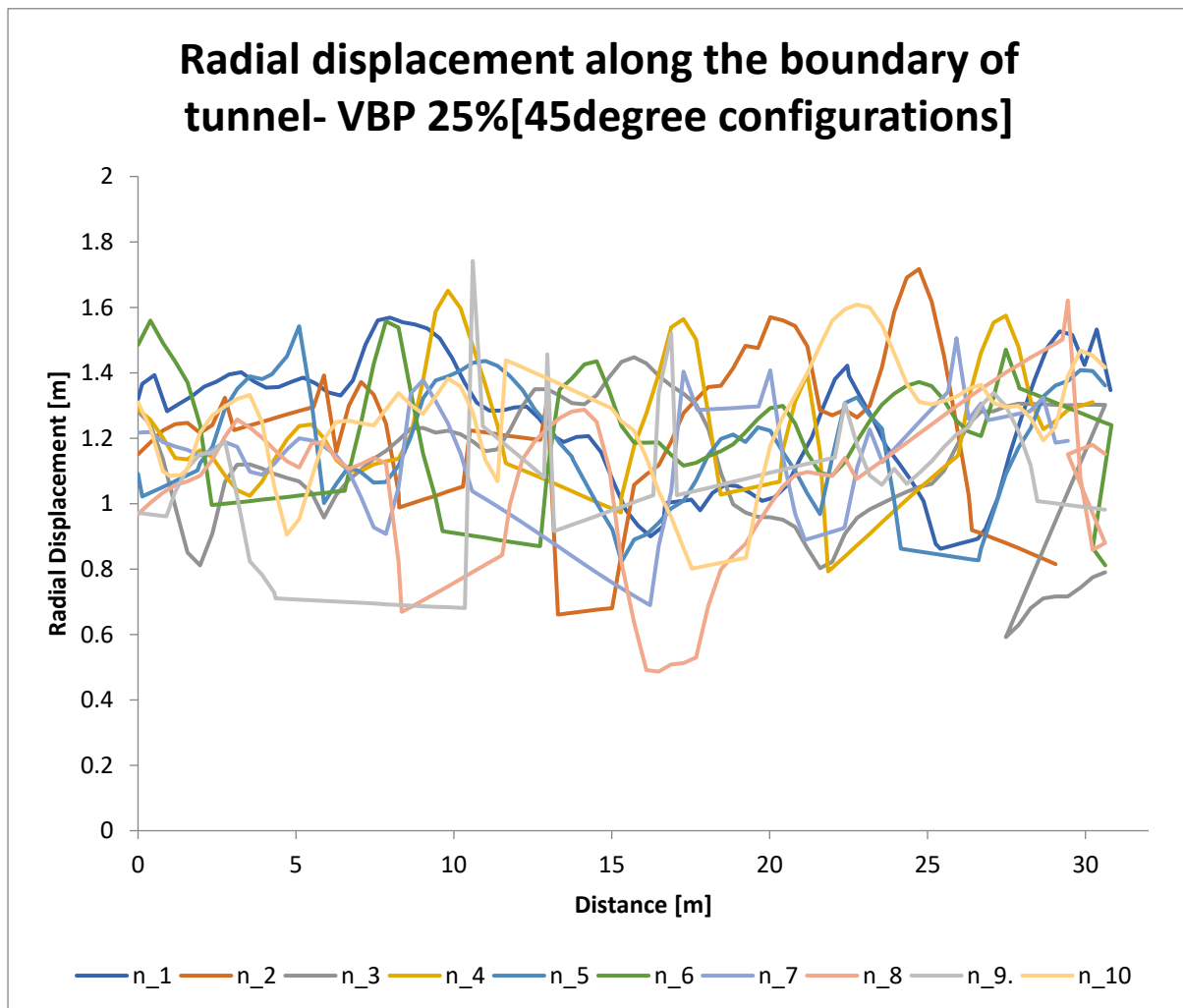


Figure 5.18 The figure of radial displacement for 45-degree orientations for VBP 25% vs. along the tunnel boundary

For 90° orientation, the displacement curves exhibit the largest scatter among the three configurations. Some realizations show noticeable local minima and maxima, reflecting the presence of blocks aligned perpendicular to the tunnel boundary. This configuration enhances stress concentration and unloading effects at specific points, leading to a more irregular displacement pattern along the perimeter. (Figure 5.19)

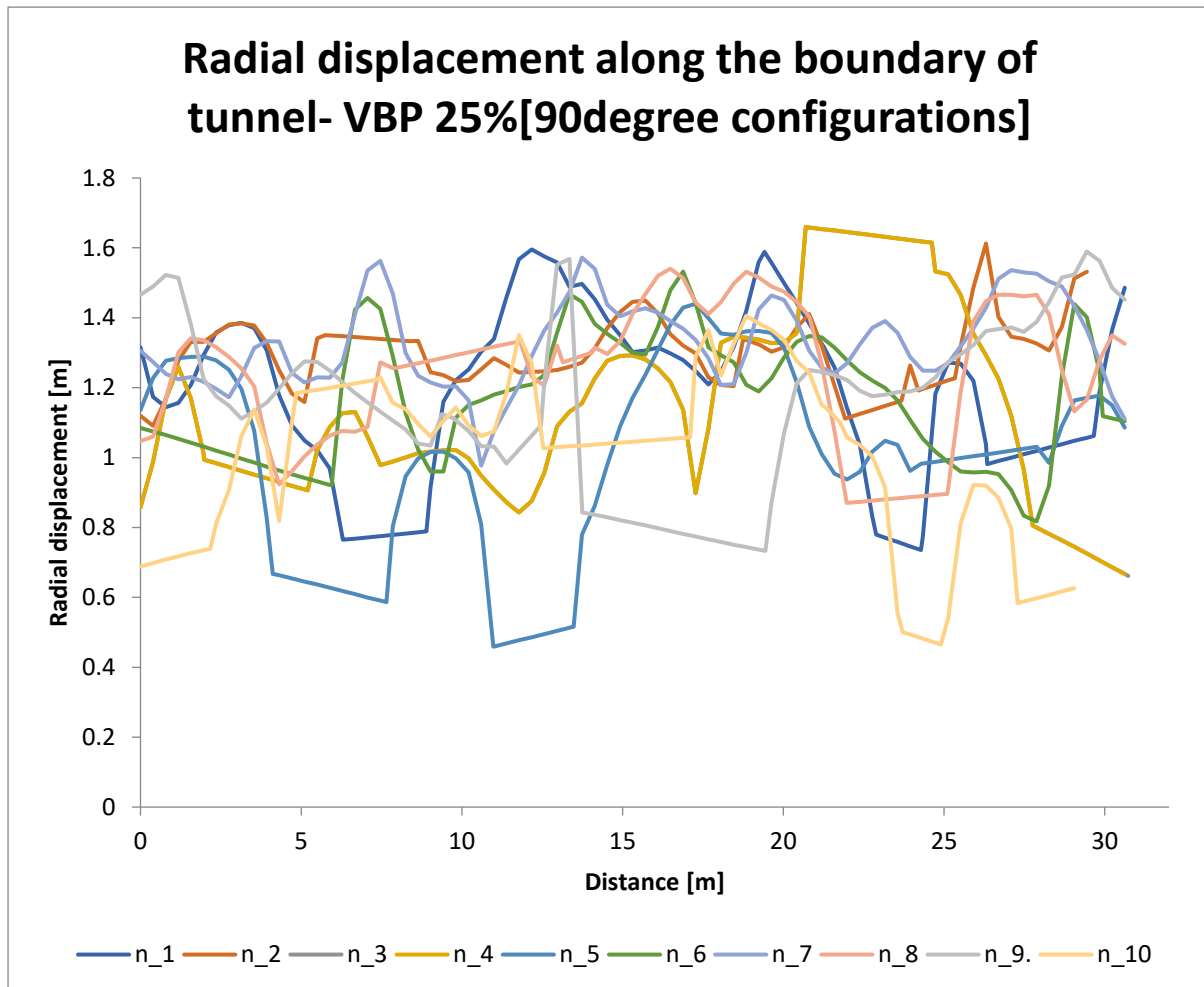


Figure 5.19 The figure of radial displacement for 90-degree orientations for VBP 25% vs. along the tunnel boundary

### 5.3.2 Radial displacement along the tunnel boundary for VBP = 40%

Increasing the volumetric block proportion to 40% results in a noticeably different mechanical response compared to the VBP = 25% case. The displacement distribution along the tunnel boundary becomes more irregular, with larger differences between realizations and more evident local fluctuations.

For the 0° configuration, the displacement profiles still follow a generally continuous pattern along the tunnel perimeter. However, the scatter between realizations is clearly greater than that observed for VBP = 25%. Local peaks and sudden drops in displacement appear more frequently, highlighting the stronger influence of block–matrix interaction at this higher block content. (Figure 5.20)

The increase in block proportion reduces the dominance of the matrix-controlled deformation mechanism observed at lower VBP values. Instead, the spatial arrangement and interaction of blocks begin to play a more significant role in controlling stress redistribution and displacement localization.

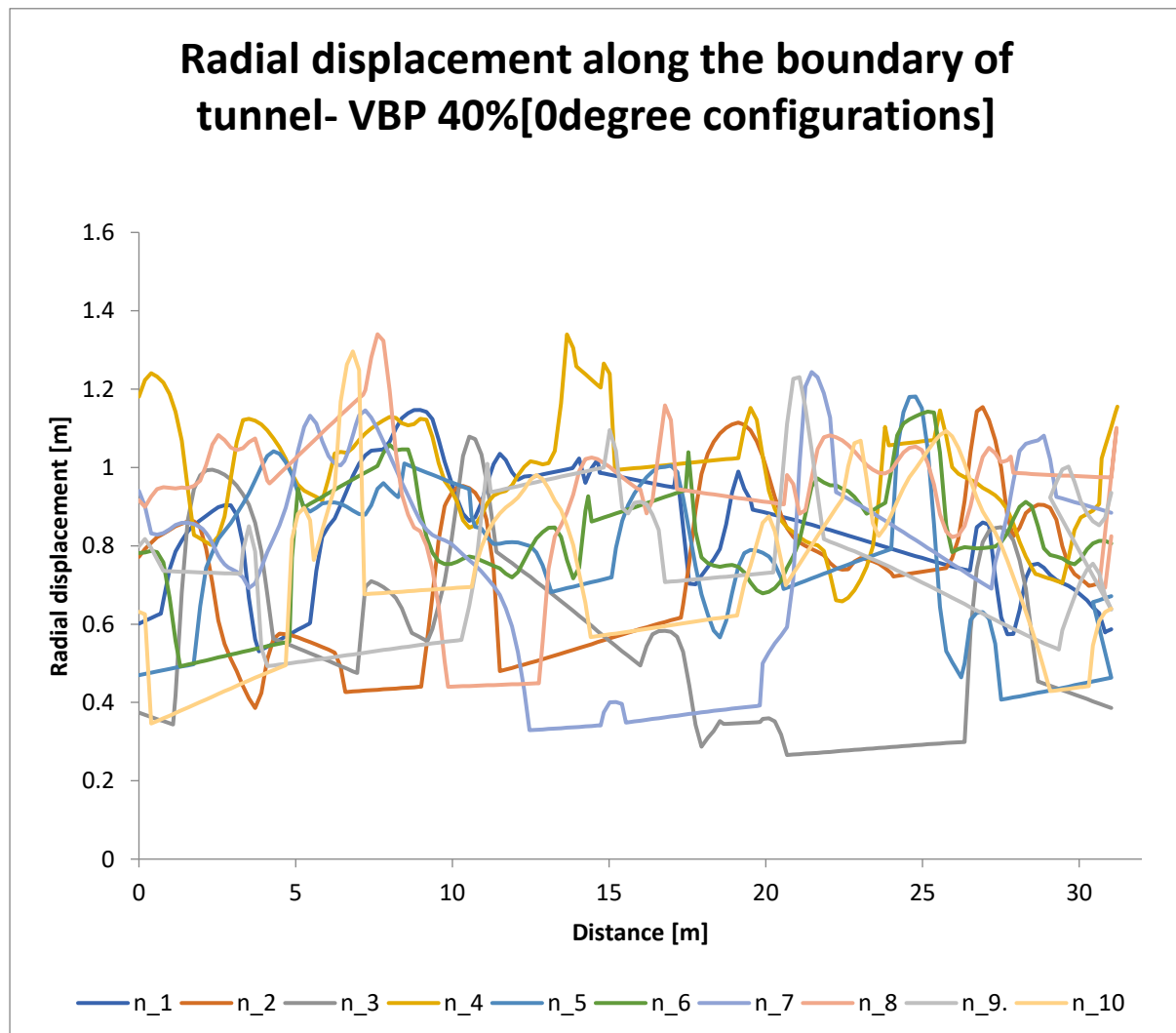


Figure 5.20 The figure of radial displacement for 0-degree orientations for VBP 40% vs. along the tunnel boundary

For 45° orientation, the displacement variability further increases. Several realizations exhibit localized zones of higher displacement, which can be associated with the interaction between inclined blocks and the tunnel excavation. The deformation pattern becomes less uniform, and the influence of block arrangement becomes more evident, even though the average displacement level remains within a comparable range. (Figure 5.21)

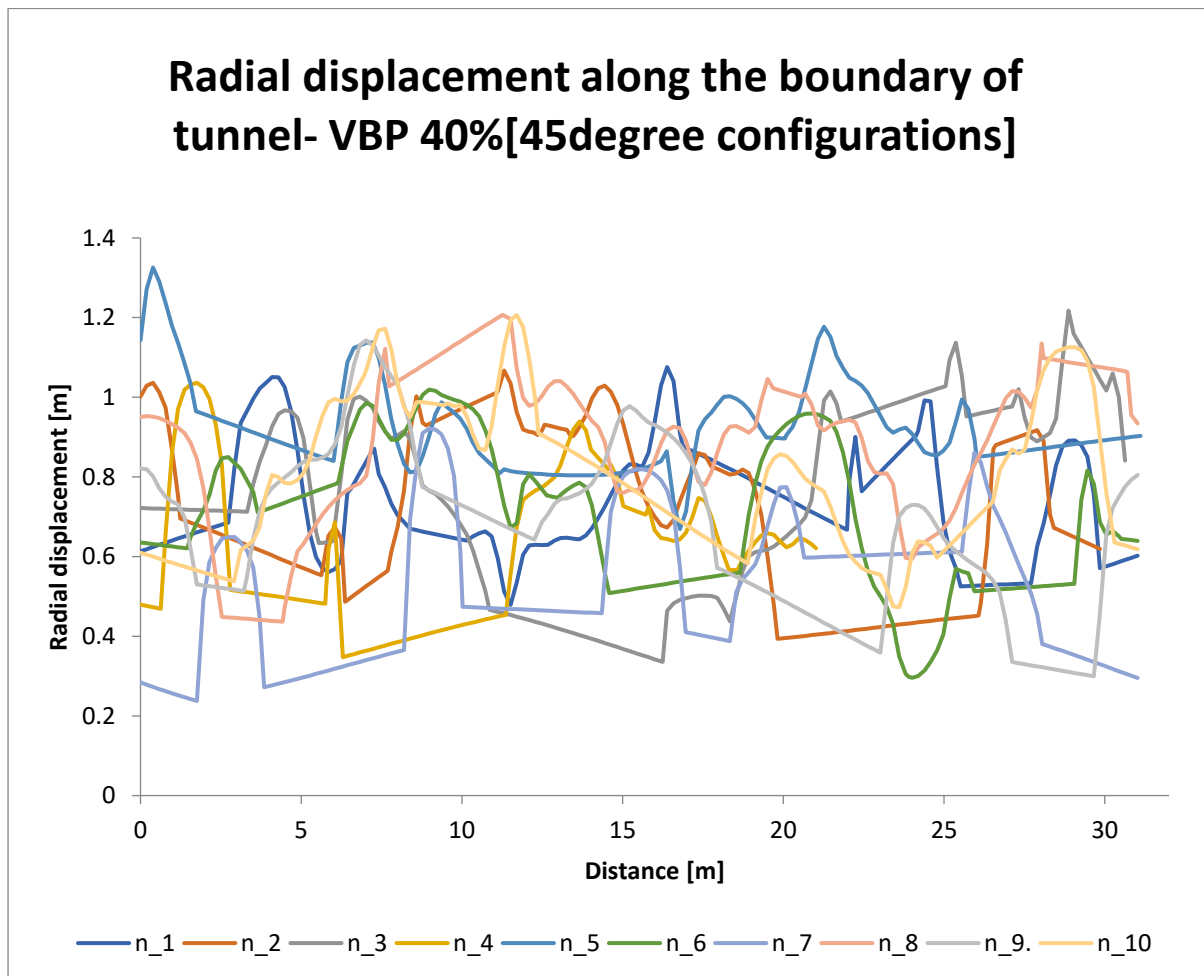


Figure 5.21 The figure of radial displacement for 45-degree orientations for VBP 40% vs. along the tunnel boundary

The most irregular response is observed for 90° orientation, where the displacement curves display marked fluctuations along the tunnel boundary. In this configuration, some realizations show distinct local displacement peaks and troughs, suggesting stronger stress redistribution effects and reduced confinement in certain sectors of the tunnel. This confirms that, at higher VBP values, the orientation of blocks plays a key role in controlling the mechanical response of the excavation. (Figure 5.22)

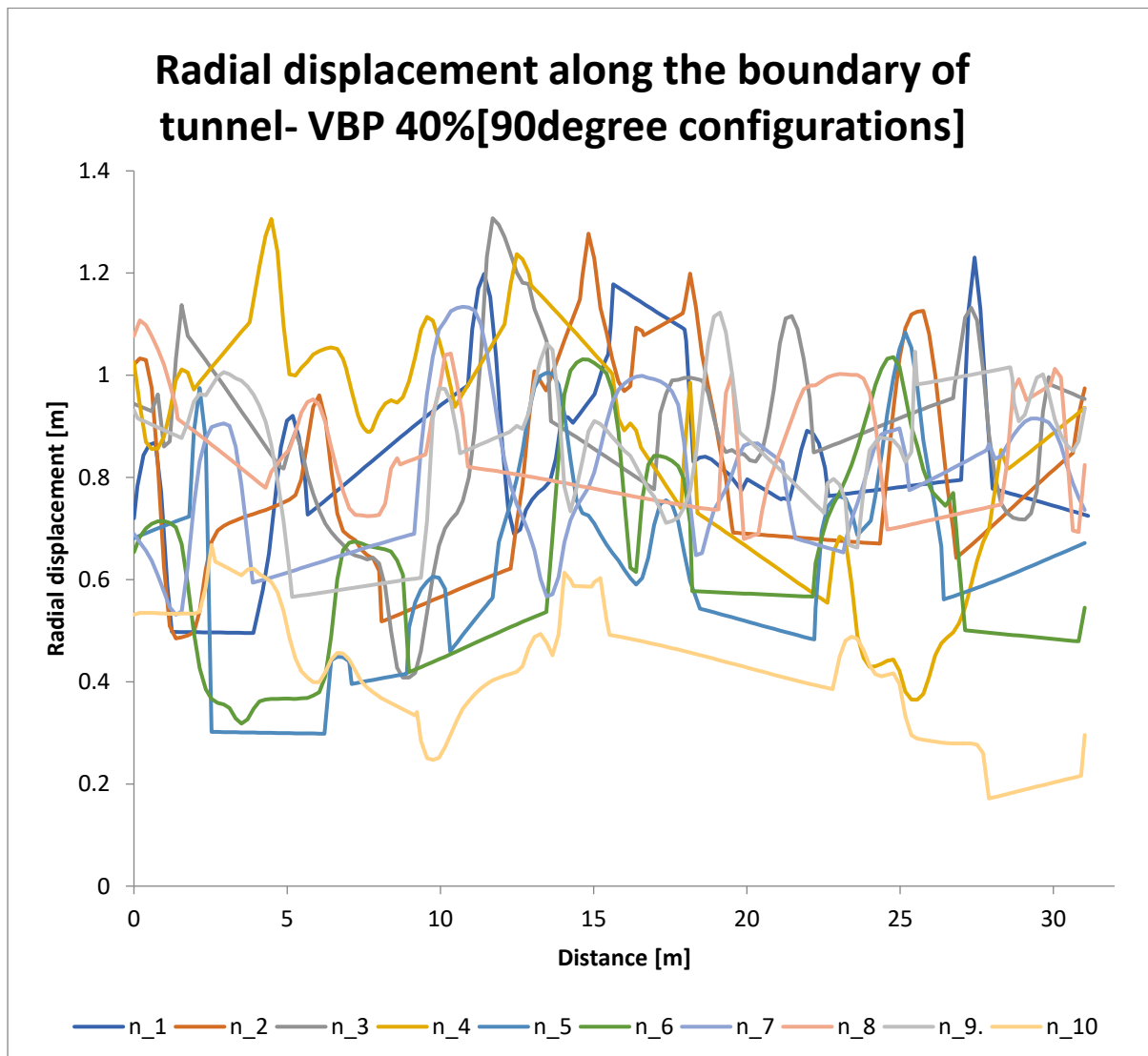


Figure 5.22 The figure of radial displacement for 90-degree orientations for VBP 40% vs. along the tunnel boundary

## 5.4 Comparative Discussion:

The comparison between the two block proportions, VBP = 25% and VBP = 40%, provides a clearer understanding of how increasing block content influences tunnel deformation. From the (Figure 5.25) showing the maximum and minimum radial displacements along the tunnel boundary, several important differences can be observed.

For VBP = 25%, the overall displacement levels are higher, with maximum values reaching approximately 1.7 m depending on block orientation. Although some variability exists between the 0°, 45°, and 90° configurations, the response remains relatively stable. In this case, the matrix still governs the overall deformation mechanism, and the influence of blocks is mainly local.

When the block proportion increases to VBP = 40%, the mechanical response changes. The maximum displacement values decrease to approximately 1.3 m, indicating a global stiffening effect caused by the higher block content. However, the deformation pattern becomes more irregular. The dispersion between minimum and maximum displacement values remains significant, and the influence of block orientation becomes more evident. This suggests that the interaction between blocks and matrix begins to play a more dominant role in controlling deformation.

The diagram directly comparing both VBP conditions confirms this behaviour. While the 25% case exhibits larger absolute displacements, the 40% case shows a more heterogeneous and spatially variable deformation pattern. Increasing the block content does not simply reduce displacement magnitude; rather, it modifies how deformation develops and how it is distributed along the tunnel boundary. (Figure 5.25)

Also, can check the variation of radial displacement at different orientations for each VBP. (Figure 5.23 – Figure 5.24)

In summary, increasing the block proportion from 25% to 40% leads to:

- A reduction in overall displacement magnitude,
- Greater variability along the tunnel boundary,
- Increased sensitivity to block orientation,
- More localized deformation mechanisms.

These results highlight the importance of considering stochastic variability and block configuration in the analysis of tunnels excavated in bimrock formations. Simplified homogeneous models may not fully capture the spatial complexity introduced by higher block content.

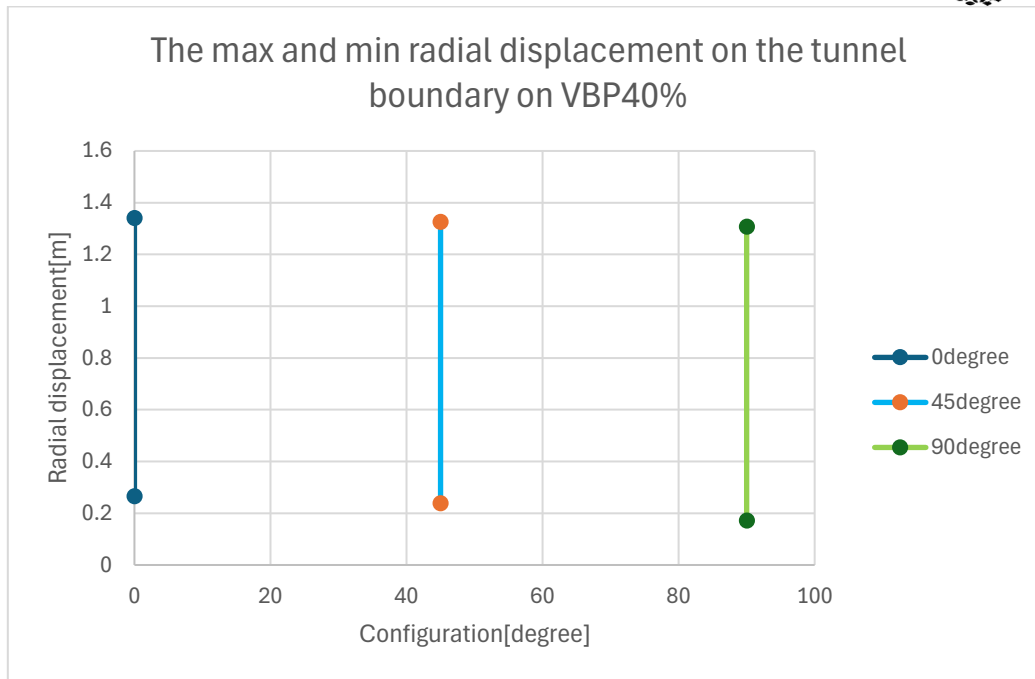


Figure 5.23 The max and the minimum radial displacement along the tunnel boundary in condition of VBP 25%

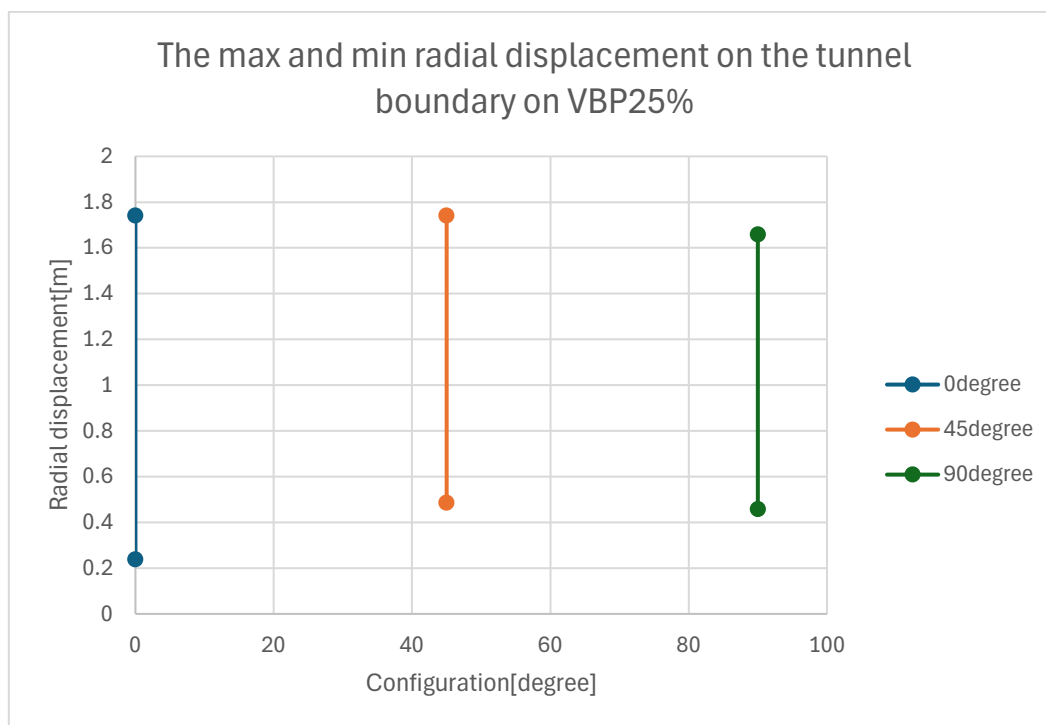


Figure 5.24 The max and the minimum radial displacement along the tunnel boundary in condition of VBP 40%

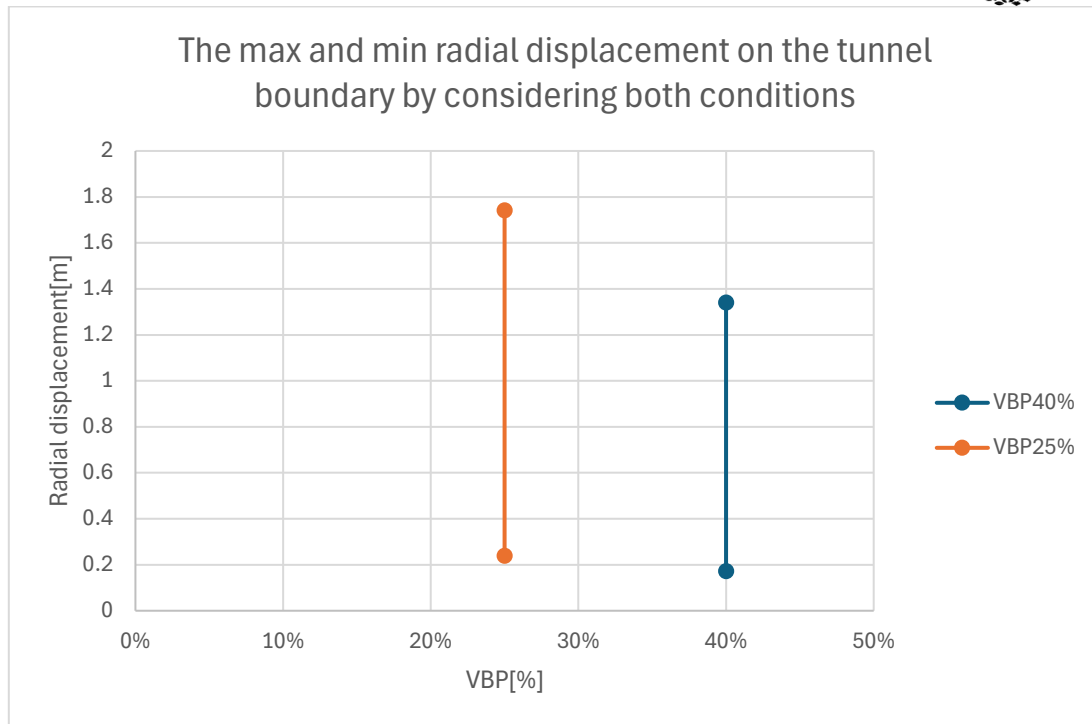


Figure 5.25 The max and the minimum radial displacement along the tunnel boundary in condition of VBP 40% and 25%

## 5.5 Analysis of radial displacement at the side walls:

### 5.5.1 Radial displacement at the right sidewall

The radial displacement values at the right sidewall were analysed for block orientations of  $0^\circ$ ,  $45^\circ$ , and  $90^\circ$ , considering both VBP = 25% and VBP = 40%.

For the  $0^\circ$  orientation, the displacement values corresponding to VBP = 25% are generally higher than those obtained for VBP = 40%. The maximum displacement recorded for VBP = 25% (1.39 m) exceeds the maximum value observed for VBP = 40% (1.16 m). Although most realizations follow this trend, one configuration shows a slightly higher displacement for VBP = 40%, reflecting the stochastic influence of block arrangement. Overall, the difference between the two VBP conditions remains noticeable but not uniform across all realizations. (Table 5.10)

For the  $45^\circ$  orientation, the separation between the two volumetric block proportions becomes more pronounced. The maximum displacement for VBP = 25% (1.60 m) is significantly higher than that recorded for VBP = 40% (approximately 0.93 m). In this case, all realizations show higher displacement values for VBP = 25%, indicating a clearer distinction between the two mechanical responses. (Table 5.11)

For the  $90^\circ$  orientation, the difference between the two VBP values remains evident. The maximum displacement for VBP = 25% (1.42 m) is higher than that observed for VBP = 40% (approximately 0.98 m). While most configurations follow this trend, minor local deviations appear in individual realizations, again confirming the stochastic nature of bimrock behaviour. (Table 5.12)

So, increasing the volumetric block proportion from 25% to 40% generally leads to a reduction in maximum right sidewall displacement. The most significant differences are observed for the  $45^\circ$  and  $90^\circ$  configurations, suggesting that the influence of block orientation becomes more relevant as block content increases.

0degree	VBP 25%	VBP40%	$\Delta$ [m]
N. configuration	right sidewall displacement[m]	right sidewall displacement[m]	
1	0.651	0.59	0.06
2	1.34	0.73	0.61
3	0.648	0.39	0.26
4	1.39	1.16	0.23
5	0.936	0.46	0.47
6	0.981	0.81	0.18
7	1.04	0.88	0.16
8	0.797	1.06	-0.26
9	0.977	0.64	0.34
10	1.29	0.64	0.65
Max	1.39	1.16	0.23

Table 5.10 The values of radial displacement at right sidewall for 0-degree orientations for VBP 40% and 25%

45degree	VBP 25%	VBP40%	$\Delta$ [m]
N. configuration	right sidewall displacement[m]	right sidewall displacement[m]	
1	1.07	0.60	0.47
2	0.68	0.58	0.10
3	1.39	0.72	0.67
4	0.99	0.48	0.51
5	0.97	0.90	0.07
6	0.96	0.64	0.32
7	0.77	0.30	0.47
8	1.11	0.93	0.18
9	1.60	0.81	0.80
10	1.21	0.62	0.59
Max	1.6	0.934	0.67

Table 5.11 The values of radial displacement at right sidewall for 45-degree orientations for VBP 40% and 25%

90degree	VBP 25%	VBP40%	$\Delta$ [m]
N. configuration	right sidewall displacement[m]	right sidewall displacement[m]	
1	1.35	0.73	0.63
2	1.42	0.98	0.45
3	1.29	0.95	0.34
4	1.29	0.94	0.35
5	1.09	0.67	0.42
6	1.33	0.55	0.79
7	1.40	0.74	0.66
8	1.33	0.83	0.51
9	0.82	0.94	-0.11
10	1.04	0.30	0.74
Max	1.42	0.975	0.45

Table 5.12 The values of radial displacement at right sidewall for 90-degree orientations for VBP 40% and 25%

### 5.5.2 Radial displacement at the crown

The displacement values at the crown are reported for 0°, 45°, and 90° block orientations, considering VBP = 25% and VBP = 40%.

For the 0° orientation, the crown displacement values associated with VBP = 25% are generally higher than those obtained for VBP = 40%. The maximum displacement recorded for VBP 25% exceeds the corresponding maximum value for VBP 40%, while the minimum values remain close for the two configurations. (Table 5.13)

For the 45° orientation, the same trend is observed. The crown displacement values for VBP = 25% consistently exceed those for VBP = 40%. The maximum displacement recorded for VBP 25% is higher, whereas the values corresponding to VBP 40% show a narrower range. (Table 5.14)

For the 90° orientation, the difference between the two volumetric block proportions becomes more evident. The maximum crown displacement for VBP = 25% is significantly higher than that recorded for VBP = 40%, while the minimum values remain distinctly lower for the higher block content. (Table 5.15)

For all considered orientations, the maximum crown displacement decreases when the volumetric block proportion increases from 25% to 40%.

0degree	VBP 25%	VBP40%	Δ[m]
N. configuration	crown displacement[m]	crown displacement[m]	
1	0.99	1.04	-0.05
2	1.13	0.43	0.70
3	0.67	0.71	-0.04
4	1.28	1.11	0.17
5	1.32	0.91	0.41
6	1.07	1.00	0.07
7	1.25	1.12	0.13
8	1.28	1.35	-0.07
9	1.18	0.53	0.65
10	1.61	0.68	0.93
Max	1.61	1.35	0.26

Table 5.13 The values of radial displacement at crown for 0-degree orientations for VBP 40% and 25%

45degree	VBP 25%	VBP40%	$\Delta$ [m]
N. configura- tion	crown displacement[m]	crown displacement[m]	
1	1.32	0.80	0.52
2	1.26	0.54	0.72
3	0.96	0.93	0.02
4	0.87	0.38	0.49
5	1.25	1.08	0.17
6	1.27	0.94	0.33
7	1.11	0.35	0.76
8	1.08	1.06	0.02
9	1.45	1.10	0.35
10	1.03	1.17	-0.14
Max	1.45	1.17	0.28

Table 5.14 The values of radial displacement at crown for 45-degree orientations for VBP 40% and 25%

90degree	VBP 25%	VBP40%	$\Delta$ [m]
N. configura- tion	crown displacement[m]	crown displacement[m]	
1	0.83	0.82	0.01
2	1.14	0.66	0.48
3	1.64	0.64	1.00
4	1.64	0.90	0.74
5	1.02	0.40	0.62
6	1.22	0.67	0.55
7	1.37	0.66	0.71
8	0.88	0.73	0.15
9	1.18	0.59	0.59
10	1.00	0.40	0.60
Max	1.64	0.9	0.74

Table 5.15 The values of radial displacement at crown sidewall for 90-degree orientations for VBP 40% and 25%

### 5.5.3 Radial displacement at the left sidewall

The displacement values at the left sidewall are reported for 0°, 45°, and 90° block orientations, for both VBP = 25% and VBP = 40%.

For the 0° orientation, the displacement values at the left sidewall for VBP = 25% are higher than those obtained for VBP = 40%. The maximum displacement recorded for VBP 25% exceeds the corresponding value for VBP 40%, while the minimum values remain comparable. (Table 5.16)

For the 45° orientation, the displacement values for VBP = 25% remain consistently higher across the realizations. The difference between the maximum displacement values of the two VBP cases increases compared to the 0° configuration. (Table 5.17)

For the 90° orientation, the separation between the two volumetric block proportions is more pronounced. The maximum displacement at the left sidewall for VBP = 25% is significantly higher than that for VBP = 40%, whereas the minimum displacement values remain lower for the higher block content. (Table 5.18)

Odegree	VBP 25%	VBP40%	
N. configuration	left sidewall displacement[m]	left sidewall displacement[m]	$\Delta$ [m]
1	1.28	0.98	0.30
2	1.45	0.57	0.88
3	0.79	0.54	0.25
4	1.32	1.00	0.32
5	1.36	0.83	0.53
6	0.81	0.89	-0.07
7	0.43	0.40	0.03
8	1.15	0.97	0.18
9	0.98	0.96	0.03
10	1.42	0.58	0.84
Max	1.45	0.996	0.45

Table 5.16 The values of radial displacement at left sidewall for 0-degree orientations for VBP 40% and 25%

45degree	VBP 25%	VBP40%	$\Delta$ [m]
N. configuration	left sidewall displacement[m]	left sidewall displacement[m]	
1	1.36	0.83	0.53
2	0.96	0.90	0.06
3	1.30	0.36	0.94
4	1.31	0.71	0.60
5	1.15	0.82	0.34
6	1.17	0.52	0.65
7	1.19	0.82	0.37
8	0.88	0.77	0.12
9	1.41	0.97	0.44
10	1.37	0.77	0.60
Max	1.41	0.972	0.44

Table 5.17 The values of radial displacement at left sidewall for 45-degree orientations for VBP 40% and 25%

90degree	VBP 25%	VBP40%	$\Delta$ [m]
N. configuration	left sidewall displacement[m]	left sidewall displacement[m]	
1	1.49	1.04	0.45
2	1.38	1.11	0.27
3	0.67	0.84	-0.17
4	0.67	1.02	-0.35
5	1.09	0.68	0.41
6	1.10	1.01	0.09
7	1.11	0.88	0.23
8	1.33	0.77	0.56
9	1.45	0.90	0.55
10	0.67	0.56	0.11
Max	1.49	1.11	0.38

Table 5.18 The values of radial displacement at left sidewall for 90-degree orientations for VBP 40% and 25%

#### 5.5.4 Summary of the displacement at the sidewalls and the crown for different VBPs

The scatter plots summarize the displacement values recorded at the crown, left sidewall, and right sidewall as a function of the volumetric block proportion (VBP).

At the crown, a clear trend can be observed. When VBP increases from 25% to 40%, the displacement values generally decrease. For VBP = 25%, most data points are concentrated at higher displacement levels, with several values approaching the upper range of the recorded response. This indicates a stronger overall deformation when the block content is lower, and the matrix plays a more dominant role. (Figure 5.26)

For VBP = 40%, the displacement values shift toward lower magnitudes. Although variability is still present due to the stochastic distribution of blocks, the overall response appears slightly more compact compared to the VBP = 25% case. This suggests that increasing the block proportion introduces a global stiffening effect, reducing the magnitude of crown displacement.

Overall, the comparison confirms that volumetric block proportion significantly influences both the magnitude and distribution of displacement at the tunnel crown. While higher block content reduces absolute displacement levels, it does not eliminate variability, which remains an inherent characteristic of bimrock formations. (Figure 5.26)

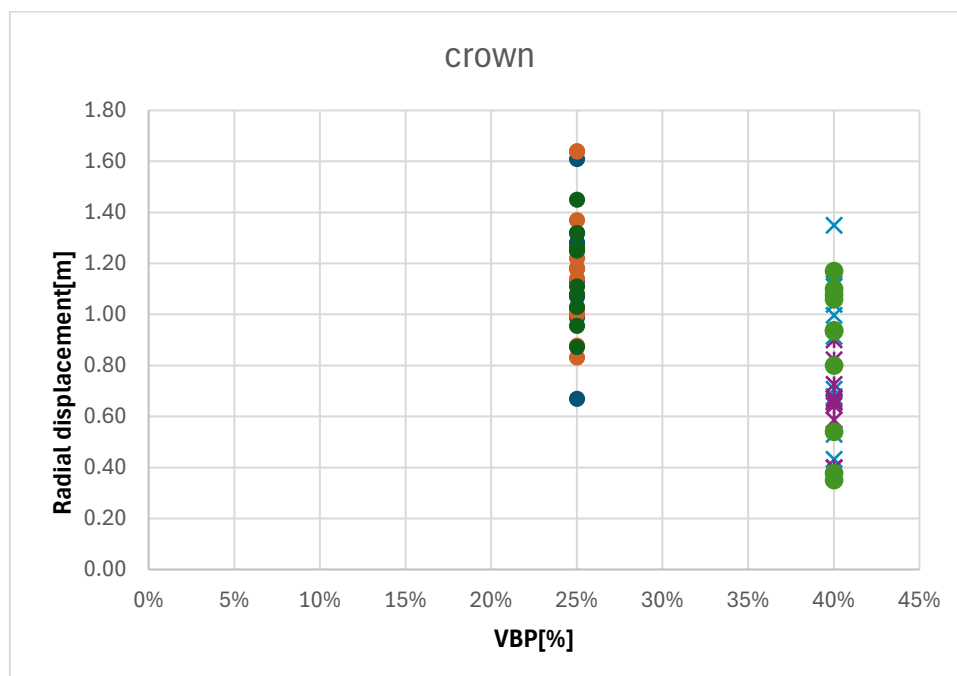


Figure 5.26 The values of displacement at crown orientations for VBP 40% and 25%

At the left sidewall, the same trend is observed, with radial displacement values progressively decreasing with increasing VBP. The largest displacement values are associated with lower block content, while higher VBP leads to a more compact distribution of points at lower displacement levels. The reduction is particularly evident when comparing the lower and higher VBP ranges. (Figure 5.27) (The results of VBP 55% and 70% are obtained from Dadone.2018)

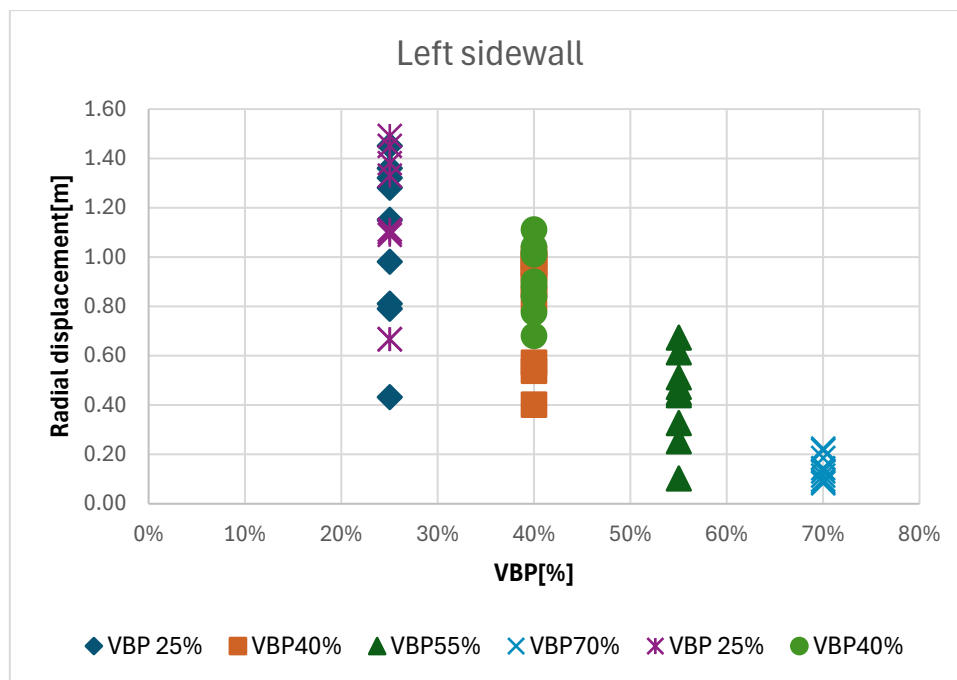


Figure 5.27 The values of displacement at left sidewall orientations for VBP 40%,55%,70% and 25%

At the right sidewall, the radial displacement values follow a similar pattern. Higher displacements are recorded for lower volumetric block proportions, while increasing VBP results in systematically lower displacement values and reduced variability among realizations. (Figure 5.28)

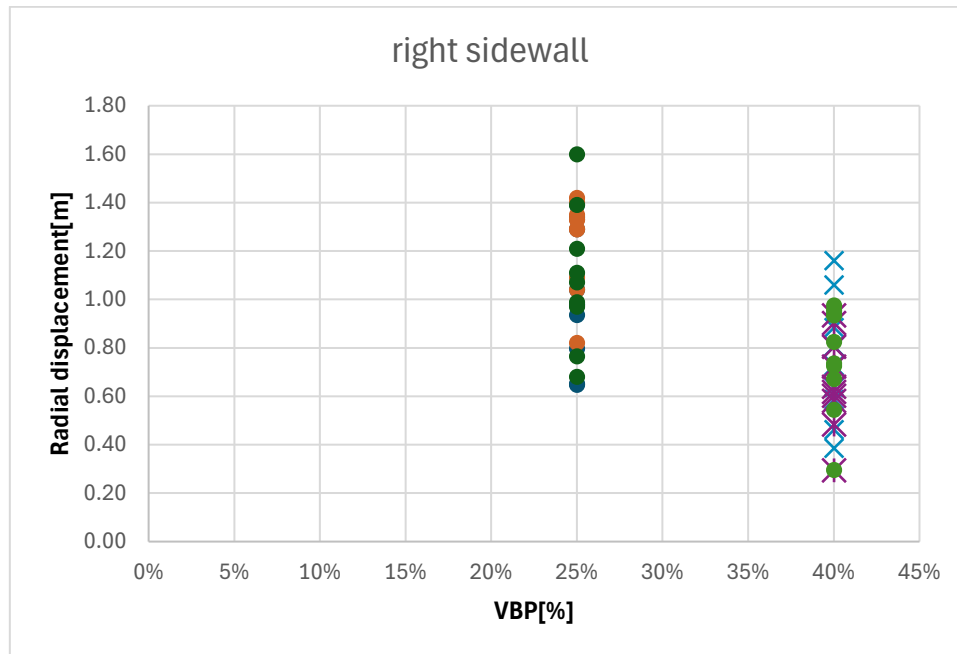


Figure 5.28 The values of displacement at right sidewall orientations for VBP 40% and 25%

## 5.6 Plastic zone extent for VBP = 25% and 40%:

According to figure 5.29 and figure 5.30 that the plastic radius depends on the configurations of blocks and increasing the VBP%, the yielded area is increased.

In the section 5.6.1, display the amount of change in VBP 25%.

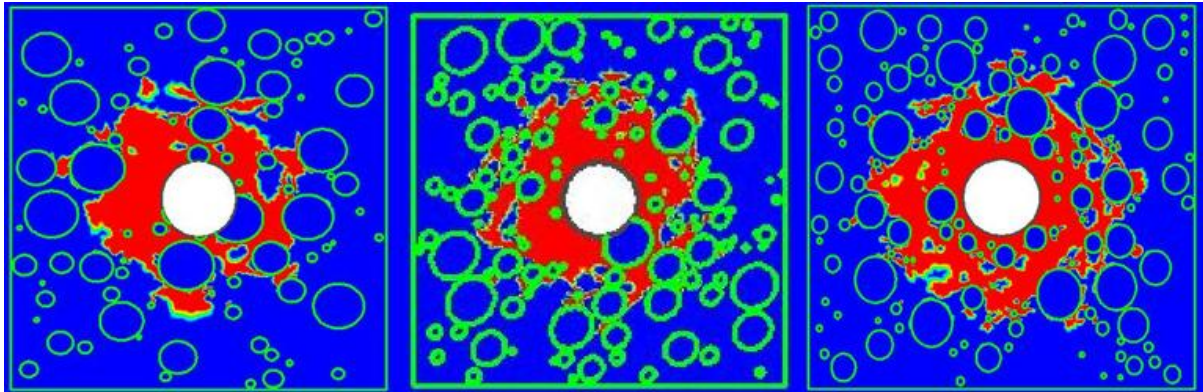


Figure 5.29 The plastic zone at VBP 25%

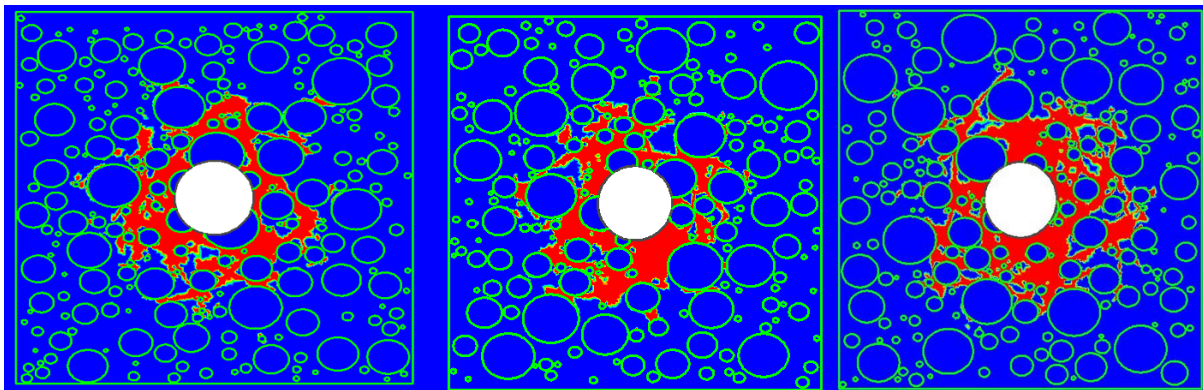


Figure 5.30 The plastic zone at VBP 40%

### 5.6.1 Plastic zone extent for VBP = 25%: comparison between 0° and 90° configurations

The extent of the plastic zone around the tunnel excavation was evaluated for VBP = 25% by comparing the 0° and 90° block orientation configurations. Figure 5.30 and figure 4.31 shows the distribution of yielded elements for the two cases, where the plasticized area is clearly identifiable around the tunnel boundary.

For the 0° configuration figure 5.31, the plastic zone extends more uniformly around the excavation perimeter, with several continuous yielded regions developing both at the sidewalls and near the crown. The calculated plastic area corresponds to 13.67% of the analyzed domain, indicating a relatively wider stress redistribution and a larger extent of irreversible deformation.

In contrast, the 90° configuration figure 4.30 exhibits a more localized plastic response. The yielded zones appear more fragmented and confined closer to the tunnel boundary, with a reduced spatial continuity. In this case, the plastic area is limited to 9.36%, representing a significant reduction compared to the 0° configuration.

The comparison highlights that, for the same volumetric block proportion, block orientation has a noticeable influence on the development of the plastic zone. Blocks oriented perpendicular to the excavation direction contribute to a more effective confinement of stresses, resulting in a smaller plastic radius, whereas the 0° configuration promotes a broader plasticized region around the tunnel.

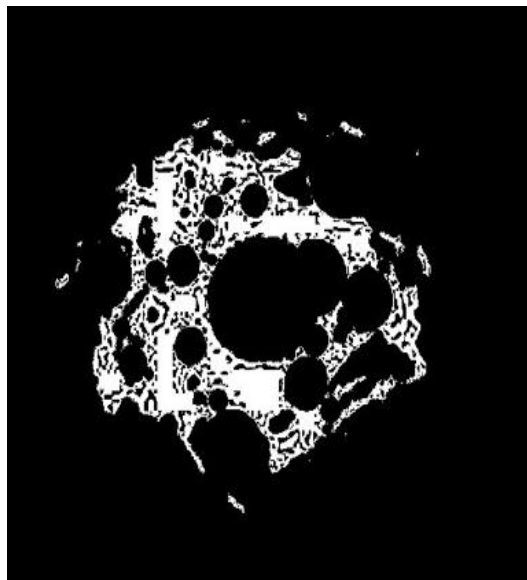


*Figure 5.31 The comparison of plastic zone in 90-degree orientation*

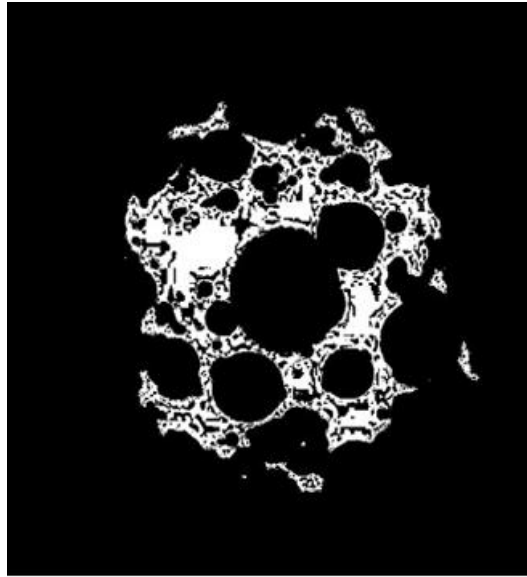


*Figure 5.32 The comparison of plastic zone in 0-degree orientation*

## 6 Conclusions

This thesis focused on the problematics related to tunnelling in block-in-matrix rocks, a class of geological formations particularly challenging from an engineering point of view due to their strong heterogeneity. Unlike conventional soils or rock masses, bim-rocks are characterized by the coexistence of a weaker matrix and competent rock blocks, whose spatial distribution is irregular and difficult to predict. This intrinsic variability makes the use of simplified homogeneous models questionable, especially for underground excavations.

To investigate these effects, a numerical approach based on finite element modelling was adopted to simulate the excavation of a circular deep tunnel in a bimrock. The geometry and position of the blocks inside the matrix were generated through a stochastic procedure, allowing different realistic configurations to be analysed by varying the volumetric block proportion and block orientation. For each configuration, the numerical results were compared with a reference case composed only of the matrix material, to isolate the influence of the blocks on the mechanical response of the ground.

The results highlight that the presence of blocks significantly alters stress redistribution and deformation patterns around the tunnel. For low volumetric block proportions, the behaviour is mainly governed by the matrix, with blocks acting as local stiff inclusions that modify the stress field but do not control the overall response. As the volumetric block proportion increases, the global stiffness of the system also increases, and tunnel convergence tends to decrease. However, this reduction in displacement is accompanied by a higher spatial variability, reflecting the heterogeneous nature of the material.

Intermediate block contents were found to represent a critical transition regime, in which neither the matrix nor the blocks clearly dominate the mechanical behaviour. In this range, numerical results show the greatest scatter, emphasizing how sensitive the tunnel response is to local block arrangement. Block orientation also plays an important role, influencing the symmetry of the displacement field and the shape and extent of the plastic zone around the excavation.

The analysis of yielding patterns confirms that plastic deformation mainly develops within the matrix, while blocks tend to constrain deformation and locally limit the extension of plastic zones. Configurations with lower block content show more widespread yielding, whereas higher block proportions lead to more confined plastic regions, although localized failure may still occur depending on block distribution.

Despite the insights provided by this study, some limitations should be acknowledged. The analyses were performed under plane-strain conditions and with idealized block

geometries, while real bimrocks may present more complex block shapes, scale effects, and time-dependent behaviour and the three-dimensional nature of the problem cannot be neglected. Further developments could include three-dimensional analyses, more realistic block morphologies, and the inclusion of hydro-mechanical coupling.

In conclusion, the results clearly demonstrate that bimrocks cannot be reliably represented as homogeneous materials in tunnelling analyses. Volumetric block proportion and block geometry strongly influence tunnel convergence, stress redistribution, and plastic zone development. The numerical approach adopted in this thesis provides a useful framework for understanding these effects and may support more informed design choices when dealing with tunnels excavated in complex geological formations.

The results highlight that the deformation around the tunnel boundary is not uniform when bimrock heterogeneity is considered. Due to the irregular distribution, size, and orientation of blocks, the tunnel experiences localized variations in displacement. This non-uniform deformation pattern may induce non-homogeneous stress states within the tunnel support system.

In practical terms, the lining or support structure may be subjected to uneven load distribution and localized stress concentrations rather than the symmetric stress state typically assumed in homogeneous ground conditions. Such irregular stress development can influence the structural performance of the support and may affect its required thickness and reinforcement.

For this reason, the inherent heterogeneity of bimrock formations should be explicitly considered during the dimensioning of the tunnel support, as simplified homogeneous assumptions may underestimate localized stress effects and lead to non-conservative design choices.

## References

- A.G.I. (Associazione Geotecnica Italiana). (1979). *Classification of complex geological formations*. Associazione Geotecnica Italiana, Rome.
- Barbero, M., Bonini, M., & Napoli, M. L. (2006). Fractal distribution of blocks in mélanges and its engineering implications. *Engineering Geology*, 85(3–4), 217–230.
- Carranza-Torres, C., & Fairhurst, C. (2000). Application of the convergence–confinement method of tunnel design to rock masses that satisfy the Hoek–Brown failure criterion. *Tunnelling and Underground Space Technology*, 15(2), 187–213.
- Cowan, D. S. (1985). Structural styles in Mesozoic and Cenozoic mélanges of the western Cordillera of North America. *Geological Society of America Bulletin*, 96(4), 451–462.
- Dadone, L. (2018). *Geometrical characterization of bimrocks for numerical modelling* (Master's thesis). Politecnico di Torino.
- D'Elia, B., Manfredini, G., & Pellegrini, M. (1986). Engineering geological problems related to complex formations in Italy. *Memorie della Società Geologica Italiana*, 31, 209–222.
- Festa, A., Pini, G. A., Dilek, Y., & Codegone, G. (2010). Mélanges and mélange-forming processes: A historical overview and new concepts. *International Geology Review*, 52(10–12), 1040–1105.
- Greenly, E. (1919). *The geology of Anglesey*. Memoirs of the Geological Survey of Great Britain.
- Hoek, E. (1999). Support for very weak rock associated with faults and shear zones. In *Proceedings of the International Symposium on Rock Support* (pp. 131–142).
- Hoek, E., & Brown, E. T. (1980). *Underground excavations in rock*. Institution of Mining and Metallurgy.
- Hoek, E., Carranza-Torres, C., & Corkum, B. (1998). Hoek–Brown failure criterion – 1998 edition. *Proceedings of NARMS-TAC Conference*, 1, 267–273.
- Lindquist, E. S., & Goodman, R. E. (1994). Strength and deformation properties of a physical model mélange. *Engineering Geology*, 36(3–4), 187–206.
- Lombardi, G. (1979). Considerations on the calculation of tunnels in squeezing ground. *Proceedings of the International Symposium on Weak Rock*, Tokyo, 1, 215–220.
- Medley, E. W. (1994). *The engineering characterization of mélanges and similar block-in-matrix rocks (bimrocks)* (PhD dissertation). University of California, Berkeley.

- Medley, E. W. (2001). Orderly characterization of chaotic Franciscan mélange. *Felsbau*, 19(6), 20–33.
- Napoli, M. L., Barbero, M., & Colombero, C. (2018). Numerical analysis of tunnel excavation in bimrocks with stochastic block distribution. *Engineering Geology*, 245, 1–15.
- Napoli, M. L., Barbero, M., & Colombero, C. (2021). Mechanical behaviour of block-in-matrix rocks: Numerical modelling and scale effects. *Rock Mechanics and Rock Engineering*, 54(3), 1205–1223.
- Panet, M., & Guenot, A. (1982). Analysis of convergence behind the face of a tunnel. *Tunnelling and Underground Space Technology*, 1(1), 41–55.
- Raymond, L. A. (1984). Classification of mélanges. In L. A. Raymond (Ed.), *Mélanges: Their nature, origin, and significance* (pp. 7–20). Geological Society of America.
- Sonmez, H., & Tuncay, E. (2008). Scale effect and block size distribution in bimrocks. *Engineering Geology*, 99(3–4), 191–206.
- Vlachopoulos, N., & Diederichs, M. S. (2009). Improved longitudinal displacement profiles for convergence confinement analysis of deep tunnels. *Rock Mechanics and Rock*